

Re-evaluation of CspZ, a complement regulator-acquiring surface protein of the Lyme disease
spirochete *Borrelia burgdorferi*, as a potential vaccine target in a canine host.

A Thesis Paper

Presented to

The College of Graduate Studies

Austin Peay State University

In Partial Fulfillment

Of the Requirements for the Degree

Masters of Science in Biology

Nerina Jusufovic

December, 2017

Copyrighted © 2017

By

Nerina Jusufovic

All Rights Reserved

December 2017

To the College of Graduate Studies:

We are submitting a thesis written by Nerina Jusufovic entitled “Re-evaluation of CspZ, an outer surface protein of the Lyme disease spirochete *Borrelia burgdorferi*, as a vaccine target in a canine host.” We have examined the final copy of this thesis for form and content. We recommend that it be accepted in partial fulfillment of the requirements for the degree of Masters of Science in Biology.

_____ Dr. Chad Brooks

Research/Committee Advisor/Chair

_____ Dr. Don Dailey

Committee Member

_____ Dr. Sarah Lundin-Schiller

Committee Member

Accepted for the Graduate and Research Council

Dr. Chad Brooks_____

Dean, College of Graduate Studies

(Original signatures are on file with official student records.)

Statement of Permission to Use

In presenting this thesis in partial fulfillment of the requirements for the Masters of Science in Biology at Austin Peay State University, I agree that the library shall make it available to borrowers under the rules of the library. Brief quotations from this field study are allowable without special permission, provided that accurate acknowledgement of the source is made. Permissions for extensive quotation or reproduction of this field study may be granted by my major professor, or in his/her absence, by the Head of the Interlibrary Services when, in the opinion of either, the proposed use of the material is for scholarly purposes. Any copying or use of the material in this thesis for financial gain shall not be allowed without my written permission.

Nerina Jusufovic

12/06/2017

Dedication

This thesis is dedicated to my family. To my Mom, Dad, Sister, and Grandma, thank you for raising me. It was just us beginning something new, in a land as foreign to us as we were about to be to it. You were always there for me when I needed it the most. Thank you for taking all the calls, especially the really late calls. Thank you for the support always. Thank you for inspiring me to never give up and always count myself in. But most importantly, thank you for raising me and shaping me into the person I am today. Each of you have left an impression of yourselves in me that I will carry for the rest of my life. Sve je ništa bez familija.

Acknowledgements

I would like to acknowledge my rock, Steven Dotson first. Thank you for all the support you've always given and dealing with the madness that was this thesis. To all my fellow graduate students and Laura Sanders, thank you for all the memories.

Austin Peay State University has been paramount in allowing the fruition and completion of this thesis by funding my Master's degree and additionally components of my research. I would also like to acknowledge specifically Daina Hunter for all her help in ordering and dealing with the nuisances of finishing a thesis off.

Dr. Hock deserves considerable acknowledgment for allowing me to use his animal facilities and providing me with animals. Without his contribution, completion of this thesis would have been nearly impossible. In addition, Dr. Scanlan has been there with advice and provided me with invaluable knowledge when I needed help. A great amount of thanks is owed to both.

I would also like to acknowledge my committee members Dr. Dailey and Dr. Schiller. I appreciate all the advice and help you have given me throughout this experience.

Lastly, I would like to acknowledge my major advisor, Dr. Chad Brooks. I appreciate you bringing me into your lab and allowing me to be your last graduate student. The approach to mentoring Dr. Brooks has is unorthodox, but I feel that it has pushed me to adapt and become a more skilled, independent researcher. I have developed the necessary skills and mental fortitude required for a potential PhD student to succeed. I feel comfortable in the scientist I have become, and I am thankful for the experience and guidance Dr. Brooks has given me.

ABSTRACT

NERINA JUSUFOVIC. Re-evaluation of CspZ, a complement regulator-acquiring surface protein of the Lyme disease spirochete *Borrelia burgdorferi*, as a potential vaccine target in a canine host. (Under the direction of Dr. Chad Brooks).

Over the past decade, studies have revealed a collection of surface proteins, collectively known as the complement regulator-acquiring surface proteins (CRASPs), expressed by *Borrelia burgdorferi* which enable the pathogenic bacterium to counteract immune defenses of the complement cascade found in various mammalian hosts and establish infection. Due to the theorized necessity of these CRASPs in the life cycle of *B. burgdorferi*, these proteins could serve as potential vaccine targets to preventing Lyme disease. This study attempted to expand on the roles of CRASPs by characterizing the protein CspZ, also known as CRASP-2. This study hypothesized CspZ is the CRASP responsible for impeding the canine complement cascade and thereby allow the bacterium to establish infection. Immunoblotting could not reveal whether CspZ is upregulated during mammalian infection due to the inability of antibodies generated against CspZ to recognize the protein in denatured lysates. In addition, determination of cell surface localization of CspZ via indirect immunofluorescence was also inconclusive and will need to be optimized. It was determined that CspZ is involved in evasion of the canine immune system, since CspZ deficient spirochetes died in the presence of dog serum. However, the B31cF mutant contains genes that code for the other CRASPs, CspA and the ErP proteins. Therefore, it could not be concluded that CspZ is the minimally necessary and sufficient CRASP which allows the survival of spirochetes in a canine host. A knockout mutant lacking all CRASPs will need to be created and then rescued with CspZ to determine if CspZ is the necessary and minimally essential CRASP required for *B. burgdorferi* survival in a canine host.

Table of Contents

| | |
|-------------------------------|-----|
| Abstract | vii |
| List of Figures | ix |
| Chapter I: Introduction | 1 |
| Chapter II: Methods | 30 |
| Chapter III: Results | 52 |
| Chapter IV: Discussion | 81 |
| Chapter V: Conclusion | 92 |
| References | 94 |
| Vitae | 109 |

List of Figures

| | |
|--|----|
| FIG 1. Structure of a spirochete..... | 3 |
| FIG 2. Image of <i>Borrelia burgdorferi</i> strain B31MI grown <i>in vitro</i> .. | 4 |
| FIG 3. Erythema migrans rash of Lyme disease and facial palsy (32). | 8 |
| FIG 4. Graph of Lyme disease cases reported for the years 1996-2016 (58). | 13 |
| FIG 5. Cases of Lyme disease in the United States for 2016 (58). | 14 |
| FIG 6. Distribution of <i>I. scapularis</i> and <i>I. pacificus</i> by county in the U.S. | 15 |
| FIG 7. The life cycle of Lyme disease transmitting <i>Ixodes</i> ticks..... | 17 |
| FIG 8. The segmented genome of <i>B. burgdorferi</i> | 21 |
| FIG 9. Regulation of gene expression in <i>B. burgdorferi</i> .. | 22 |
| FIG 10. Molecular mechanisms that contribute to complement evasion by <i>Borrelia</i> | 25 |
| FIG 11. Hydrophobicity plots..... | 34 |
| FIG 12. Cloning schematic of the creation of the recombinant plasmids..... | 37 |
| FIG 13. Bradford assay BSA standard curve..... | 40 |
| FIG 14. Layout of dot blot titration membrane..... | 43 |
| FIG 15. Layout of the nitrocellulose membranes for native dot-blot of whole cell lysates. | 48 |
| FIG 16. 100 μ L PCR reactions of the genes of interest..... | 54 |
| FIG 17. Selection plates from transformations with various ligation conditions.. | 55 |
| FIG 18. Colony PCR results performed on transformants from selection plates.. | 56 |
| FIG 19. Diagnostic restriction enzyme digestion of pGEX: <i>tmspZ</i> PCR + colony.. | 57 |
| FIG 20. Nucleotide sequence alignment of colony 71..... | 58 |
| FIG 21. Protein sequence alignment of colony 71..... | 59 |
| FIG 22. SDS-PAGE of IPTG induced and overexpressed <i>E. coli</i> BL21 DE3..... | 62 |
| FIG 23. SDS-PAGE gels showing the protein purification process..... | 63 |

| | |
|---|----|
| FIG 24. Thrombin cleavage of GST:tCspZ and GST:tOspA.. | 64 |
| FIG 25. Dot blot antibody titration with recombinant proteins on PVDF membranes..... | 67 |
| FIG 26. Immunoblots of 500ng of recombinant protein probed with the proper antibodies..... | 69 |
| FIG 27. ECL immunoblotting of <i>Borrelia</i> whole cell lysates.. | 72 |
| FIG 28. Native dot-blot of recombinant proteins and <i>Borrelia</i> whole cell lysates..... | 74 |
| FIG 29. A control of fixed spirochetes via indirect immunofluorescence..... | 77 |
| FIG 30. Cell-surface (unfixed cells) localization via indirect immunofluorescence.. | 78 |
| FIG 31. Serum sensitivity assay results. | 80 |

CHAPTER I

Introduction

***Borrelia burgdorferi* background**

The causative agent of Lyme disease is a gram negative, microaerophilic, and cork-screw shaped (spirochete) bacterium called *Borrelia burgdorferi*. *B. burgdorferi* is uniquely transmitted by hard bodied ticks found in the genus *Ixodes* to wild reservoir predominantly mammalian hosts which include small mammals and birds. Humans and domestic animals such as canines are intermediate or incidental hosts for the spirochete and not thought to be a part of the larger enzootic cycle (1, 2). Upon successful transmission of the spirochete to non-reservoir hosts, Lyme disease results.

Lyme disease is a multi-organ system illness that may result in neurological, cardiac, dermatological, and rheumatic symptoms. The spirochete was first successfully isolated from an *Ixodes scapularis* (formerly *Ixodes dammini*) tick described in a publication in 1982 by William Burgdorfer et al. and proposed as the infectious agent of Lyme disease (3). Burgdorfer's proposal of a Lyme disease causing spirochete was later confirmed when similar spirochetes were recovered from patient samples afflicted with a disease consistent with Lyme arthritis in 1983 by Steere et al. (4). In 1984, the Lyme disease causing spirochete was officially characterized and named by Johnson et al. as *Borrelia burgdorferi* in honor of Burgdorfer's isolation of the bacterium (5).

Like other spirochetes, *B. burgdorferi* cells observe a helical shape and motility, with a protoplasmic cylinder complex that includes the cytoplasm, inner cell membrane, and peptidoglycan collectively which are surrounded by an outer membrane, and finally a

endoflagellum (6). The flagella of spirochetes such as *B. burgdorferi* and the syphilis causing agent, *Treponema pallidum*, are tucked into the periplasmic space just underneath the outer membrane (7). Cross-sections of cells viewed by electron microscopy reveal the presence of a varying number of axial filaments, also known as endoflagella, which correspond to the number of endoflagella present in a given cell (3). The structure of the endoflagella provide high motility to the spirochete allowing travel through viscous environments (8, 9). Figure 1 displays electron micrographs of the structure of the spirochete (10). Cell size varies from species to species of *Borrelia* and from cell to cell of a single species (7). In regards to *B. burgdorferi*, cell sizes (length) range from 10 μ m to 30 μ m when observed via dark-field microscopy (3). Spirochetes can also take the form of aggregates which are now thought to be biofilm formations due to unfavorable culture conditions (7, 11, 12). An image of typical spirochetes at mid-late logarithmic phase versus a formed aggregate is shown in figure 2.

Currently, the spirochete is categorized into a genospecies of 18 related *Borrelia* species called *B. burgdorferi* sensu lato (in the loose sense) complex which cause Lyme borreliosis (13). Of the 18 species, three are confirmed to cause the majority of Lyme disease cases in humans: *B. afzelii*, *B. garnii*, and *B. burgdorferi* sensu stricto (in the strict sense) (5, 14, 15). In the United States, *B. burgdorferi* sensu stricto is the predominant strain of Lyme disease and will be referred to as *B. burgdorferi* from this point forward. The other two species are the major causes of Lyme disease in Europe, but *B. burgdorferi* sensu stricto is present as well (14, 16).

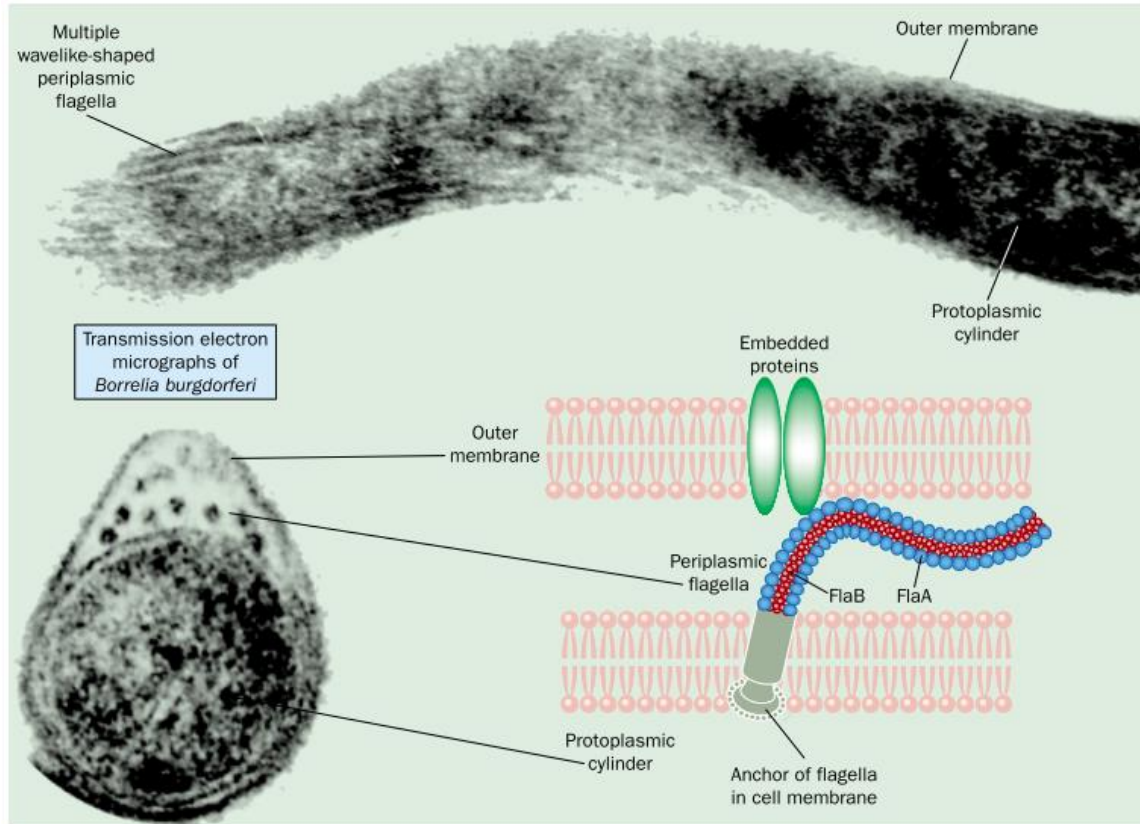


Figure 1. Ultrastructural morphology of *B burgdorferi* electron micrographs and schematic line drawings illustrate the structural morphology of *B burgdorferi*. The spirochetes consist of a protoplasmic cylinder covered by the cell membrane. A second outer membrane covers the periplasm containing the flagella. Flagella consist of two major proteins, flagellin A and flagellin B (FlaA and FlaB).

FIG 1. Structure of a spirochete. This image was obtained from a study by Singh et al. (10).

Cross section of a spirochete shows the presence of endoflagella located in the periplasm. These endoflagella wrap around the protocylinder of the cell and rotate around the cell body to provide a corkscrew like motility.

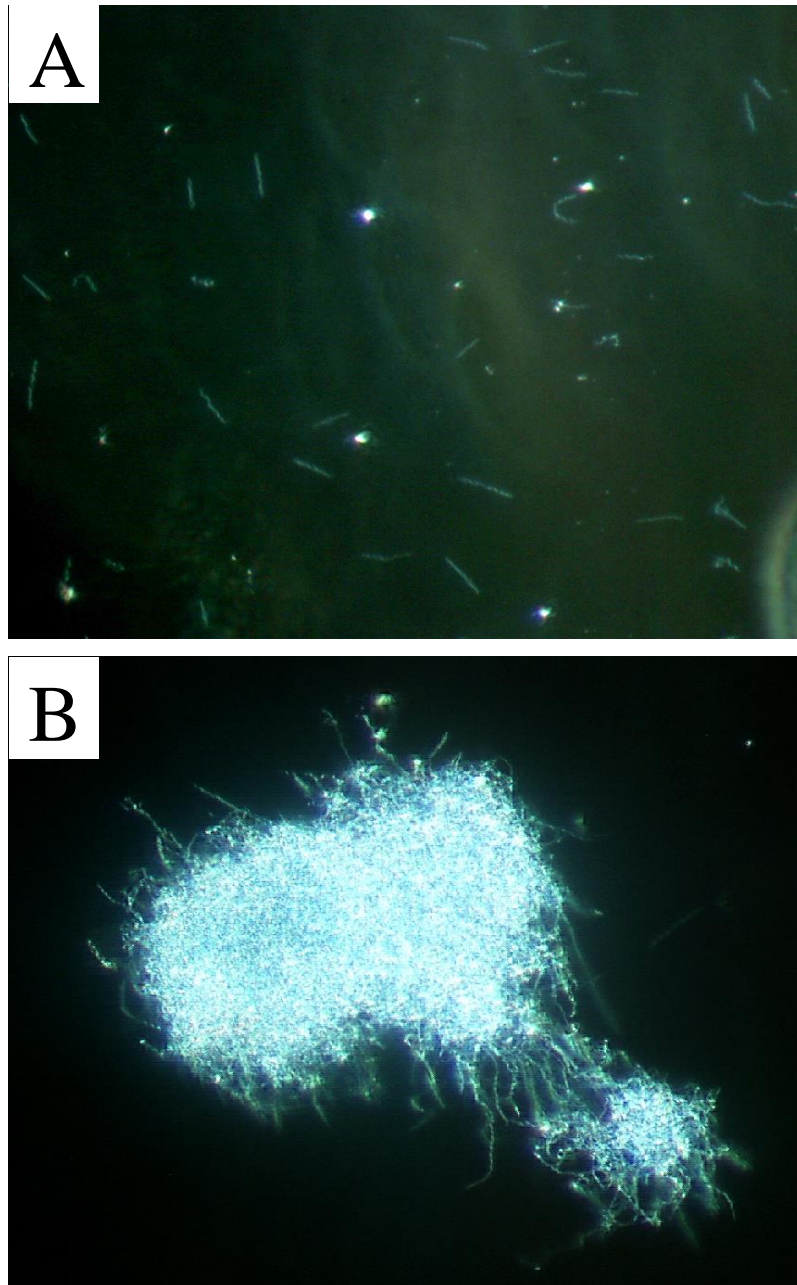


FIG 2. Image of *Borrelia burgdorferi* strain B31MI* grown *in vitro*. *Borrelia* are assessed by their motility for viability, and spirochetes are counted per field of view at 400x for density (A). Aggregate formation can be observed during *in vitro* cultivation (B). Images were taken at 400x total magnification by Nerina Jusufovic. *Strain B31MI is the virulent strain originally isolated by Burgdorfer et al. and is often used in *B. burgdorferi* research labs as the entire genome has been sequenced (3, 8, 17).

Laboratory cultivation of Borrelia burgdorferi

Cultivation of spirochetes *in vitro* requires a specialized medium called BSK-II (Barbour-Stoenner-Kelly-II) or the modified version BSK-H (Sigma Aldrich) supplemented with 6% heat inactivated rabbit serum (18). This is due to the absence of genes in *Borrelia* for anabolic reactions and thus requires the supplementation of animal serum (8). *Borrelia* spp. best grow at temperatures of 30-37°C under microaerophilic conditions (5, 18). Temperatures above 40°C inhibits growth completely even when temperatures are lowered according to Barbour (18). Growth does occur at ambient temperatures (23-24°C) but is slower requiring longer lengths of cultivation (19). Culture density and viability is assessed via dark-field microscopy as *Borrelia* do not grow well on solid media. Growth can also be identified through color change from red to yellow due to acidification of the media as BSK contains the pH indicator phenol red. Viability is based on observed motility in approximately 90-95% of the spirochetes on a wet mount slide (20, 21). When grown in the laboratory, researchers must be cautious about cultivation techniques as they can affect downstream experiments. This is due to two factors: 1) variation in the formulation of BSK media can affect the ability of different strains to grow optimally if at all, as well as affect gene regulation (20–24) and 2) *Borrelia* strains have been shown to spontaneously lose plasmids during *in vitro* cultivation which can alter the infectivity of the organism (25–27). Regarding the latter, this has been shown to occur as early as passages 5-10 for some plasmids. Also, strains are classified as high passage, low infectivity (passed more than 10 times) or low passage, high infectivity (passed no more than 5-10 times). All of these factors must be considered when working with *Borrelia burgdorferi* and studying aspects of its pathogenicity and genetics.

Lyme disease

The etiologic agent of Lyme disease, *Borrelia burgdorferi*, was not known until its isolation from an Ixodid tick by Burgdorfer in 1982 as mentioned previously (3). Manifestations of the disease such as the bull's eye rash, however, have been documented as early as 1909 (28). The syndrome known as Lyme disease was first detailed after a string of unusual child arthritis cases were investigated by rheumatologists and researchers as a new form of inflammatory arthritis in the town of Lyme, Connecticut in 1975. This is also where the name Lyme disease comes from (29). Lyme disease manifests in three stages in humans: early localized, early disseminated, and late or chronic infection (30, 31). The most prominent feature of early localized infection is the development of erythema chronicum migrans (ECM, bull's eye rash) at the site of the tick bite approximately 3-32 days after the bite which will expand over the course of the first few days up to 12 inches (32, 33). An example of a common ECM rash is shown in figure 3. This symptom, however, does not present in all patients but in roughly 70-80% of cases. Besides the rash, early localized infection can also present with flu-like symptoms including nausea, headache, stiff neck, fatigue, fever, chills, muscle and joint pain, and lymphadenopathy (30, 31, 33). Left untreated, the spirochetes will spread via the bloodstream to other organs leading to the second stage called early-disseminated Lyme disease.

Manifestations of early-disseminated Lyme disease occur days to months after the tick bite and include more neurological and cardiac symptoms as the spirochetes spread to the tissues. Neurological symptoms include stiff neck and headaches as before with addition of more severe manifestations such as facial palsy (drooping of face), dizziness or shortness of breath, nerve pain, loss of sensations and shooting pains in hands or feet, and short term memory issues (33). Figure 3 displays facial palsy. Lyme carditis includes symptoms of dizziness, shortness of breath,

chest pain, and heart palpitations. The result of such symptoms is referred to as heart or AV block (32–35). The last stage of the disease is the development of chronic arthritis characterized by extreme joint pain and swelling especially of large joints as well as extreme fatigue (32, 33). Prolonged exposure of the host immune system to spirochetes can result in a chronic Lyme disease state, which is the result of an autoimmune response not the presence of active spirochetes (10, 36). This autoimmune response might be due to the development of antibodies by Lyme arthritis patients to outer surface protein A of *B. burgdorferi* throughout infection, from immune responses to damage of host neuronal tissue, cross-reactivity to a *B. burgdorferi* antigen (molecular mimicry), or the presence of a superantigen (36).

Lyme borreliosis in canines does not exhibit all of the characteristics that occur in human illness. For example, canines do not develop the ECM rash or many of the early-localized symptoms seen in humans. Instead, symptoms appear in dogs only after the infection has already disseminated. In addition, many dogs remain asymptomatic but still seroconvert making the diagnosis of Lyme disease in dogs difficult (37). When dissemination does occur, symptoms include fever, lack of appetite and swollen lymph nodes (38). A common sign is lameness in limbs of where the tick bite occurred. While not definitively proven to be associated with *B. burgdorferi*, a serious complication observed in infected dogs is Lyme nephropathy. This complication can be fatal and is characterized by renal failure with symptoms such as dehydration, vomiting, anorexia, wasting, and polyuria (37, 38). Due to the high fatality rate of this complication, as well as the large number of dogs that present with no symptoms, finding new a vaccine that protect dogs from *B. burgdorferi* is warranted.



FIG 3. Erythema migrans rash of Lyme disease and facial palsy. ECM is commonly referred to as a bull's eye rash due to its appearance of having a target and is a symptom of early-localized Lyme disease. Early-disseminated Lyme disease produces neurological symptoms such as facial palsy which is drooping of one side of the face. These images were obtained from the CDC (33).

Treatment, prevention, and Lyme disease vaccines

Treatment of Lyme disease consists of taking antibiotics such as doxycycline, cefuroxime axetil, and amoxicillin over the course of 10-21 days (39). For humans and dogs, doxycycline is the preferred antibiotic of choice (37, 38). Treatment, if caught early, is usually successful in clearing the infection. Antibiotics are taken over the course of two months. Successful treatment however is dependent on how quickly the diagnosis is made. Another problem is the development of post-treatment Lyme disease syndrome or antibiotic refractory Lyme arthritis in some individuals (40). This is thought to result from an autoimmune response or from a persistent infection (36, 40). The syndrome involves the non-specific symptoms of Lyme disease such as joint pain, fatigue, and muscle aches that persist after antibiotic therapy (40). Prevention of Lyme disease outside of vaccines includes tick control, reservoir host management, and good hygiene measures to check for and remove ticks after outdoor activity in endemic areas (41, 42). Prompt removal of ticks can prevent transmission of *B. burgdorferi* as it takes about 24 hours for the transmission of the organism from the tick to the host (43).

Given the prevalence of *Borrelia burgdorferi* in the United States and Europe and the complications of Lyme disease after treatment, attempts have been made to make a vaccine for Lyme disease. The original Lyme disease vaccine designed, vetted, and then marketed in 1999 (41, 44, 45) was against the protein OspA (46, 47). OspA is involved in the survival of *B. burgdorferi* in the tick guts. The vaccine worked by blocking the transmission of *B. burgdorferi* by killing the spirochetes that migrated to the saliva where they would be exposed to antibodies of the host from the tick having obtained a blood meal (47). The efficacy of the recombinant OspA vaccine was 49% after one dose and 76% after three doses for symptomatic disease. For asymptomatic disease, the efficacy was 83% after one dose and 100% after three doses (48).

Even though the vaccine was effective, fear of autoimmune reactions from potential molecular mimicry of OspA, inability of the vaccine to protect against various strains, and low compliance with the required boosters, it experienced low sales and has been removed from the market (45). In 2011, Steere et al. determined that the rOspA vaccine did induce antibiotic-refractory Lyme arthritis in a mouse model (49). With the incidence of Lyme disease increasing rather than decreasing and expansion of the disease carrying ticks throughout the U.S., the continuation of a search for a vaccine is not only warranted but needed (50, 51). Despite waning public interest, researchers are continuing the study of *Borrelia burgdorferi* proteins as potential vaccine targets (45). As a side note, perhaps public perception will change, since the possibility of contracting Lyme disease could increase due to tick range expansion.

Currently, an OspA vaccine is still being used to prevent Lyme disease in dogs. There is debate on its use because of the variation in efficacy found by different trials and studies. Efficacy ranges from 50-85% and up to three doses are needed (37, 52). One hypothesis for the wide range of efficacy is considered a result of the well-known expression pattern of OspA. Basically, OspA is expressed well on the surface of spirochete within the tick, however, soon after the tick consumes a blood meal, the spirochetes significantly down regulate OspA protein expression (47). The down regulation of OspA in mammalian hosts limits the protective function of anti-OspA antibodies. Regardless, several of the same concerns with the human OspA vaccine exist with the canine vaccine; thus, many are divided on whether it should be administered (37). Further research of the Lyme disease spirochete, *B. burgdorferi*, is needed to reach a more complete understanding of the host-microbe dynamics and bring the medical and scientific communities closer to the production of a viable and safe vaccine against Lyme disease.

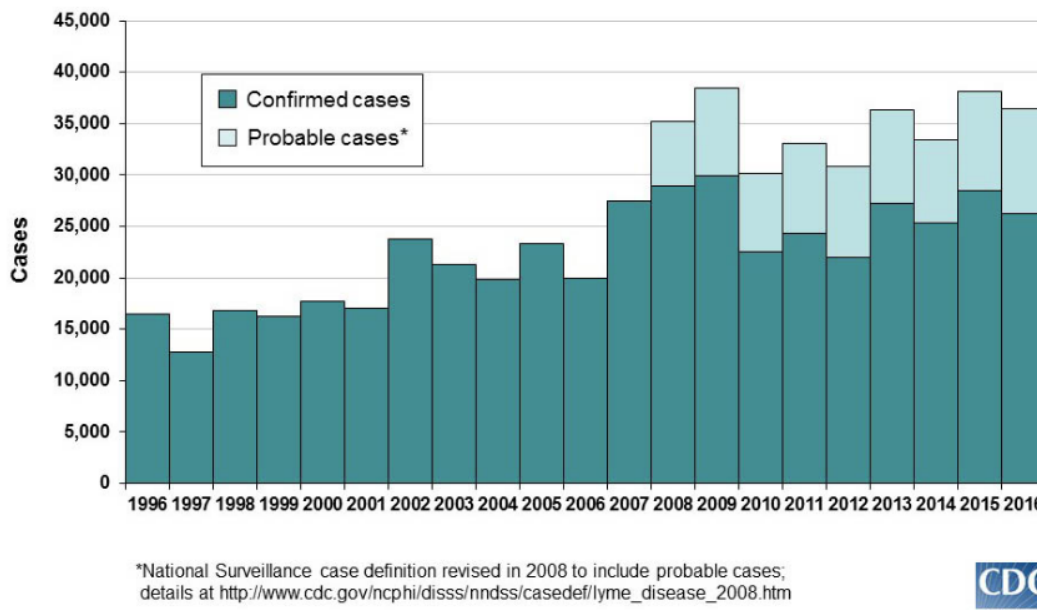
Lyme disease epidemiology and geographical distribution Ixodes scapularis

For the past decade, Lyme disease has consistently been the most prevalent tick borne illness in the United States and Europe, with cases steadily increasing year to year (53). Roughly 15,000 people were diagnosed as having Lyme disease in 1996. By 2015, the number of cases reported per year has doubled to ~35,000 per year. This trend is displayed in a chart from the CDC in figure 4. According to the CDC, an estimated 30,000 cases of Lyme disease are confirmed annually (54). The most recent surveillance data of Lyme disease were just published from 2008-2015 (35). In that time span, roughly 275,589 cases of Lyme disease were reported with 208,834 of those being confirmed while the rest were classified as probable cases (35). Figure 5 shows a map of the U.S. overlaid with the reported cases of Lyme disease for 2016.

Lyme disease transmission involves a complex enzootic cycle between tick and mammalian reservoirs as the hosts were first described in 1982 by Burgdorfer et al. (3). In the United states, two species of *Ixodes* ticks are the primary vectors of Lyme disease, *I. scapularis* and *I. pacificus*, while *I. ricinus* and *I. persulcatus* dominate Europe (55). The locality of Lyme disease is based on the geographical distribution of the ticks which itself is complicated by aspects of climate such as humidity levels and temperature. In addition, the geographic range of reservoir hosts such as white footed mice and incompetent host such as white-tailed deer that contribute to mating of the ticks (51, 55, 56). Due to the climate preferences of the species, *I. scapularis* is responsible for spreading Lyme in the Northeastern U.S. while *I. pacificus* is the culprit on the Western coast (55, 57). Studies have shown that increased numbers of deer and mice correlate to increased incidence of Lyme disease outbreaks (58, 59). Therefore, assessing the risk of Lyme disease involves surveillance of not only ticks, but the mammalian reservoirs and other hosts involved in keeping the enzootic life cycle going.

In 1998, Dennis et al. created the first definitions of reporting the presence and establishment of *Ixodes scapularis* and *pacificus* ticks in counties of the United States. Established counties had to present at least six ticks or two life stages of the tick during tick collection. The study generated a total of 2,120 county-specific records on the two tick species, and a map was generated showing the geographic distribution of the ticks in the United States by county from 1907-1996 (60). That map would not be updated for 16 years until Eisen et al. published their work in 2016 of a new map based on the criteria of the Dennis et al. study. The updated map displays data on established and reported *Ixodes* spp. in U.S. counties from 1907-2015 (51). The 1998 map shows ticks spanning the areas where Lyme disease has historically been localized, Northeastern U.S. and California. The 2015 map on the other hand, displays how the geographic range of the tick is expanding to Southeastern states as well as North-Central states such as Michigan, Wisconsin, and Minnesota. This coincides with the trend of increasing numbers of Lyme disease cases seen in neighboring states of those with traditionally high incidences (35). The 1998 and 2015 maps are shown in figure 6.

Reported Cases of Lyme Disease by Year, United States, 1996-2016



The graph displays the number of reported cases of Lyme disease from 1996 through 2016.

FIG 4. Lyme disease cases reported for the years 1996-2016 (53). Lyme disease cases consistently increase each year which is due to a multitude of factors such as expansion of the tick vector range and changes in climate (51).

Reported Cases of Lyme Disease -- United States, 2016

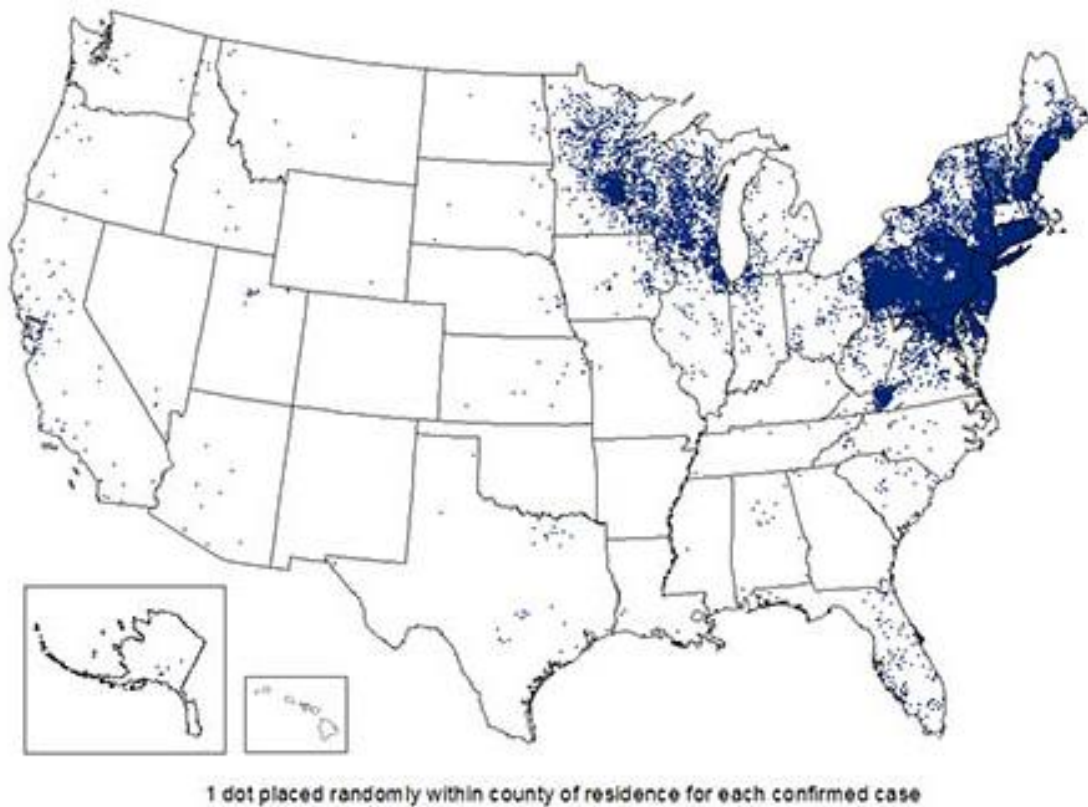


FIG 5. Cases of Lyme disease in the United States for 2016. The majority of Lyme disease cases are still concentrated to the Northeastern U.S., but more cases are starting to occur in other areas further south. This map was obtained from the CDC (53).

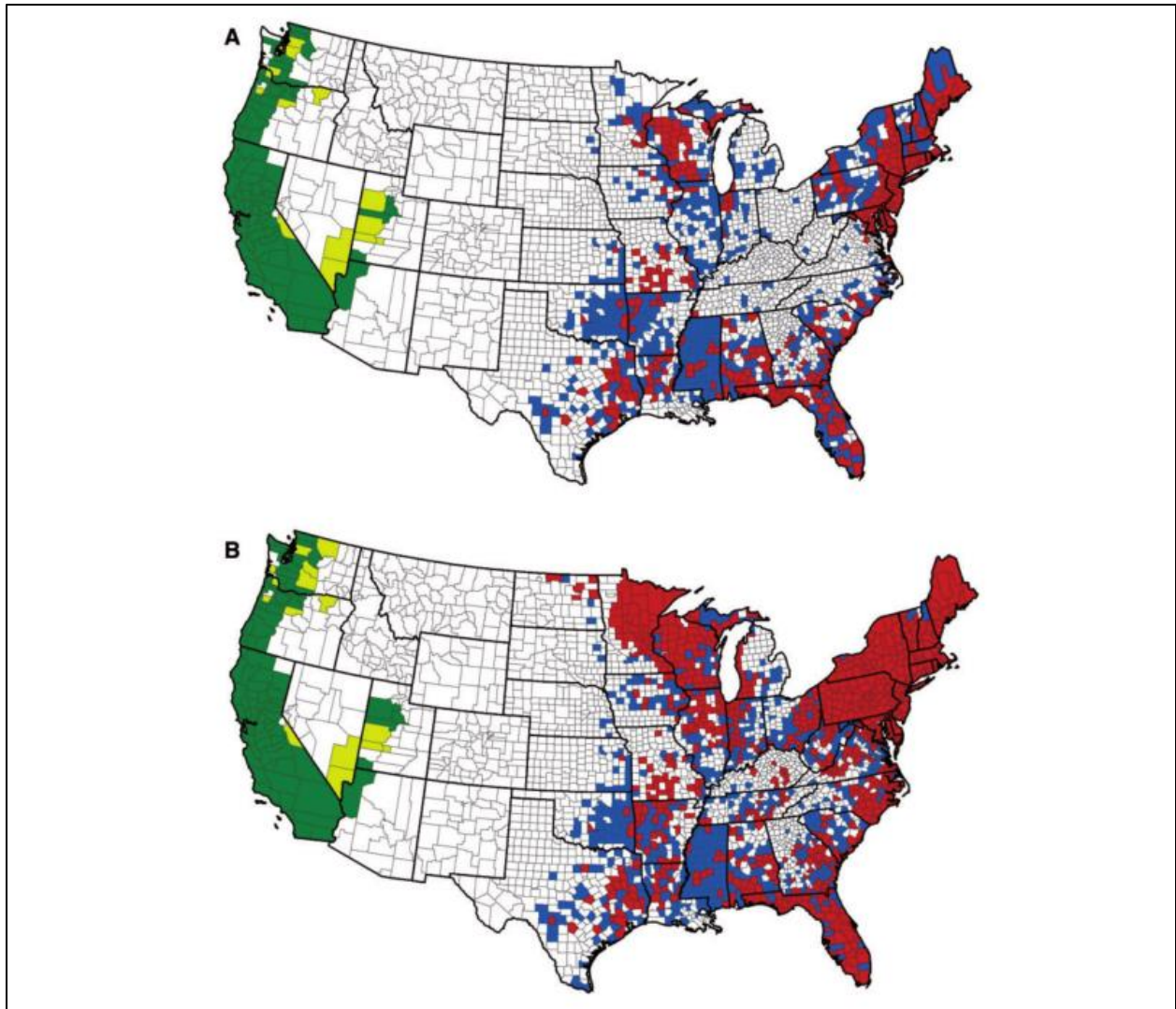


FIG 6. Distribution of *I. scapularis* and *I. pacificus* by county in the U.S. This figure is the geographic map displaying expansion range of *Ixodes* spp. by Eisen et al. (51). The top map (A) displays the 1998 map by Dennis et al. (60) while the bottom map (B) shows the updated version by Eisen et al. (51). Comparing the two maps, it is evident that the tick vector of Lyme disease is spreading to previously unestablished and reported regions of the U.S. As the tick expands its range, the chances of contracting Lyme disease might also increase.

Enzootic life cycle of B. burgdorferi

Ixodes scapularis has a two-year life cycle that occurs in three stages: larval, nymphal, and adult. Each stage requires a blood meal to keep the life cycle going (61). The enzootic life cycle of *B. burgdorferi* starts when uninfected *Ixodes* tick larva hatch from eggs and quest for a host to take a blood meal. Typically, larvae feed on birds and small rodents, like squirrels and the white-footed mouse, which are considered reservoir hosts for *B. burgdorferi* and subsequently these larvae become infected. The infected larva will molt into the nymph stage and must take another blood meal to continue the tick life cycle. Nymphs take blood meals from larger mammals such as the white-tailed deer and fox, as well as the same rodent reservoirs used by the larvae stage, and thereby these infected nymphs infect the mammalian hosts. The nymph stage is the first and main stage in the tick life cycle where the theoretically dead-end hosts such as humans and incidental hosts such as domestic animals (dogs) can be infected with spirochetes from infected nymphs when they take a blood meal (55, 61, 62). The ticks will molt once more from nymphs to adult ticks. The adult ticks can take blood meals from the same range of hosts as nymphal stage ticks. Unlike other tick-borne pathogens such as *Rickettsia rickettsii* and as noted by the description of the enzootic cycle above, *Borrelia burgdorferi* does not undergo transovarial transmission. This means that infected adult ticks will not pass *Borrelia burgdorferi* to their eggs. Ticks do remain infected throughout the entire molting process (63). The life cycle of *Ixodes* spp. is displayed in figure 7.

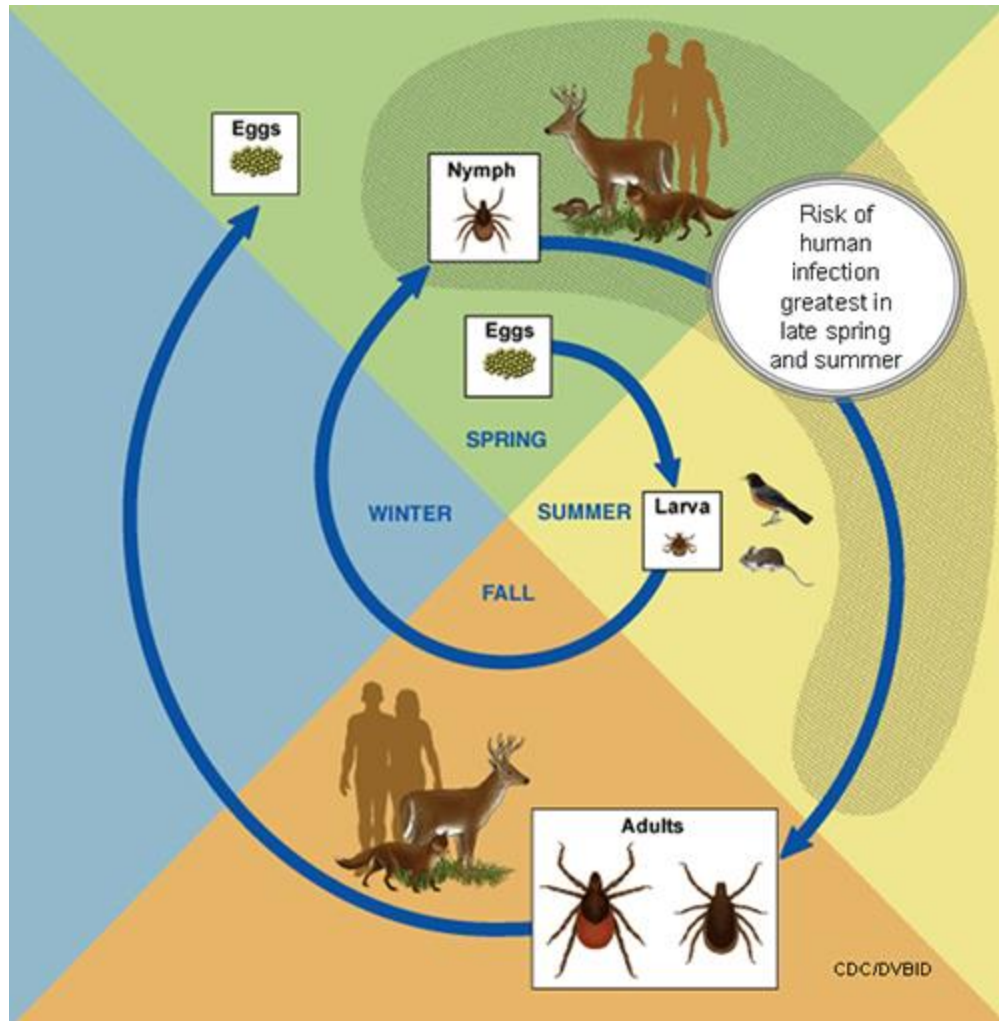


FIG 7. The life cycle of Lyme disease transmitting *Ixodes* ticks. *B. burgdorferi* does not undergo transovarial transmission meaning tick eggs are hatched Lyme free. Nymph and adult ticks are the primary transmitters of the disease to larger mammals while larva infect small reservoir hosts such as birds and rodents. The image was obtained from the CDC (64).

***Borrelia burgdorferi* genetics and immune evasion**

In 1997, the segmented genome of *Borrelia burgdorferi* strain B31MI was sequenced in part by Fraser et al. and concluded in 2000 by Casjens et al. (8, 17). *B. burgdorferi* is often considered to have one of the most elaborate genomes among prokaryotes consisting of a single linear chromosome, 12 linear plasmids, and 9 circular plasmids. The plasmids are named by a combination of whether they are linear (lp) or circular (cp) and by size in kilobase pairs (Kb). Figure 8 displays the genome of *B. burgdorferi*.

Some suggest that the complexity of the genome could be attributed to the many different hosts and therefore environments in which the spirochete must survive to maintain the enzootic cycle (8, 17, 19, 65–69). This theory is supported by data that reveals a survival reliance on several genes found on specific plasmids in specific environments during the enzootic life cycle. For example, the gene *ospA* which is located on lp54 is upregulated when spirochetes are present in the midgut of unfed ticks. When the spirochetes migrate from the gut to the salivary glands post feeding, *ospA* is downregulated while other genes such as *ospC* are upregulated. *OspA* is believed to be essential for the survival of the organism in the tick gut, while *OspC* is believed to be crucial for transmission from tick to mammalian host (47, 65, 70–72). Figure 9 shows a figure from Singh et al. showing the regulation of genes from tick to mammalian hosts by *B. burgdorferi* (10). This genetic control can be mimicked *in vitro* with some proteins such as *OspC*, which shows the same response to temperature changes that mimic the tick and mammalian host (19, 65). Others such as *OspA*, do not observe the same regulation with *in vitro* temperature shifts simulating tick and host environments.

Another important mechanism of survival in hosts by *B. burgdorferi* is a mechanism of genetic recombination by the variable major protein like sequence gene locus (*vlsE*) located on

linear plasmid 28-1 which encodes for a surface exposed protein that is 34 kilodalton (kDa). This protein allows antigenic variation of the spirochete's surface proteins during infection. The *vlsE* gene locus contains 15 silent cassettes and an expression site. The silent cassettes each have six variable regions and six conserved regions (73, 74). These variable regions are located on the surface exposed side of the membrane where contact with host immune responses will occur (75). The gene is downregulated during tick feeding and then upregulated during persistent vertebrate infection (76). It is believed that during mammalian infection, the *vlsE* locus alters the six variable regions with portions of the silent cassettes thus allowing the outer surface protein profile of the spirochete to change and evade the immune system of the host. This occurs throughout the duration of infection leaving the host one step behind (73, 74).

Unique for pathogenic bacteria, DNA sequencing also revealed that *B. burgdorferi* does not have an iron importing system suggesting it does not use iron and therefore it is not limited by host sequestering of iron (17). Other researchers have determined that *B. burgdorferi* replaces iron with manganese further contributing to the virulence of the organism (77).

A puzzling and challenging aspect of *Borrelia burgdorferi* genetics mentioned in the laboratory cultivation section, is its loss of plasmids and subsequently infectivity when cultured *in vitro*. This anomaly was first observed by Schwan et al. when proteins bands were missing on SDS-PAGE gels from cultures upon continual passage *in vitro* (26). In addition, the cultured strains lost infectivity in mice when studies were undertaken to characterize proteins involved in infectivity of the bacterium. It was noted that after 5-15 passages, certain plasmids were lost in culture. This sparked the notion that certain genes on plasmids were primarily involved in virulence of *Borrelia burgdorferi* while the main linear chromosome largely consists of housekeeping genes (26). Figure 8 shows a total of 23 plasmids rather than 21 plasmids. Studies

have hypothesized that the original *B. burgdorferi* B31MI isolate contained a total of 23 plasmids, but two cp32 variants, cp32-2 and cp32-5, were lost during propagation *in vitro* (8, 17, 78–81). B31MI is infectious, so therefore it is believed these circular plasmids are not needed for infectivity of the strain (17, 78, 79). Other studies have confirmed this loss of plasmids during *in vitro* cultivation results in a loss of infectivity (25, 27, 82). The loss of infectivity due to plasmid loss of *Borrelia burgdorferi* has also spawned the notion that key plasmids are involved in the maintenance and persistence of the organism in each mammalian species that can serve as a host. Work investigating this phenomenon has postulated that perhaps plasmid retention is correlated to host environments (82).

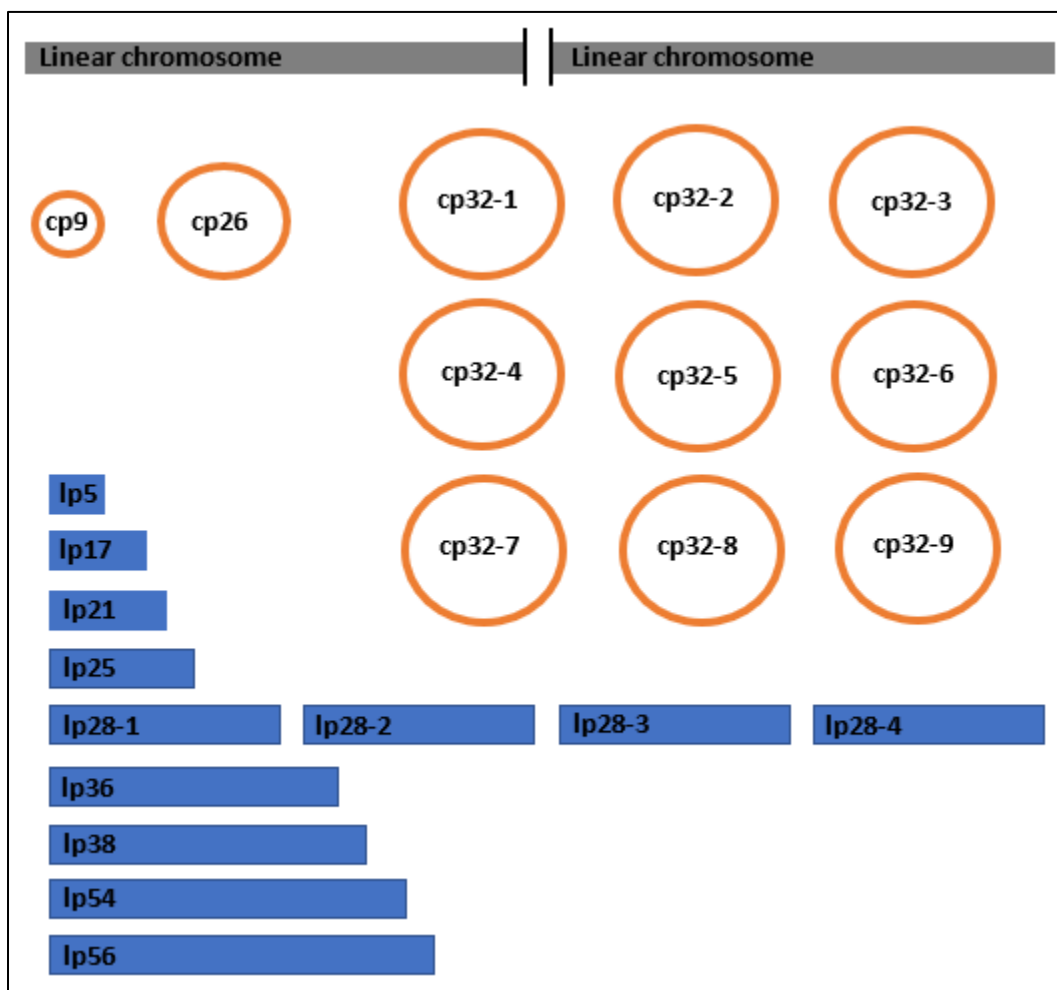


FIG 8. The segmented genome of *B. burgdorferi*. The genome contains a linear chromosome and 21 circular (cp) and linear (lp) plasmids. Strains of *B. burgdorferi* contain a varying number of cp32 copies at a time, but six to seven copies are present typically (8, 17, 78–81). Figure was adapted from reference (81).

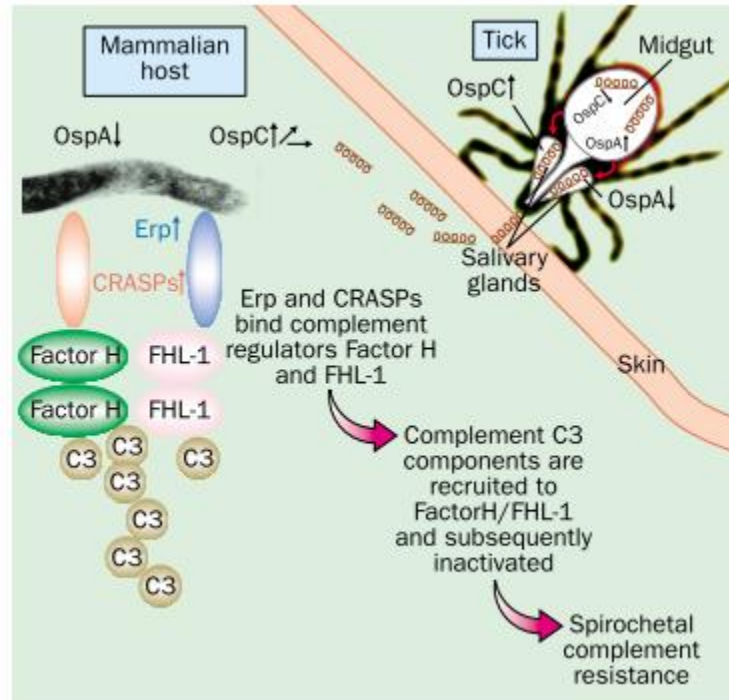


FIG 9. Regulation of gene expression in *B. burgdorferi*. This image was obtained from a study by Singh et al. (10). Certain genes are up or down regulated dependent on host environment. Of note is the down-regulation of OspA within the tick midgut while the upregulation of OspC occurs after entering the mammalian host.

Complement Regulator Acquiring Surface Proteins (CRASPS)

B. burgdorferi must evade a major factor of the mammalian host immune system known as the alternate pathway of the complement cascade. An important family of proteins responsible for activating this pathway is the Factor H family of proteins such as Complement Regulator Factor H (CFH) and Factor H-Like Protein 1 (CFHL). The action of CFH and CFHL is to regulate the complement pathway through interaction with complement cascade related proteins such as complement component 3b (C3b). C3b will bind to the surface of pathogens and then recruit factor B to promote the cleavage of many C3 molecules which results in opsonization and destruction of the target cell. To prevent the harm of self-cells and promote destruction of pathogens, Factor H proteins recognize glycosaminoglycans of self-cells and prevent factor B binding to C3b or promote C3 protein dissociation from the cell (83, 84).

To evade the complement cascade, many pathogens including *B. burgdorferi* have several proteins that interact with the aforementioned Factor H proteins to regulate activation of the alternative complement cascade (85, 86). Those proteins are collectively called CRASPS, Complement Regulator Acquiring Surface Proteins. By using CRASPs to bind negative regulators of complement like CFH and CFHL, *B. burgdorferi* essentially uses these proteins as a shield to prevent complement attack such as the formation of the membrane attack complex. Figure 10 displays the binding mechanisms of the CRASP proteins in complement evasion from a review by de Taeye et al. (84).

To date, five CRASP proteins have been identified: CspA (BbCRASP-1), CspZ (BbCRASP-2), ErpP (BbCRASP-3), ErpC (BbCRASP-4), and ErpA (BbCRASP-5) (85). The Erp proteins are also collectively referred to as OspE in the literature. Table 1 displays features of the CRASP proteins.

Of the five CRASPS, only CspA and CspZ bind both CFH and CFHL (87). Studies with CspA and CspZ have shown that the two proteins are involved in different parts of the transmission cycle of Lyme disease. The *cspA* gene has been found to be expressed at high levels in the midguts of unfed nymphs, during feeding, and then subsequently dropped off after established mammalian infection (88). The *cspZ* gene, however, was found to be expressed at high levels during established disseminated mammalian infection (89, 88). No expression was observed during the tick phases (88). As *cspA* is downregulated, *cspZ* is upregulated. It is suggested that CspA is involved in overcoming the host immune response during transmission, while CspZ helps to maintain resistance to the host complement system during established mammalian infection.

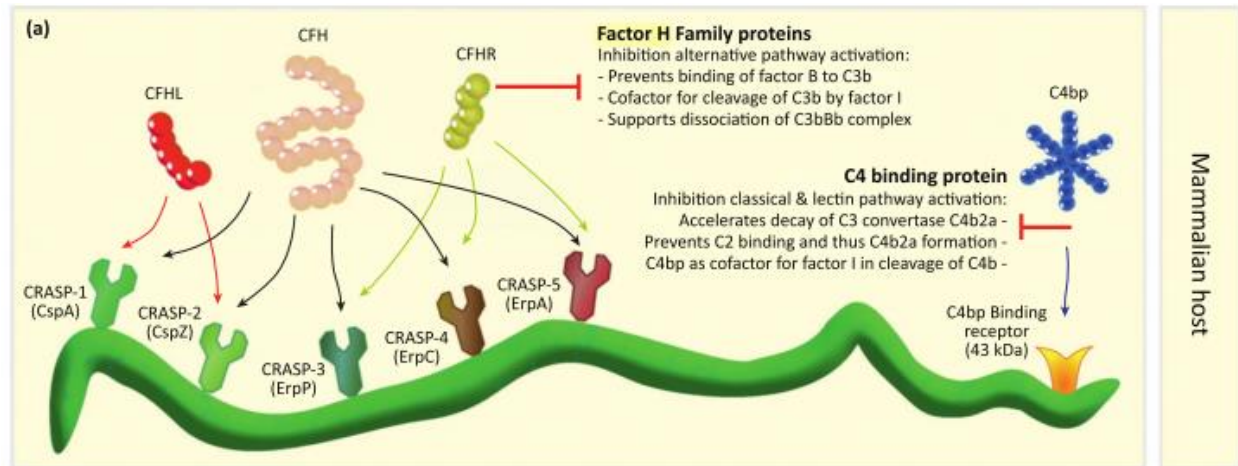


FIG 10. Molecular mechanisms that contribute to complement evasion by *Borrelia*. This image was obtained from a study by de Taeye et al. (84). Of note, CspZ binds to CFHL or CFH and thereby uses those host proteins to inhibit factor B and further downstream activation of the complement cascade.

Table 1. CRASP family features.

| Protein designation | Gene name | Gene Localization | Binding Capability | Reference |
|---------------------|-------------|-------------------|-------------------------|--|
| CspA (BbCRASP-1) | <i>cspA</i> | lp54 | FH, FHL-1 | Kraiczy et al. (90) |
| CspZ (BbCRASP-2) | <i>cspZ</i> | lp28-3 | FH, FHL-1 | Hartmann et al. (89) |
| ErpP (BbCRASP-3) | <i>erpP</i> | cp32-9 | FH, FHR-1, FHR-2, FHR-5 | Kraiczy et al. (91), Haupt et al. (92), Siegal et al. (93) |
| ErpC (BbCRASP-4) | <i>erpC</i> | cp32-2 | FH, FHR-1, FHR-2, FHR-5 | Hammerschmidt et al. (94) |
| ErpA (BbCRASP-5) | <i>erpA</i> | cp32-1 | FH, FHR-1, FHR-2, FHR-5 | Kraiczy et al. (91), Haupt et al. (92) |

a. Gene localization is based on sequencing data of strain B31 (8, 17).

b. Binding capability includes denatured and native CRASP binding.

c. Table was adapted from reference (89).

NA, not available; lp, linear plasmid; cp, circular plasmid; FH, Factor H; FHL-1, Factor H-like protein-1; FHR, Factor H-related proteins.

CspZ as a potential canine vaccinogen

Some criteria that makes a protein an efficacious vaccine target include:

1. The antigen is located on the surface of *Borrelia burgdorferi*, since it is an extracellular pathogen.
2. Conservation of the antigen is observed across different species and strains of *Borrelia* that cause Lyme disease.
3. The antigen is involved in both stages of the enzootic life cycle, tick and mammal.

CspZ is thought to be cell-surface localized, but studies using differing approaches have had mixed results. Surface exposed proteins should be sensitive to protease treatment such as proteinase K. Studies by Hartmann et al. and Coleman et al. revealed that CspZ is resistant to proteinase K and trypsin cleavage suggesting it is not cell surface localized (89, 95). When indirect immunofluorescence was performed on intact spirochetes, however, CspZ was observed to be expressed in a spotted pattern on the cell surface (89, 88). Other outer surface proteins have shown resistance to protease treatment as well, thus, CspZ cleavage sites are likely blocked due to the way the protein anchors to the membrane (96). Studies by Hartmann et al. and Kraiczky et al. have shown that *cspZ* sequences are highly conserved across genospecies, while Rogers et al. showed sequence divergence at the interspecies level (89, 97, 98). Furthermore, immune responses to *B. burgdorferi* antigens also have variation within species which was observed in a study by Baum et al. The study utilized a protein microarray to determine which antigens resulted in a universal immune response among experimentally infected beagle dogs. Pixel intensities from the arrays were calculated and revealed several proteins that the dogs showed a consistent immune responses to including CspZ (99). CspZ, however, is not involved in both stages of the life cycle. CspZ has been shown to be highly expressed during established

mammalian infection but not in the tick based on murine infection models and *cspZ* transcript levels during the tick stages of the enzootic cycle (89, 88). Strong humoral immune responses are produced against CspZ during murine and human infections with *B. burgdorferi* as determined by serological analyses with infected animal or patient serum (89, 97).

In a gene knockout experiment by Brooks et al., it was shown that mutants lacking CspA (BbCRASP-1) were killed when exposed to human serum, while non-mutants were resistant to killing by the host's immune response (100). Following the same theory, similar experiments were done to evaluate if CspZ has similar effects in a canine system. In a thesis done by Kay, a serum resistant strain *B. burgdorferi* B31MI was serially passed *in vitro* into culture medium incubated with different host animal sera. It was discovered that linear plasmid 28-3 (lp28-3) which harbors the *cspZ* gene was always retained in canine hosts (101). CspZ (also referred to as BbCRASP-2 in the literature) has been shown in the thesis done by Takalo-Lund to be required for survival in a canine host. Continuing with the insights gained in the Kay study, the Lund study experimented with *B. burgdorferi* clone F (Bb31cF) which harbors only 8 plasmids needed for basal survival and lacks lp28-3 and therefore the *cspZ* gene. When Bb31cF was exposed to canine serum, the spirochetes were undetectable and could not survive exposure. Bb31cF was then electroporated with a recombinant plasmid re-introducing the *cspZ* gene into the mutant denoted as cF:pBSV2*cspZ*. Upon exposure to canine sera, cF:pBSV2*cspZ* regained serum resistance and survived (102). Therefore, CspZ is likely necessary for *B. burgdorferi* to survive the canine immune system and persist in a canine host. Based on the observations from the Kay and Lund studies, it is hypothesized that CspZ is an immunological determinant in canine infection therefore making it a novel target vaccine candidate. Taking the above information collectively, CspZ has several characteristics of a potential vaccine target.

Objective

The ultimate goals of this study were to determine if CspZ is the necessary and minimally essential CRASP of *B. burgdorferi* required for survival in a canine host, and if it can be used to develop a new vaccine against Lyme disease in canines. To evaluate these goals, an expression vector was designed to allow for the purification of CspZ, OspA, and FlaB (the latter two served as controls) to allow for further studying of the proteins. Antibodies generated against the proteins allowed for immunoblot analyses to be performed to examine the expression levels of CspZ in different host environments, as well as to determine if CspZ is a cell surface localized protein via indirect immunofluorescence. Lastly, a serum sensitivity assay was performed to evaluate the necessity of CspZ to spirochete survival in a canine host using a mutant strain of *B. burgdorferi* which lacks CspZ, B31cF, and B31MI which contains all 21 linear plasmids.

From these goals, a few hypotheses and predictions were made:

1. If CspZ is up-regulated during mammalian infection, then western blot analyses will show up-regulation of CspZ in mimicked mammalian environmental conditions.
2. If CspZ is a cell surface localized protein, then indirect immunofluorescence with antibodies against CspZ will produce fluorescence on the outer surface of intact *B. burgdorferi*.
3. If CspZ is required for *B. burgdorferi* survival in a canine host, then mutant *B. burgdorferi* strain B31cF lacking CspZ will die in the presence of dog serum while the infectious strain B31MI expressing CspZ will survive.

If the hypotheses are accepted, CspZ could be a reasonable vaccine target against Lyme disease in dogs.

CHAPTER II

Methods

Bacterial strains and culture conditions

Borrelia burgdorferi strains used in this study include the wild-type strain B31M1 (B31) and clonal mutant B31cF. *B. burgdorferi* B31 is an infectious strain which harbors all 21 plasmids and is resistant to complement mediated killing. The clonal mutant B31cF contains only 8 plasmids required for maintenance and does not contain lp28-3 which carries the gene for *cspZ*. Spirochetes were cultivated in modified Barbour-Stoenner-Kelly (BSK-H) (Sigma-Aldrich, St. Louis, MO) complete (contains 6% rabbit serum) growth medium. Spirochetes were initially inoculated from frozen glycerol stocks and grown to mid-logarithmic phase ($1-5 \times 10^7$ spirochetes/ml) at 34°C unless otherwise noted. Cultures were monitored and enumerated every 24 or 48 hours via dark field microscopy. Briefly, 10ul of non-diluted or a 1:5 dilution of culture was placed on a clean microscope slide and covered with a 18x18mm coverslip. Subsequently, 10-20 microscopic fields were counted at 400x magnification and an average was taken. The average was then multiplied by a constant of 2.5×10^5 to determine the concentration of spirochetes/ml of culture (20). Viability of cultures was assessed by motility of the spirochetes. A 1:1000 dilution of culture was passed once mid-logarithmic phase was achieved into fresh BSK-H supplemented with 6% rabbit serum in a 15mL conical tube.

For temperature shift experiments, *Borrelia* strains were grown at 34°C to mid logarithmic density before passage to 23°C. Once cultures reached mid logarithmic phase at 23°C, they were then temperature shifted from 23°C to 34°C and allowed to reach mid logarithmic density. Spirochetes were also host-adapted by temperature shifting into 20% dog

serum and allowed to reach mid logarithmic density. A previous study by Tokarz et al. showed that culturing of spirochetes in whole blood and incubating them at tick temperature resulted in the increase of gene expression for tick related proteins (103). The same rational is applied here to increase protein expression of mammalian related proteins such as CspZ by temperature shifting them into media containing dog serum at 34°C. All media were calibrated to the appropriate temperature before passage. All *Borrelia* strains were screened for plasmid content by PCR before protein studies were performed to confirm the proper retention of plasmids for each strain.

Strains of *Escherichia coli* used in cloning experiments were DH5 α for plasmid maintenance and BL21 DE3 (New England Biolabs, Ipswich, MA) for protein expression except where otherwise noted. All *E. coli* cell lines were cultivated in either Luria-Bertani (LB) media or 2x-YT media. Media was supplemented with ampicillin to a final concentration of 100ug/ml for the selection of clones harboring plasmid constructs.

Designing of pGEX:recombinant protein constructs (pGEX:rProteins)

Primers were designed to isolate the *cspZ* (gene of interest), *ospA* (positive outer surface control), and full-length *flaB* (negative outer surface control) genes from the genome of *B. burgdorferi* B31MI using the NCBI nucleotide database and BLAST (Basic Local Alignment Search Tool) (National Center for Biotechnology Information, Bethesda, MD) to analyze gene and genome sequences. Primers directly targeting the *cspZ* gene resulted in non-specific binding to other parts of the genome, and therefore primers targeting a flanking region approximately 100bp upstream and downstream of the *cspZ* gene (outer *cspZ*) that did not produce multiple amplicons were created. Nested primers (inner *cspZ*) targeting the *cspZ* gene sequence within the flanked regions were then used on amplicons generated from the outer *cspZ* primers via nested PCR. Primers for *cspZ*, *ospA*, and *flaB* were designed for in frame cloning into the plasmid expression vector pGEX 4T-3 (GE Healthcare Life Sciences, Pittsburgh, PA) by the inclusion of 5' BamHI and 3' XhoI restriction sites.

Primers for *cspZ* and *ospA* were designed to exclude the signal peptides resulting in mature protein products denoted as truncated *cspZ* (*tcspZ*) and *ospA* (*tospA*). Nucleotide sequences were translated to protein sequences utilizing the ExPASy Translate Tool (Swiss Institute of Bioinformatics, Lausanne, Switzerland). Hydrophobicity plots shown in figure 11 were generated utilizing the ExPASy ProtScale program (Swiss Institute of Bioinformatics, Lausanne, Switzerland) based on the Kyte and Doolittle method (104) with a window size of 7 to analyze the peptide sequence.

Table 2. Oligonucleotides used for traditional PCR and cloning

| Primer Name | Primer Sequence (5' → 3') ^a | Description | Size |
|-------------------------------------|--|--|---------|
| outer <i>cspZ</i> F (3020-2996) | GCGTCTAGAA CTTGTGCTA | Amplification of a flanking region of DNA 83bp upstream and 92bp downstream from the <i>cspZ</i> gene from B31MI genome that will produce nonspecific binding. | 852bp |
| outer <i>cspZ</i> R (2168-2192) | GAGGCTATGAATCTC GCGGCATGCC AAAAGAGA AGTATGCAAAGTATGC | | |
| inner <i>tcspZ</i> F (2913-2890) | GATGTTAGTAGATTAAATCA | Amplification of the <i>tcspZ</i> gene without restriction enzyme sites attached. | 654bp |
| inner <i>tcspZ</i> R (2260-2285) | GAGA CTATAATAAAGTTTGCTTAA TAGCTT | | |
| <i>tcspZ</i> F (2913-2890) | GCGGGATCC GATGTTAGTA | Used to amplify the <i>cspZ</i> gene excluding the signal peptide sequence with nested PCR of the amplified region produced from the outer <i>cspZ</i> primers. | 671bp |
| <i>tcspZ</i> R (2260-2285) | GATTAAATCAGAGA GCGCTCGAG CTATAATAAAA GTTTGCTTAATAGCTT | | |
| <i>tospA</i> F (9505-9528) | GCGGGATCC TGTAAGCAAAA | Used to amplify the <i>ospA</i> gene excluding the signal peptide sequence from the B31MI genome. | 788bp |
| <i>tospA</i> R (10275-10251) | ATGTTAGCAGCCTT GCGCTCGAG TTTTAAAGCG TTTTTAATTCATCA | | |
| <i>flaB</i> F (148653-148625) | GCGGGATCC ATCAATCATA | Used to amplify the full-length <i>flaB</i> gene from the B31MI genome. | 1,022bp |
| <i>flaB</i> R (147649-147676) | ATACATCAGCTATTAATGC GCGCTCGAG TTATCTAAGC AATGACAAAACATATTGG | | |
| <i>tflaB</i> F (148167-148153) | GCGGGATCC CTCAGGGTCTC | Used to amplify an immunodominant region of the <i>flaB</i> gene from the recombinant plasmid pGEX: <i>flaB</i> to produce a soluble GST fusion protein for purification. | 346bp |
| <i>tflaB</i> R (147839-147855) | AAGCG GCGCTCGAG TCTATTTTGG AAAGC | | |
| pGEX (MCS) F | GGGCTGGCAAGCCACGTTT | Vector backbone specific primers recognizing the multiple cloning site of the expression vector pGEX-4-T3. | 171bp |
| pGEX (MCS) R | GGTG CCGGGAGCTGCATGTGTCA GAGG | | |
| <i>tcspZ</i> F (2913-2890) | GCGGGATCC GATGTTAGTA | Orientation specific primers used to screen <i>E. coli</i> transformants for the presence and proper orientation of the <i>tcspZ</i> gene after transformation. | 742bp |
| pGEX (MCS) R | GATTAAATCAGAGA CCGGGAGCTGCATGTGTCA GAGG | | |
| pGEX (MCS) F | GGGCTGGCAAGCCACGTTT | Orientation specific primers used to screen <i>E. coli</i> transformants for the presence and proper orientation of the <i>tospA</i> gene after transformation. | 855bp |
| <i>tospA</i> R (10275-10251) | GGTG GCGCTCGAG TTTTAAAGCG TTTTTAATTCATCA | | |
| pGEX (MCS) F | GGGCTGGCAAGCCACGTTT | Orientation specific primers used to screen <i>E. coli</i> transformants for the presence and proper orientation of the <i>flaB</i> gene after transformation. | 1,089bp |
| <i>flaB</i> R (147649-147676) | GGTG GCGCTCGAG TTATCTAAGC AATGACAAAACATATTGG | | |
| <i>tflaB</i> F (148167-148153) | GCGGGATCC CTCAGGGTCTC | Orientation specific primers used to screen <i>E. coli</i> transformants for the presence and proper orientation of an immunodominant region of the <i>flaB</i> gene after transformation. | 434bp |
| pGEX (MCS) R | AAGCG CCGGGAGCTGCATGTGTCA GAGG | | |

^a Bolded and underlined nucleotides indicate restriction enzyme sites.

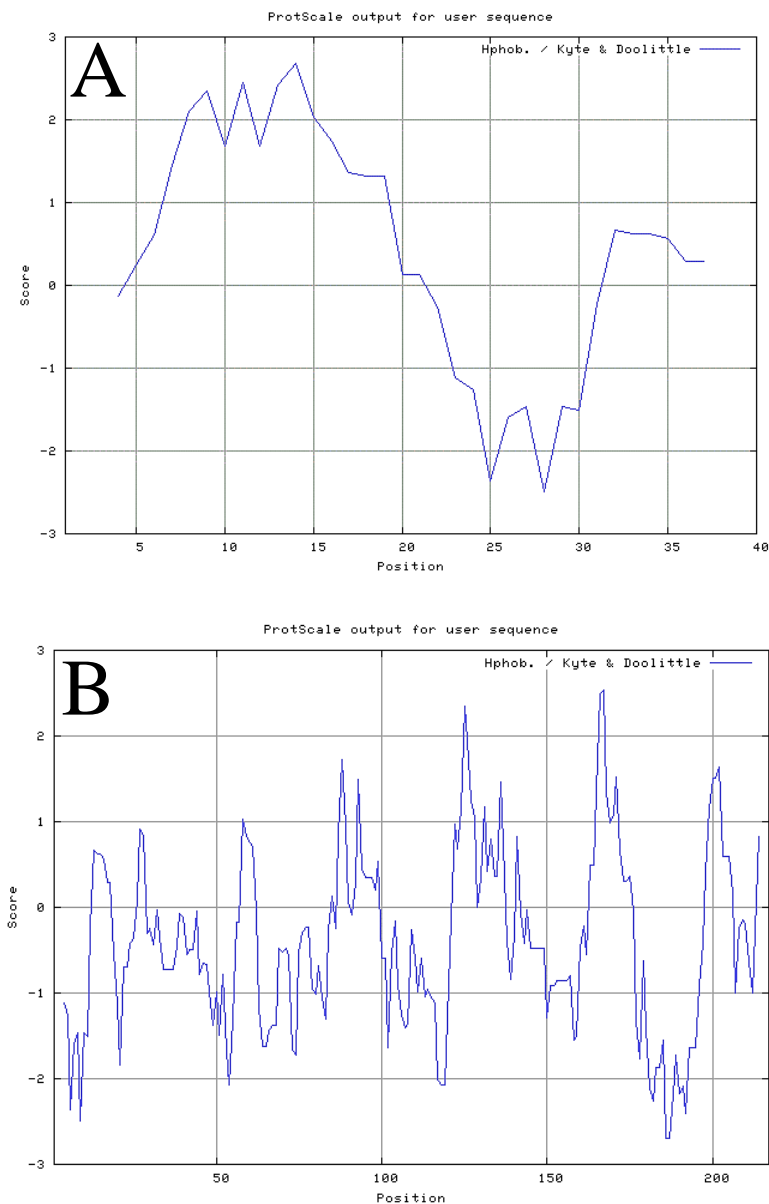


FIG 11. Hydrophobicity plots. Plots were analyzed to determine the signal peptide location of each protein. Hydrophobicity plot of the first 40 amino acids of the full length CspZ protein (A). A hydrophobic region is indicated at the N terminal region of the protein from around amino acid 1 to 20. Hydrophobicity plot of the truncated CspZ protein after amino acids 1 through 19 have been excluded (B). The hydrophobic region is no longer present at the N terminus of the protein. The forward primer was designed to exclude the 57 nucleotides corresponding to amino acids 1-19 of the protein.

Cloning

DNA was isolated from *B. burgdorferi* B31MI by lysing the bacteria via boiling. Spirochetes were grown to moderate density and harvested by centrifugation at maximum speed in a microcentrifuge. The spirochetes were then resuspended in 100ul of molecular grade water and boiled for 5 minutes. Using the primers listed in Table 1, *cspZ*, *ospA*, and the full-length *flaB* gene were PCR amplified, and the reactions subsequently cleaned up using the Wizard® SV Gel and PCR Clean-UP System (Promega, Madison, WI) for future restriction enzyme digestion and ligation into an expression vector plasmid. The expression plasmid vector pGEX-4T-3 was propagated in *E. coli* DH5α and plasmid DNA was isolated with a Plasmid PureYield™ Miniprep System (Promega, Madison, WI). All DNA was quantified utilizing a Nanodrop ND-1000 spectrophotometer and stored at -20°C until further use. Restriction enzyme digestion was performed on the inserts and vector with BamHI and XhoI (Promega, Madison, WI) restriction enzymes. Digests were incubated at 37°C and monitored via gel electrophoresis until an optimum incubation time was determined. The reactions were inactivated by incubation at 70°C for 15 min and cleaned up with a Wizard® SV Gel and PCR Clean-UP System. Following restriction enzyme digestion, the cleaned DNA of the genes of interest were ligated into the BamHI and XhoI sites of the cut pGEX 4T-3 vector utilizing T4 DNA ligase (Promega, Madison, WI) with an insert to vector ratio of 1:3. For cloning, one microliter of each ligation reaction was then electroporated into *E. coli* DH5α for plasmid maintenance. Clones positive for the recombinant plasmids pGEX:*tcspZ*, pGEX:*tospA*, and pGEX:*flaB* were determined utilizing colony PCR with backbone specific and orientation specific primers (Table 1) as well as restriction enzyme analysis. The resulting constructs contain the genes of interest fused to

Glutathione-S-Transferase (GST), an N-terminal fusion protein tag, to allow for future protein purification. The cloning schematic is depicted in figure 12.

Positive colonies were inoculated into LB media overnight at 37°C for subsequent plasmid DNA isolation, and the generation of glycerol stocks of the recombinant plasmids in DH5 α for future experimentation. Approximately, 75ng of plasmid DNA from five positive pGEX:*tspZ* clones were sent to the sequencing facility at Yale University to verify insert orientation and reveal any mutations. The constructs pGEX:*tospA* and pGEX:*flaB* were not sent off for sequencing.

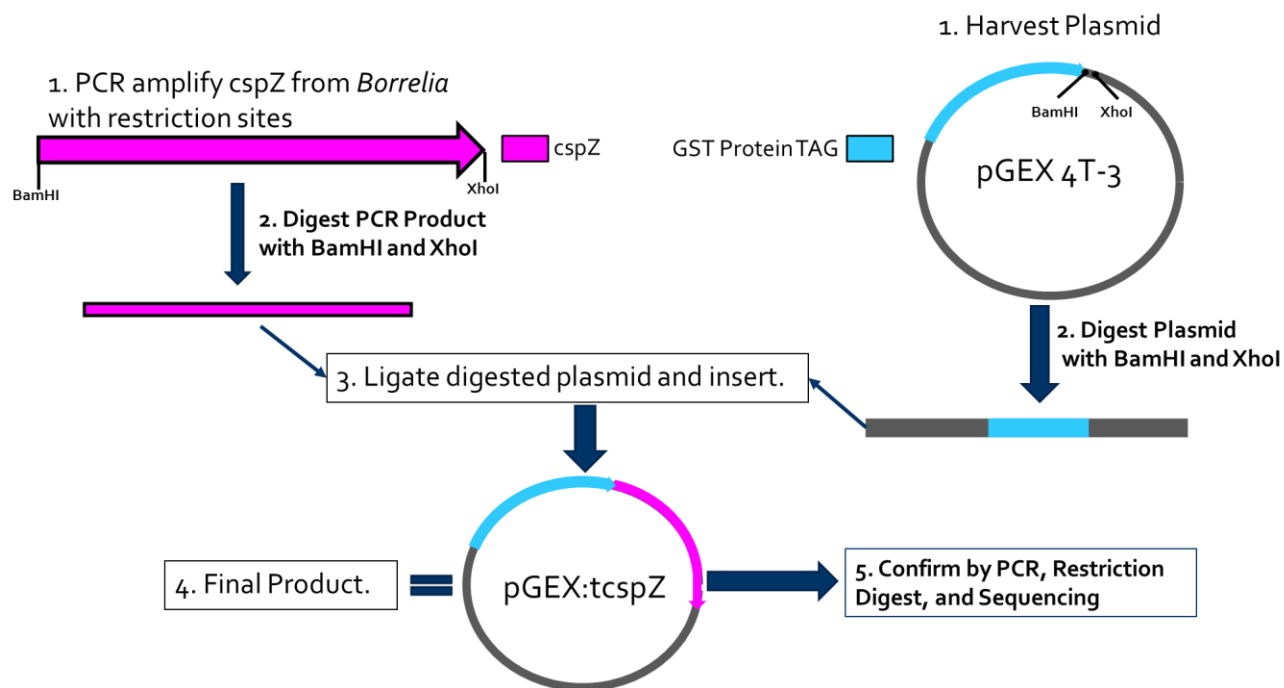


FIG 12. Cloning schematic of the creation of the recombinant plasmids. The process of creating the recombinant plasmid pGEX:tcspZ is shown above. BamHI and XhoI restriction sites were designed into primers used to amplify the genes of interest to allow for cloning into the pGEX 4T-3 expression vector. The same process shown above was followed to generate pGEX:tospA, and pGEX:flaB.

Protein expression and purification of recombinant proteins

For protein expression experiments, proteins were either expressed in the *E. coli* DH5 α strain or *E. coli* BL21 DE3 strain (New England Biolabs, Ipswich, MA). In the case of the latter, BL21 DE3 cells were chemically transformed following manufacturer protocol (NEB) with the respective recombinant plasmid DNA. Positive clones for pGEX:*tcspZ*, pGEX:*tospA*, and pGEX:*flaB* were confirmed with methods previously mentioned. Optimal protein expression conditions such as concentration of isopropyl β -D-thiogalactoside (IPTG) (Promega), medium of growth, length of induction, and temperature of induction were determined empirically with small scale trials for each recombinant protein. Full length recombinant GST:FlaB protein was determined to be insoluble and located in inclusion bodies even after attempts were made to optimize induction conditions. Therefore, the *flaB* gene was re-cloned into the pGEX-4T-3 vector to include only the immunodominant region of the FlaB protein (tFlaB) as determined by Berland et al. which is soluble (105). The primers used for cloning of *tflaB* are listed at the end of Table 1. Once optimal conditions were determined, clones positive for the genes of interest were inoculated into LB media supplemented with ampicillin overnight at 37°C with shaking (155 RPM). Overnight starter cultures were then diluted 1:100 into fresh 2xYTA or LB media and incubated until cultures reached an OD₆₀₀ of 0.5 to 0.8 before induction of fusion protein expression with IPTG (Promega). For the recombinant fusion proteins GST:tCspZ and GST:tOspA, cultures were induced with 0.5mM IPTG, incubated at 34-37°C, and allowed to grow for an additional 3 to 4 hours with shaking (160RPM). For GST:tFlaB, cultures were induced with 0.5 or 1mM IPTG and incubated overnight at room temperature with shaking (160RPM). Cells were harvested by centrifugation at 3050 x g for 35 minutes at 4°C and were frozen at -40°C until protein purification was performed.

For protein extraction, cells were thawed and subsequently lysed via sonication in 15 second bursts on and off while kept on ice. Sufficient lysis by sonication was monitored via microscopy with methylene blue staining. Depending on the culture volume, the sonicates were pelleted by microcentrifugation at 10,000 x g for 10min or at 3,050 x g for 40min at 4°C to separate the insoluble and soluble protein fractions. The clarified soluble lysates containing the recombinant fusion proteins were loaded onto glutathione agarose beads (Pierce Thermo Fisher Scientific, Rockford, IL) for protein purification by affinity chromatography according to manufacturer's guidelines for batch method purification (GE Healthcare Life Sciences, Pittsburgh, PA). tFlaB was left fused to the GST tag, while CspZ and OspA were cleaved free of the GST tag with bovine thrombin while still bound to the glutathione beads (GE Healthcare Life Sciences, Pittsburg, PA) according to manufacturer's protocol for on column cleavage. For GST:tFlaB, the GST elution buffer was subsequently exchanged for PBS, and the protein was concentrated using an Amicon® Ultra 0.5mL Centrifugal unit (EMD Millipore, Billerica, MA). The purity of all proteins was analyzed by SDS-PAGE on either 10 or 12.5% separating gels and 4% stacking gels with Coomassie brilliant blue R250 (BioRad, Hercules, CA) staining. Protein concentrations were determined with the Bradford Coomassie Protein Assay (Pierce Thermo Fisher Scientific, Rockford, IL) utilizing Bovine Serum Albumin as the standard. The standard curve generated is shown in figure 13. The standard curve was utilized to determine recombinant protein concentration as well as whole cell lysate protein concentration prior to performing assays.

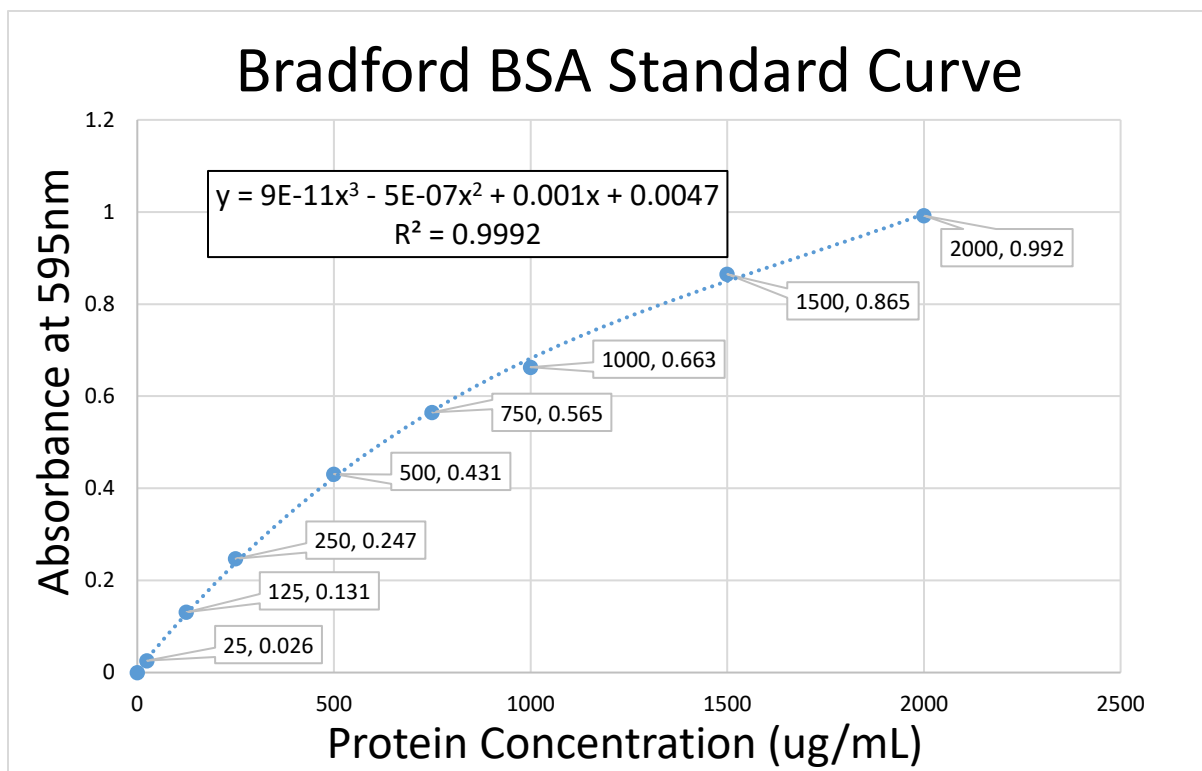


FIG 13. Bradford assay BSA standard curve generated for determination of protein concentration. A polynomial to the third order was used to fit the trendline as recommended by the manufacturer. Protein solutions mixed with Bradford Coomassie blue reagent were measured in a spectrophotometer at 595nm to obtain absorbance readings.

Polyclonal antibody generation and dot blot titration

To generate polyclonal antibodies, two Long-Evans rats per purified recombinant protein were immunized by intraperitoneal injection with 50 μ g of either cleaved tCspZ, cleaved tOspA, or GST:tFlaB in PBS (pH 7.4) in a 1:1 emulsion with Freund's complete adjuvant (Sigma Aldrich, St. Louis, MO). Two booster immunizations followed at two-week intervals with 50 μ g of each purified protein in PBS (pH 7.4) in a 1:1 emulsion with incomplete Freund's adjuvant (Sigma Aldrich, St. Louis, MO). Two weeks after the final booster immunization, all rats were exsanguinated to collect antisera. Serum was separated from blood components by centrifugation at 10,000 x g for 10min at room temperature. Sera was carefully collected, aliquoted, and frozen at -40°C until further experimentation. All animal procedures were performed in accordance with the Institutional Animal Care and Use Committee (IACUC) guidelines and with protocol approval by the Austin Peay State University IACUC. Normal rat serum (Invitrogen™ Thermo Fisher Scientific, Rockford, IL) was purchased as a negative control for immunological assays.

To determine the optimal concentration of primary and secondary antibodies, antibodies were titrated against purified recombinant proteins via dot blot in a checkerboard layout. The layout of the gridded membrane is depicted in figure 14. For each antiserum generated, the same concentration of appropriate purified recombinant protein (100ng) was spotted onto a gridded PVDF membranes (Immobilon P) and allowed to dry. The membranes were then blocked for 1 hour at room temperature in PBS (pH 7.4) with 0.05% Tween 20 (PBS-T) and 1% BSA (bovine serum albumin). The membranes were then cut into 1x1cm squares along the grids and placed into separate chambers for incubation with the appropriate antibody concentrations. Rat polyclonal antisera directed against the recombinant proteins and goat anti-rat IgG (H+L) HRP conjugated secondary antibody (Invitrogen) were applied at varying combinations of dilutions to

each square. Membranes were incubated with each antibody for 1 hour at room temperature and washed with PBS-T three times for five minutes in between each application. Dot blots were developed with the chromogenic substrate 4-chloro-naphthol (Pierce) and hydrogen peroxide per manufacturer instructions.

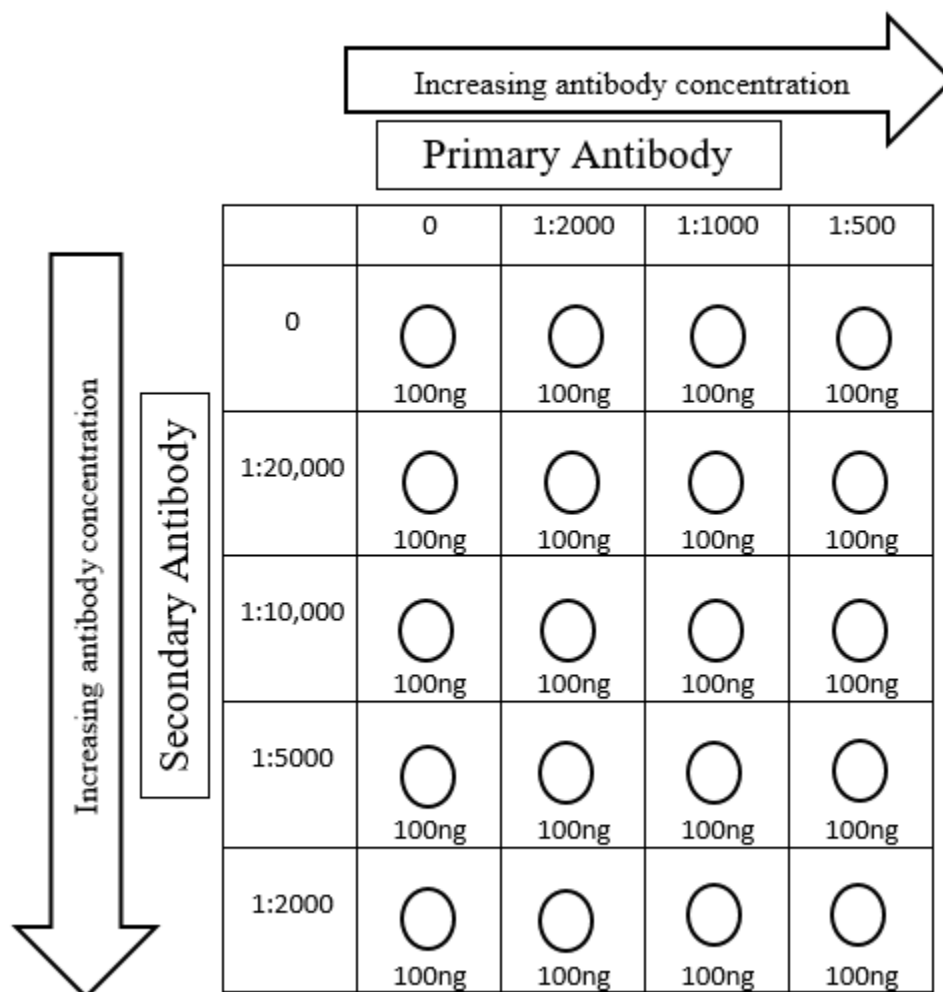


FIG 14. Layout of dot blot titration membrane. Approximately 100ng of recombinant protein was spotted onto each square of a gridded membrane.

SDS-PAGE and immunoblotting

For protein expression analysis, spirochetes were grown at 23°C, temperature-shifted from 23°C to 34°C, or host adapted in dog serum to mid logarithmic density. Spirochetes were then harvested via centrifugation at 3050g for 30 min at 4°C and gently washed three times in 1X PBS (HyClone Laboratories, Logan, UT). The spirochetes were then resuspended in 150uL of 1X PBS and stored at -40°C until immunoblotting was to be performed. Borrelial whole cell lysates were prepared by addition of an equal volume of SDS-PAGE loading buffer (62.5µM Tris Base [pH6.8], 10% [vol/vol] glycerol, 5% [vol/vol] β-mercaptoethanol, 5% SDS, 0.01% bromophenol blue) to spirochete suspensions mentioned above and subsequently boiled for 10 min. Purified recombinant proteins were also prepared via boiling to serve as antibody recognition controls. Borrelial whole cell lysates (1×10^7 spirochetes per lane) and recombinant proteins (500ng-2ug) were then passed through 4% stacking and 12.5% separating gels to separate the proteins. Protein migration was monitored by iBright™ prestained protein ladder (Invitrogen) to ensure maximum separation of the proteins. Gels were then electro-transferred by wet transfer in 1X transfer buffer (Towbin buffer: 25mM Tris, 192mM Glycine, 20% Methanol) to 0.45µm nitrocellulose membranes (GVS Life Sciences, Sanford, ME) or 0.45µm Immobilon-P polyvinylidene difluoride (PVDF) membranes (MilliporeSigma) for immunoblotting.

For initial testing of western blotting procedure and antibody recognition of denatured recombinant proteins, immunoblots containing the recombinant proteins tOspA, GST:tFlaB, and tCspZ were blocked in blocking buffer consisting of PBS-T-1% BSA for 1 hour at room temperature. Subsequently, blots were incubated with the appropriate primary antibodies (polyclonal rat serum) anti-OspA (1:1000), anti-GST:tFlaB (1:500), and anti-CspZ (1:500) for 1 hour at room temperature. The blots were then washed three times with PBS-T (5 min each

wash) and then incubated with goat anti-rat IgG (H+L) HRP conjugated secondary antibody (Invitrogen) at a dilution of 1:2000. Blots were then washed three times with PBS-T for 15, 5, and 5 min followed by a final wash in PBS for 5 min. Immunoblots were developed with the chromogenic substrate 4-chloro-naphthol (Pierce) and hydrogen peroxide per manufacturer instructions.

For analysis of protein expression in borrelial whole cell lysates, enhanced chemiluminescence (ECL) immunoblotting was performed. Membranes containing borrelial whole cell lysates and the appropriate recombinant protein (as a control) mentioned previously were first blocked in PBS-T-2% BSA for 1 hour at room temperature. After blocking, membranes were incubated with either anti-OspA (1:1000), anti-GST:tFlaB (1:1000), or anti-CspZ (1:1000) for 1 hour at room temperature. Three 10 min washes with PBS-T were performed before blots were incubated with a 1:40,000 dilution of goat anti-rat IgG (H+L) HRP conjugated secondary antibody (Invitrogen). Blots were subsequently washed in PBS-T three times (15 min, 10 min, and 5min) followed by a last wash in PBS (5min). The immunoblots were developed with SuperSignal™ West Pico Plus ECL substrate (Pierce) per manufacturer protocols. Exposure of the blots was carried out with a UVP Biospectrum 810 Imaging System with an exposure time of 1 min for each blot. Images were inverted to a white background with black bands, and the gamma of the images was adjusted to 0.4 for all immunoblots.

Native dot-blot with borrelial whole cell lysates

To determine if anti-CspZ antibodies are capable of binding native (non-reduced and non-denatured) CspZ from borrelial whole lysates, a dot-blot was performed. Whole cell lysate was prepared using temperature shifted B31MI spirochetes which were sonicated on ice three times for five seconds on and off to lyse the cells. Protease inhibitor cocktail (Promega) was added to prevent protein degradation by released proteases. Total protein concentration was then determined with the Coomassie Bradford Assay and standard curve generated previously (Figure 13). A nitrocellulose membrane was then cut into strips and gridded for each protein of interest (CspZ, FlaB, and OspA). Figure 15 shows the layout of the nitrocellulose strips. As a control, recombinant proteins were also spotted for the dot blot alongside borrelial whole cell lysates. Negative primary antibody controls were done for all recombinant proteins and for whole cell lysates. To preserve the amount of lysate left, the no primary antibody control for the lysates was only done to one gridded square located on the OspA strip. Nothing was spotted on the square for CspZ and FlaB. The last squares for all strips was a no protein control (neither lysate nor rProtein) to determine that primary antibodies were not binding to the membranes themselves. Each gridded square of the strip was spotted with the amount of protein or lysate. Spotted proteins were allowed to dry and then were blocked in PBS-T-2% BSA for 1 hour at room temperature. After blocking, membranes were incubated with either anti-rOspA (1:1000), anti-rGST:FlaB (1:1000), or anti-rCspZ (1:500) for 1 hour at room temperature. Three, 10-minute washes with PBS-T were performed before blots were incubated with a 1:20,000 dilution of goat anti-rat IgG (H+L) HRP conjugated secondary antibody (Invitrogen). Blots were subsequently washed in PBS-T three times (15 min, 10 min, and 5min) followed by a last wash in PBS (5min). The dot-blot was developed with SuperSignal™ West Pico Plus ECL substrate (Pierce) per

manufacturer protocols. Exposure of the blots was carried out with a UVP Biospectrum 810 Imaging System with varying exposure times of either 15 sec, 1 min, or 5 min for each strip. Images were inverted to a white background with black bands, and the gamma of the images was adjusted to 0.4 for all dot-blot.

| | | | | |
|-----------------------|-------------------------|-----------------------|-----------------------------------|-----------------------|
| 5 μ g rProtein | 2.5 μ g rProtein | 1 μ g rProtein | 2.5 μ g rProtein No 1Ab | 0 μ g rProtein |
| 5 μ g Lysate | 2.5 μ g Lysate | 1 μ g Lysate | 2.5 μ g Lysate No 1Ab | 0 μ g Lysate |

FIG 15. Layout of the nitrocellulose membranes for native dot-blot of whole cell lysates. Only the OspA nitrocellulose strip received the 1 μ g lysate but no primary antibody control (No1Ab) due to a limiting amount of lysate available

Cell Surface Localization via Indirect Immunofluorescence

Spirochetes were grown at 34°C to a cell density of at least 1×10^7 spirochetes/mL. Cells were washed twice in 1mL of fresh BSK-H media and spun at 4000 x g for 4 min to pellet the cells. Subsequently, cells were diluted or concentrated to 5×10^6 spirochetes/mL in a 100 μ L volume in three separate tubes. For surface localization, a 1:100 dilution of rat polyclonal antibody directed against either CspZ, FlaB, or OspA was added to the tube of motile spirochetes and allowed to incubate for 1 hour at room temperature. FlaB is the periplasmic flagellin protein and will serve as a negative outer surface control verifying membrane integrity, while OspA is a known outer surface protein serving as a positive control. Cells were then washed three times with sterile 1X PBS and harvested by centrifugation at 4,000 x g for 4 min. The pellets were then resuspended in 100 μ L of PBS and 10 μ L aliquots were spotted onto glass slides to air dry overnight. After drying, cells were fixed by pipetting 150 μ L of ice cold acetone to the slide for 10 min at 4°C. Following fixation, the slides were blocked by the addition of 40 μ L of 0.2% BSA in PBS (pH 7.4) for 30 min. The slides were then incubated with a 1:500 dilution of Alexa Fluor 488-conjugated goat anti-rat antibody (Invitrogen) for 45 min at room temperature in a dark humidified chamber. Alexa Fluor 488 produces a green fluorescence. Slides were washed three times with 0.2% BSA in PBS (pH 7.4) before being incubated for 10 min with a 1:1000 dilution of 2.5mg/mL of the permeable DNA-binding stain 4',6-diamidino-2-phenylindole dihydrochloride (DAPI; Polyscience). DAPI counterstaining was used to identify spirochetes within a given field and gives off a blue fluorescence. Slides were then visualized using a Nikon Eclipse fluorescence microscope at both 400x and 1000x magnification. Spirochetes within the same field of view were captured for DAPI and Alex Fluor 488. A fixed control was also done for all three proteins to validate antibody recognition and the procedure. For the fixed control,

10 μ L aliquots of 5×10^6 spirochetes/mL were spotted onto glass slides and air dried overnight. The slides were then fixed in acetone and blocked first before being incubated with a 1:100 dilution of the appropriate primary antibody. All blocking, wash, secondary antibody, and DAPI incubation steps were performed as stated for the surface localization experiment.

Serum Sensitivity Assay

Dog serum used was either donated from a canine with no history or previous exposure to Lyme disease or purchased. For donated blood, samples were obtained and allowed to clot at room temperature for 60 minutes. Samples were then spun at 1,300 x g for 10 minutes at room temperature. Serum was harvested and aliquots of 100 μ L were stored at -40°C until further use. Additional dog complement serum (Innovative Research) was purchased to complete all the necessary assays and was shipped on dry ice to ensure complement activity was not degraded. Purchased serum was stored at -80°C until needed for use. A serum sensitivity assay was performed in accordance with a published protocol (106). Strains B31MI and B31cF were grown to a density of at least 1 x 10⁷ spirochetes/mL. Once the proper cell density was reached, one (1) mL of culture was microcentrifuged at 6,000 x g for 10 minutes. The medium was decanted, and pellets were washed three times in one mL of BSK-H media. Pellets were then resuspended to a density of 1 x 10⁷ spirochetes/mL. Serum was thawed, and an aliquot of serum was heat inactivated at 56°C for 30 minutes to use as a control. For the assay, two different reactions were performed for each strain in triplicate: 20% normal dog serum (NDS) and 20% heat inactivated dog serum (HiDS). Serum was diluted with BSK-H media to 40% and an equal volume of bacteria (5 x 10⁶ spirochetes/mL final concentration) were added to the reaction to bring the final dilution of serum to 20%. Reactions were performed in 200 μ L “PCR” tubes at a final volume of 140 μ L and incubated at 34°C for the course of the experiment. Aliquots of 10 μ L were taken from each reaction at 0, 2, 4, and 16h after addition of serum for viability analysis using dark-field microscopy. Spirochetes were enumerated by counting 10 fields of view at 400x total magnification as previously described. Significant differences in sensitivity were determined utilizing a 2-sample t-test comparing heat inactivated controls to normal sera experiments.

CHAPTER III

Results

Cloning of pGEX 4T-3 with cspZ, ospA, and flaB

The first step of cloning was PCR amplifying the genes of interest and harvesting vector plasmid DNA. Figure 16 shows the results of PCR amplifying *tcspZ*, *tospA*, and *flaB* from the genome of *B. burgdorferi* B31MI. A truncated version of *flaB* (*tflaB*) was later created due to protein purification problems of the full length *flaB* and therefore *tflaB* is the immunodominant region of *flaB* (105). The PCR results for *tflaB* are also shown in figure 16. As shown in figure 16, all amplicons were the correct sizes for each gene of interest.

Once genes were amplified and enough pGEX 4T-3 plasmid DNA was harvested, a restriction enzyme digestion was performed on the genes and plasmid with BamHI and XhoI to allow for cloning. After digestion, the cut vector and gene inserts were ligated and subsequently transformed into the propagation host *Escherichia coli* DH5 α . Seven colonies were chosen for analysis of successful ligation: Colonies 14, 17, 40, 57, 66, 67, and 71. To preliminarily confirm the presence as well as orientation of the inserts, colony PCR was performed on colonies chosen from selection plates such as those in figure 17. Colony PCR was performed with two sets of primers for each of the genes of interest. One primer set was backbone specific only, which targeted the vector backbone of the plasmid. Backbone specific primers only reveal the presence of the insert in the plasmid but not the orientation. Therefore, a second primer set was orientation specific consisting of one primer targeting the gene insert while the other primer targeted the vector backbone. This primer set confirms both the presence of the insert as well as if the orientation of insert is correct. Clones positive for the insert were anticipated to yield PCR

products roughly the size of the MCS of pGEX 4T-3 (171bp) plus the size of the inserts for backbone specific primers as shown in table 1. A negative clone would produce a PCR product the size of the MCS only at 171bp. Orientation specific primers were anticipated to yield positive PCR products slightly smaller than those of the backbone specific primers, while negative clones would yield no PCR products since the insert would not be in proper orientation to be amplified. Figure 18 displays the results of colony PCR performed on transformed colonies. All of the clones were positive for the *cspZ* insert and proper orientation except for colony 40. Clones were also confirmed with a restriction enzyme analysis to further confirm the size and contents of the constructs. The results of the restriction enzyme analysis of a clone are displayed in Figure 19. Glycerol stocks of colonies 14, 17, 57, 66, 67, and 71 were created for storage of the created expression plasmids until further use.

For the plasmid construct pGEX:*tcspZ*, five clones that were PCR positive and of correct size as confirmed by restriction analysis were sent off for Sanger sequencing. The designed plasmid constructs were confirmed to have the genes of interest inserted in the proper orientation. Sequence alignments were performed on NCBI BLAST to determine if any mutations occurred. All clones had 99% nucleotide sequence homology to the *cspZ* sequence of *B. burgdorferi* B31 from the BLAST database. All five clones contained at least one point mutation. Of the five clones, two clones designated as colony 17 and colony 71 had point mutations that did not alter the final amino acid sequence as a tyrosine was still translated at amino acid position 209. These two clones were used for all future protein expression and purification experiments. Figures 20 and 21 show the results of the nucleotide and the protein sequence alignments performed on colony 71 respectively. Sequence alignments were based on the Sanger sequencing results.

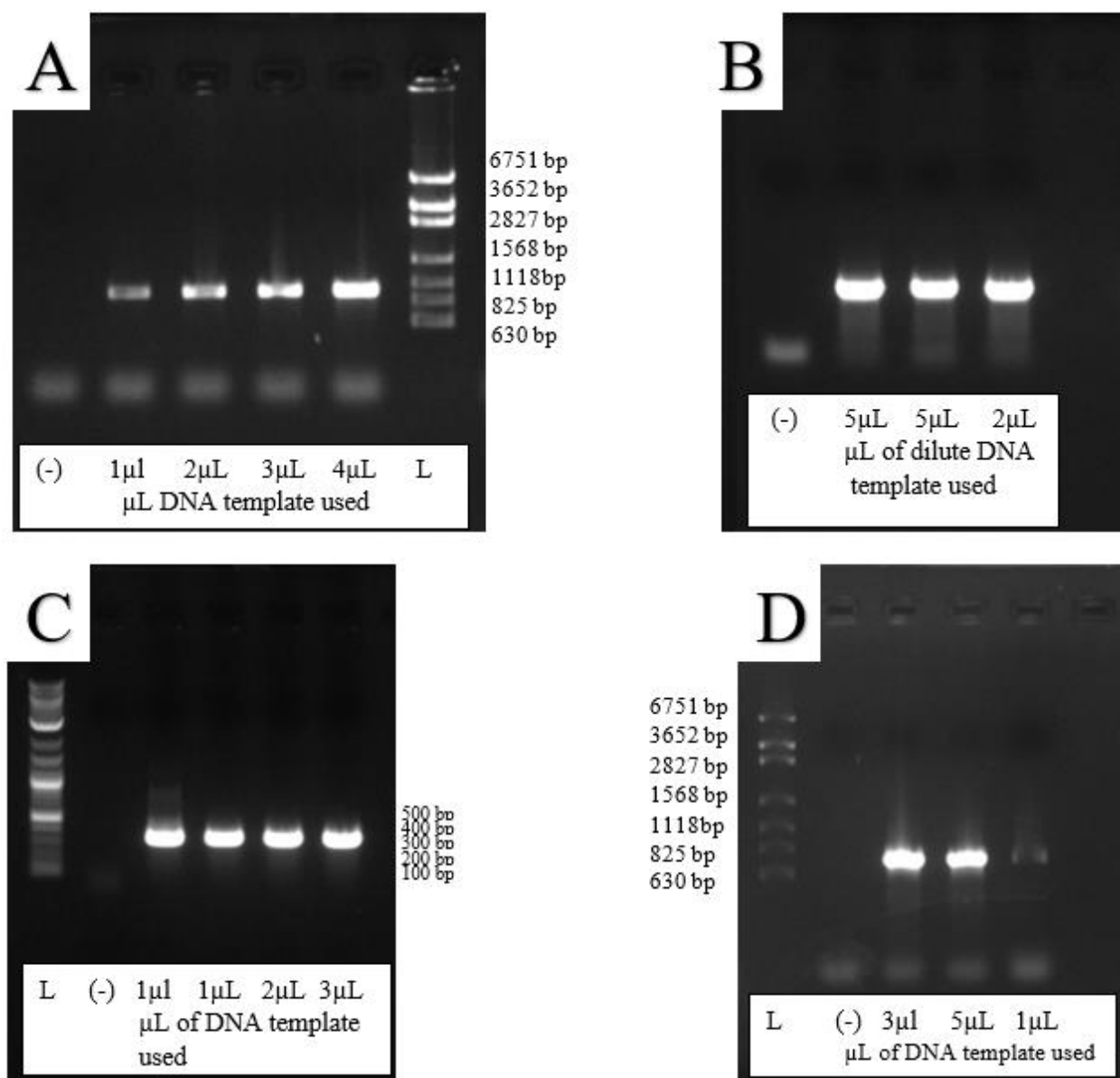


FIG 16. PCR reactions (100 μ L) of the genes of interest. PCR reactions were optimized by determining the appropriate annealing temperatures and DNA template concentrations of small scale reactions (20 μ L). Once optimized, the PCR reactions were scaled up to 100 μ L to harvest enough DNA for cloning. Full length *flaB* is approximately 1,022bp (A). Truncated *cspZ* is approximately 671bp with restriction sites (B). Truncated *flaB* is approximately 346bp (C). Truncated *ospA* is approximately 788bp (D).

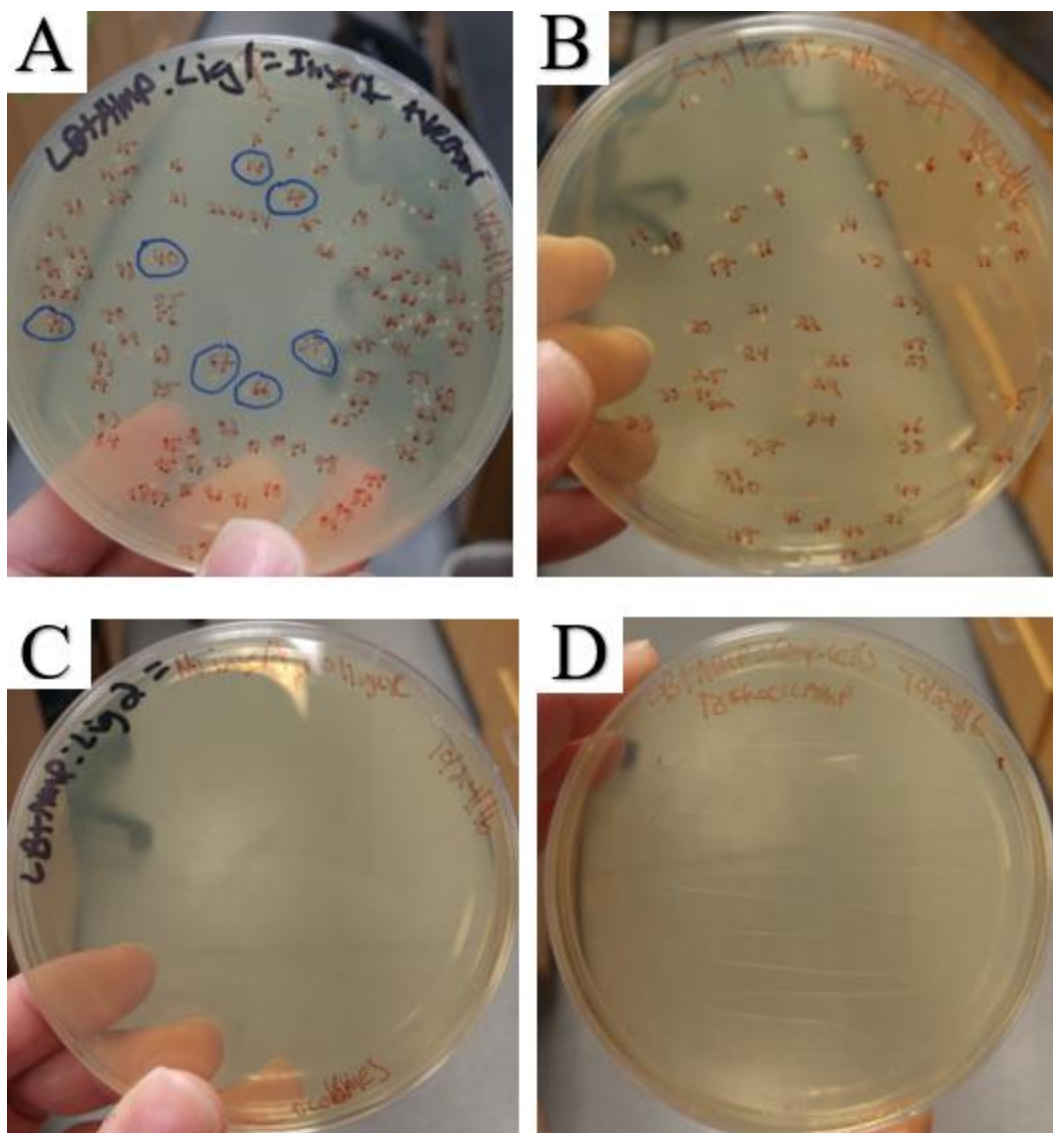


FIG 17. Selection plates from transformations with various ligation conditions. Many colonies are present on the selection plate from a ligation reaction containing the insert of interest and vector (A). After incubation, seven colonies were randomly chosen for PCR analysis: Colony 14, 17, 40, 57, 66, 67, and 71. The no insert control plate (B) shows how many colonies on plate (A) may be vector that self-ligated and contain no insert. A ligation control with no insert or ligase (C) should have no colonies as displayed above. An ampicillin plate was inoculated with competent *E. coli* which received no foreign DNA (D). Competent DH5 α cells do not have resistance to ampicillin prior to transformation.

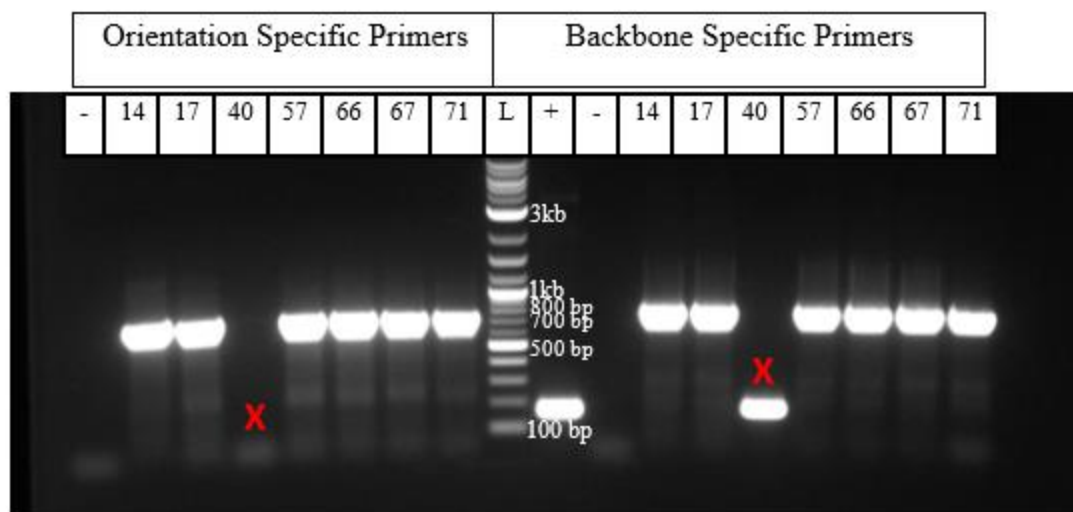


FIG 18. Colony PCR results performed on transformants from selection plates. Orientation specific primers yielded a PCR product of approximately 721bp for positive pGEX:*tospZ* clones while negative clones resulted in no amplicons. Backbone specific primers resulted in a slightly larger PCR product of 809bp for positive clones. Negative clones resulted in an amplicon with the size of 171bp matching the MCS of pGEX 4T-3. All transformants were positive for the insert except for colony 40 denoted by the red X's. The five positive clones were sent off for sequencing. Colony PCR for pGEX:*tospA* and pGEX:*tflaB* was also performed in similar fashion (results not shown). (L=Ladder, (-) = negative control, #'s= transformants tested from ligation plates).

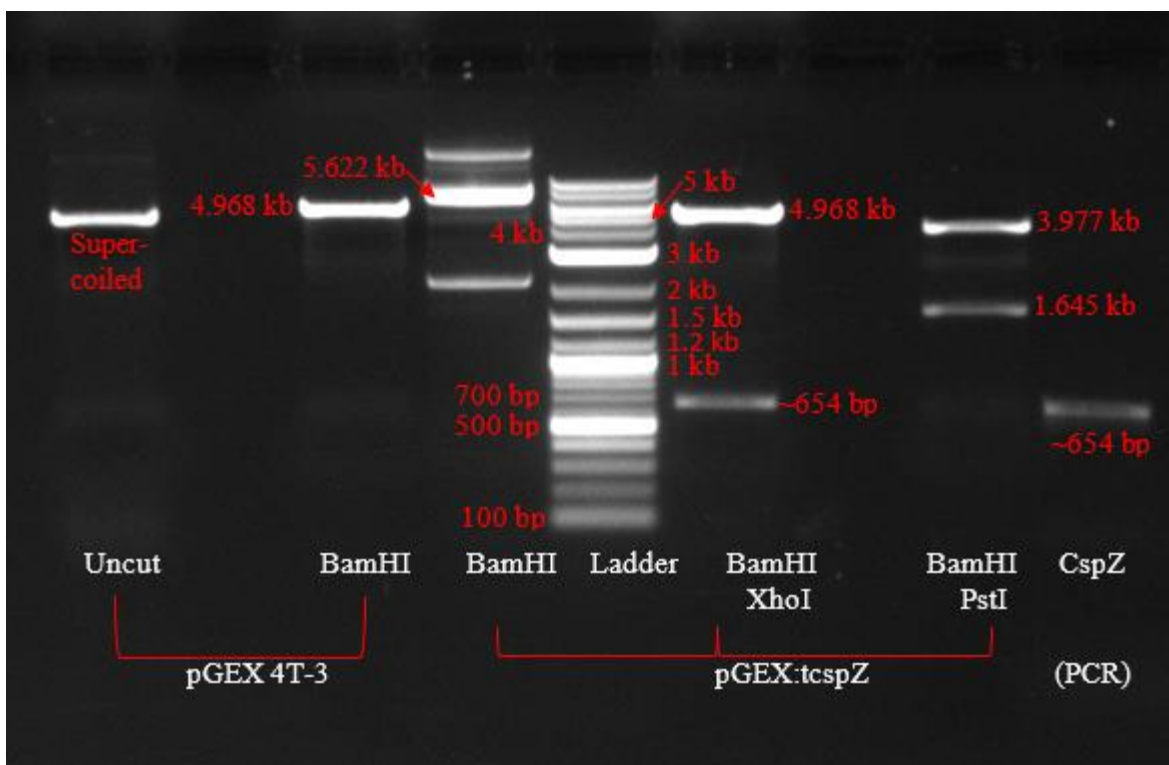


FIG 19. Diagnostic restriction enzyme digestion of pGEX:*tcspZ* PCR + colony. Linear pGEX 4T-3 is approximately 4.968 kb. pGEX 4T-3 inserted with *tcspZ* should have an extra 654bp and there linearized equal to 5.622 kb. The single BamHI digest of pGEX:*tcspZ* contains some erroneous banding patterns which was observed in other BamHI digests of other DNA and likely due to incomplete digestion. A double digest was performed with a different restriction enzyme, PstI to further confirm the insert presence. PstI cuts pGEX 4T-3 out of the MCS at 1.921 kb. A double digest of pGEX:*tcspZ* with BamHI and PstI resulted in two fragments with the appropriate sizes of 3.977kb and 1.645kb based on the restriction sites of the plasmid. A double digest of pGEX:*tcspZ* with BamHI and XhoI resulted in two fragments corresponding to the size of linearized pGEX 4T-3 at 4.968 kb and of the insert *tcspZ* at 654bp. The diagnostic digest corroborated with colony PCR of the clones and five were sent off for sequencing.

Sequence ID: Query_190017 Length: 711 Number of Matches: 1

Range 1: 58 to 711 [Graphics](#) ▼ Next Match ▲ Previous Match

| Score | Expect | Identities | Gaps | Strand |
|----------------|--|--------------|-----------|-----------|
| 1203 bits(651) | 0.0 | 653/654(99%) | 0/654(0%) | Plus/Plus |
| Query 1 | GATGTTAGTAGATTAAATCAGAGAAATATTAATGAGCTTAAAAATTTTGTGAAAAGGCC | 60 | | |
| Sbjct 58 | GATGTTAGTAGATTAAATCAGAGAAATATTAATGAGCTTAAAAATTTTGTGAAAAGGCC | 117 | | |
| Query 61 | AAGTATTATTCTATAAAATTAGACGCTATTTATAACGAATGTACAGGAGCATATAATGAT | 120 | | |
| Sbjct 118 | AAGTATTATTCTATAAAATTAGACGCTATTTATAACGAATGTACAGGAGCATATAATGAT | 177 | | |
| Query 121 | ATTATGACTTATTCGGAAGGTACATTTTCTGATCAAAGTAAGGTTAATCAAGCTATATCT | 180 | | |
| Sbjct 178 | ATTATGACTTATTCGGAAGGTACATTTTCTGATCAAAGTAAGGTTAATCAAGCTATATCT | 237 | | |
| Query 181 | ATATTTAAAAAAGACAATAAAATTGTTAATAAGTTTAAGGAGCTTGAAAAGATTATAGAA | 240 | | |
| Sbjct 238 | ATATTTAAAAAAGACAATAAAATTGTTAATAAGTTTAAGGAGCTTGAAAAGATTATAGAA | 297 | | |
| Query 241 | GAATACAAACCTATGTTTTAAGTAAATTAATTGATGATTTTGCTATAGAATTAGACCAA | 300 | | |
| Sbjct 298 | GAATACAAACCTATGTTTTAAGTAAATTAATTGATGATTTTGCTATAGAATTAGACCAA | 357 | | |
| Query 301 | GCTGTAGATAAATGATGTGTCTAATGCCAGACATGTTGCTGATTCTTATAAAAACTTAGA | 360 | | |
| Sbjct 358 | GCTGTAGATAAATGATGTGTCTAATGCCAGACATGTTGCTGATTCTTATAAAAACTTAGA | 417 | | |
| Query 361 | AAATCTGTTGTATTAGCCTACATTGAGAGTTTTGATGTTATATCTTCTAAGTTTGTGAT | 420 | | |
| Sbjct 418 | AAATCTGTTGTATTAGCCTACATTGAGAGTTTTGATGTTATATCTTCTAAGTTTGTGAT | 477 | | |
| Query 421 | AGTAAGTTTGTGAAGCTTCTAAAAAATTTGTCAATAAAGCTAAAGAGTTTGTAGAGGAA | 480 | | |
| Sbjct 478 | AGTAAGTTTGTGAAGCTTCTAAAAAATTTGTCAATAAAGCTAAAGAGTTTGTAGAGGAA | 537 | | |
| Query 481 | AATGATCTTATAGCTCTTGAGTGTATTGTGAAAACATTGGAGATATGGTTAATGATAGG | 540 | | |
| Sbjct 538 | AATGATCTTATAGCTCTTGAGTGTATTGTGAAAACATTGGAGATATGGTTAATGATAGG | 597 | | |
| Query 541 | GAAATAAATCAAGAAGCAGGTATAATAATTTTATAAAAAAGAAGCAGATTTTTTAGGT | 600 | | |
| Sbjct 598 | GAAATAAATCAAGAAGCAGGTATAATAATTTTATAAAAAAGAAGCAGATTTTTTAGGT | 657 | | |
| Query 601 | GCTGCTGTAGAACTTGAGGGGGCTTACAAAGCTATTAAGCAAACCTTATTATAG | 654 | | |
| Sbjct 658 | GCTGCTGTAGAACTTGAGGGGGCTTATAAAGCTATTAAGCAAACCTTATTATAG | 711 | | |

FIG 20. Nucleotide sequence alignment of colony 71. Colony 71 containing pGEX:*tospZ* yields 99% sequence homology of *tospZ* to *cspZ* of the B31 strain of *B. burgdorferi*. The single point mutation results in a C instead of T (black arrow).

Sequence ID: Query_144453 Length: 217 Number of Matches: 1

Range 1: 1 to 217 [Graphics](#) ▼ Next Match ▲ Previous Match

| Score | Expect | Method | Identities | Positives | Gaps |
|----------------|---|------------------------------|---------------|---------------|-----------|
| 429 bits(1102) | 4e-160 | Compositional matrix adjust. | 217/217(100%) | 217/217(100%) | 0/217(0%) |
| Query 1 | DVSRLNQRNINELKIFVEKAKYYYSIKLDAIYNECTGAYNDIMTYSEGTFSDQSKVNQAIS | | | | 60 |
| Sbjct 1 | DVSRLNQRNINELKIFVEKAKYYYSIKLDAIYNECTGAYNDIMTYSEGTFSDQSKVNQAIS | | | | 60 |
| Query 61 | IFKKDNKIVNKFKELEKIIIEEYKPMFLSKLIDDFAIELDQAVDNDVSNARHVADSYKKLR | | | | 120 |
| Sbjct 61 | IFKKDNKIVNKFKELEKIIIEEYKPMFLSKLIDDFAIELDQAVDNDVSNARHVADSYKKLR | | | | 120 |
| Query 121 | KSVLAYIESFDVISSKFVDSKFVEASKKFVNKAKEFVEENDLIAECIVKTIGDMVNDR | | | | 180 |
| Sbjct 121 | KSVLAYIESFDVISSKFVDSKFVEASKKFVNKAKEFVEENDLIAECIVKTIGDMVNDR | | | | 180 |
| Query 181 | EINSRSRYNNFYKKEADFLGAAVELEGAYKAIKQTLL | | 217 | | |
| Sbjct 181 | EINSRSRYNNFYKKEADFLGAAVELEGAYKAIKQTLL | | 217 | | |



FIG 21. Protein sequence alignment of colony 71. Colony 71 containing pGEX:*tcsz* yields 100% sequence homology of the cloned tCspZ to CspZ of the B31 strain of *B. burgdorferi*. The single point mutation still results in the amino acid tyrosine (Y) being translated at amino acid position 209 (indicated by the black arrow).

Protein expression and purification of recombinant proteins

The designed plasmid constructs were able to successfully express the recombinant proteins of interest CspZ, OspA, and FlaB of *Borrelia burgdorferi* in the propagation host *E. coli* DH5 α . To enhance protein expression, however, the plasmid constructs pGEX:*tcspZ*, pGEX:*tospA*, and pGEX:*tflaB* were transformed into the *E. coli* protein expression strain BL21 DE3 (NEB). To confirm expression, a new protein band that is thick near the size of the anticipated fusion protein should be visible in *E. coli* whole cell lysates transformed with each construct but not in *E. coli* harboring an empty pGEX 4T-3 vector. The approximate sizes of GST and the GST:rProteins are as follows: GST ~ 25kDa, GST:tCspZ ~ 50kDa, GST:tOspA ~57kDa, and GST:tFlaB ~38kDa. Each construct resulted in the production of a protein band corresponding to the approximate sizes. Overexpression of induced proteins was able to be visualized via SDS-PAGE for each construct as seen in Figure 22 and protein bands are circled in red representing the corresponding fusion proteins in the whole cell lysates. The optimal IPTG concentration and induction incubation time were determined empirically to be 0.5mM IPTG and four hours of incubation as seen in figure 22 (A).

After preliminary confirmation of expression, the proteins of interest needed to be purified from the rest of the whole cell lysates to be used as pure antigens for antibody generation. This was accomplished by ligand affinity chromatography using glutathione agarose beads to bind GST which was fused to the proteins of interest. Visual analysis of purity was conducted again with SDS-PAGE. Figure 23 displays SDS-PAGE gels showing the process of purification from whole cell lysate, to flow through, to washes, to final elutions. Figure 23 (c) shows the attempted purification of full length FlaB protein. All of the fusion protein remained stuck in the insoluble fraction. All attempts to shift expression from insoluble to soluble failed

for full length FlaB and therefore a truncated version of an immunodominant region of the protein was designed (tFlaB). Figure 23 (d) shows the successful purification of GST:tFlaB. Some extra bands are noticed in the elutions, but purity is still relatively high (~80-85%). Those bands likely represent proteins from host *E. coli* such as chaperones that were carried over through the purification process due to oversonication of the lysates.

For recombinant tCspZ and tOspA, an addition step was performed to free the proteins from the GST fusion partner. This was accomplished via thrombin cleavage. The pGEX 4T-3 vector comes with a thrombin cleavage site at the end of the GST protein. Optimal cleavage conditions were determined empirically. Figure 24 shows SDS-PAGE gels showing optimization of cleavage conditions and successful cleavage of tCspZ and tOspA from the GST moiety. After cleavage, tCspZ is approximately 27kDa, and tOspA is approximately 31 kDa which is consistent with their anticipated sizes (107). Both proteins showed high purity as no other erroneous bands were visible. The immunodominant region of FlaB is only ~13kDa. Due to the small size of this truncated version of FlaB, it was left fused to the GST moiety to ensure the antigen would be large enough to produce an immune response in animals during immunization. Purified GST:tFlaB is shown in figure 23 (D) and is approximately 45kDa. Proteins were then quantitated using a standard curve generated via a Coomassie Bradford Assay with BSA as the standard.

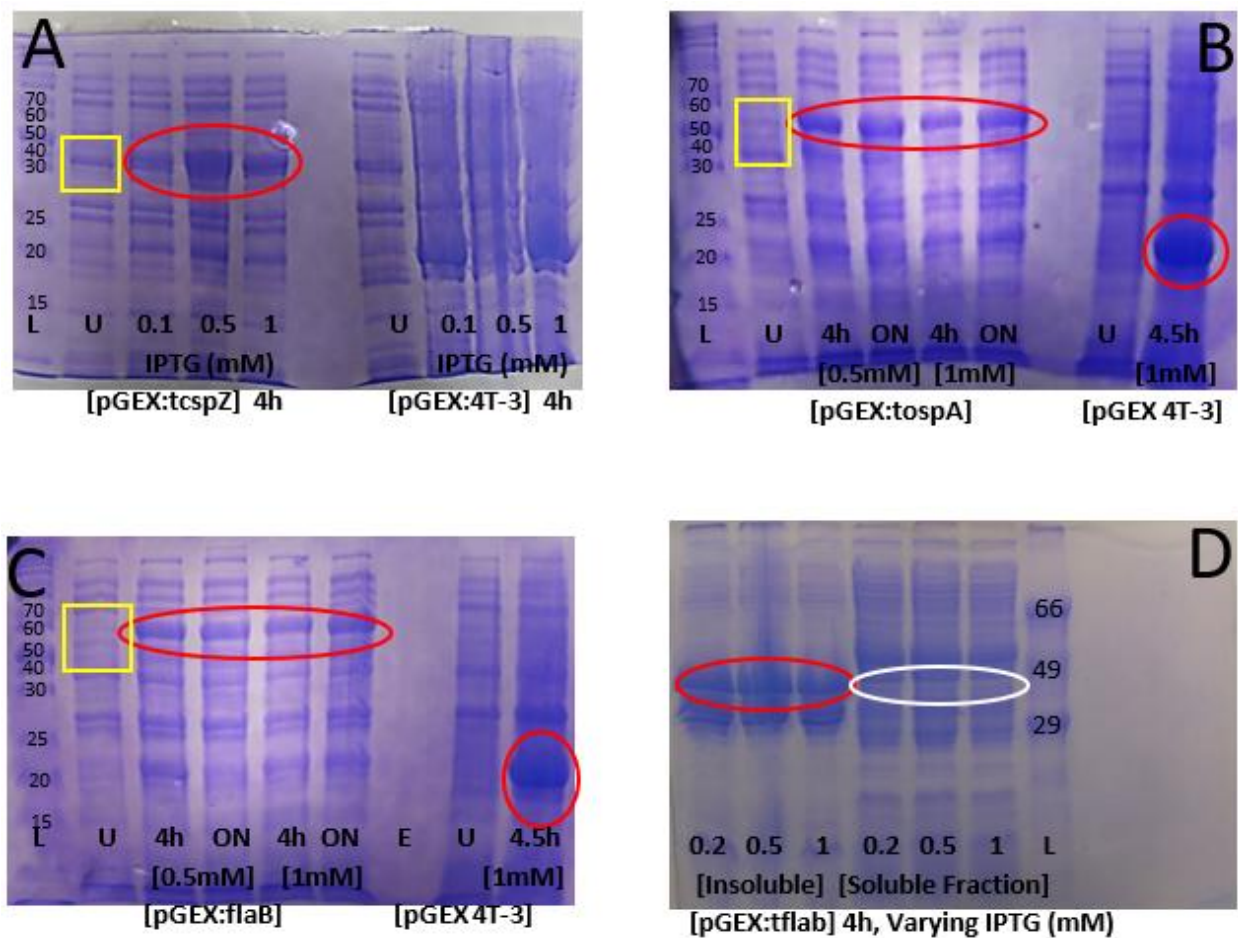


FIG 22. SDS-PAGE of IPTG induced and overexpressed *E. coli* BL21 DE3. *E. coli* containing constructs shows overexpression of recombinant fusion proteins. Protein bands corresponding to the appropriate sizes of each GST fusion protein are indicated by red circles. Yellow squares represent uninduced whole cell lysates lacking a protein band at the anticipated size to serve for comparison. pGEX:*tcspZ* lysates (A) resulted in protein bands at approximately 40kDa. pGEX:*tospA* lysates (B) resulted in proteins bands at approximately 55kDa. pGEX:*flaB* lysates (C) resulted in protein bands at approximately 60kDa. pGEX:*tflaB* lysates (D) resulted in protein bands at approximately 45 kDa. The white circle indicates faint bands present in the soluble fraction that match the size of GST:tFlaB. (L=Ladder, U=Uninduced)

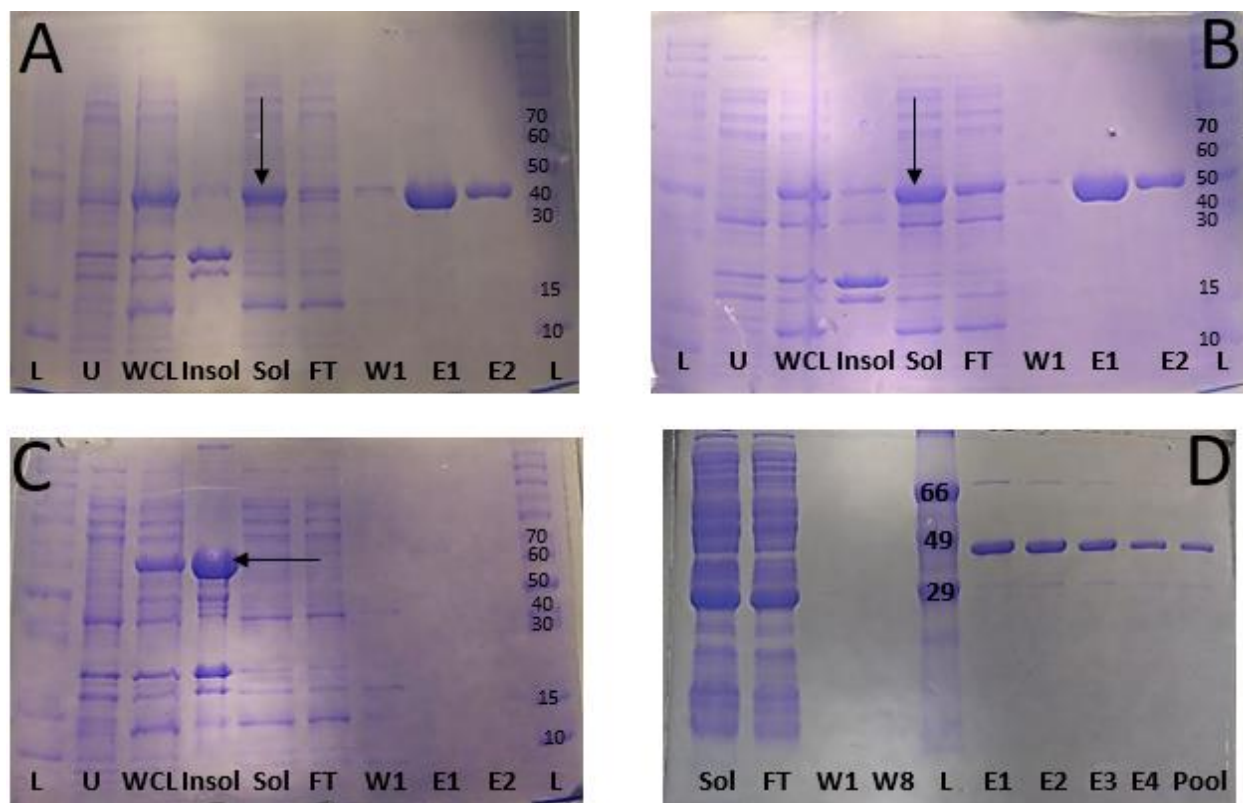


FIG 23. SDS-PAGE gels showing the protein purification process. *E. coli* BL21 DE3 containing the various pGEX:rProtein constructs is displayed in each respective image. Lane 2 of pGEX:*tspZ* (A), pGEX:*tospA* (B), and pGEX:*flaB* (C) shows uninduced (U) lysates which do not show protein bands like induced whole cell lysates (WCL) in lane 3. Only GST:tCspZ (A) and GST:tOspA (B) were located in the soluble fraction (Sol) of lysates (lane 5 indicated by arrows) while all GST:FlaB (C) was found in the insoluble fraction (lane 4 indicated by arrow). GST:tFlaB (D) was able to be purified despite also appearing to be predominantly insoluble (data not shown). GST:tCspZ bound to the beads well indicated by very little of it in the flow-through (FT) while some GST:tOspA was lost. GST:tCspZ, GST:tOspA, and GST:tFlaB were able to be purified away with minimal contamination of host protein in the elution fractions (E). To improve yield, elutions were pooled (pool) and resuspending to desired concentration in some instances such as in lane 10 of D above.

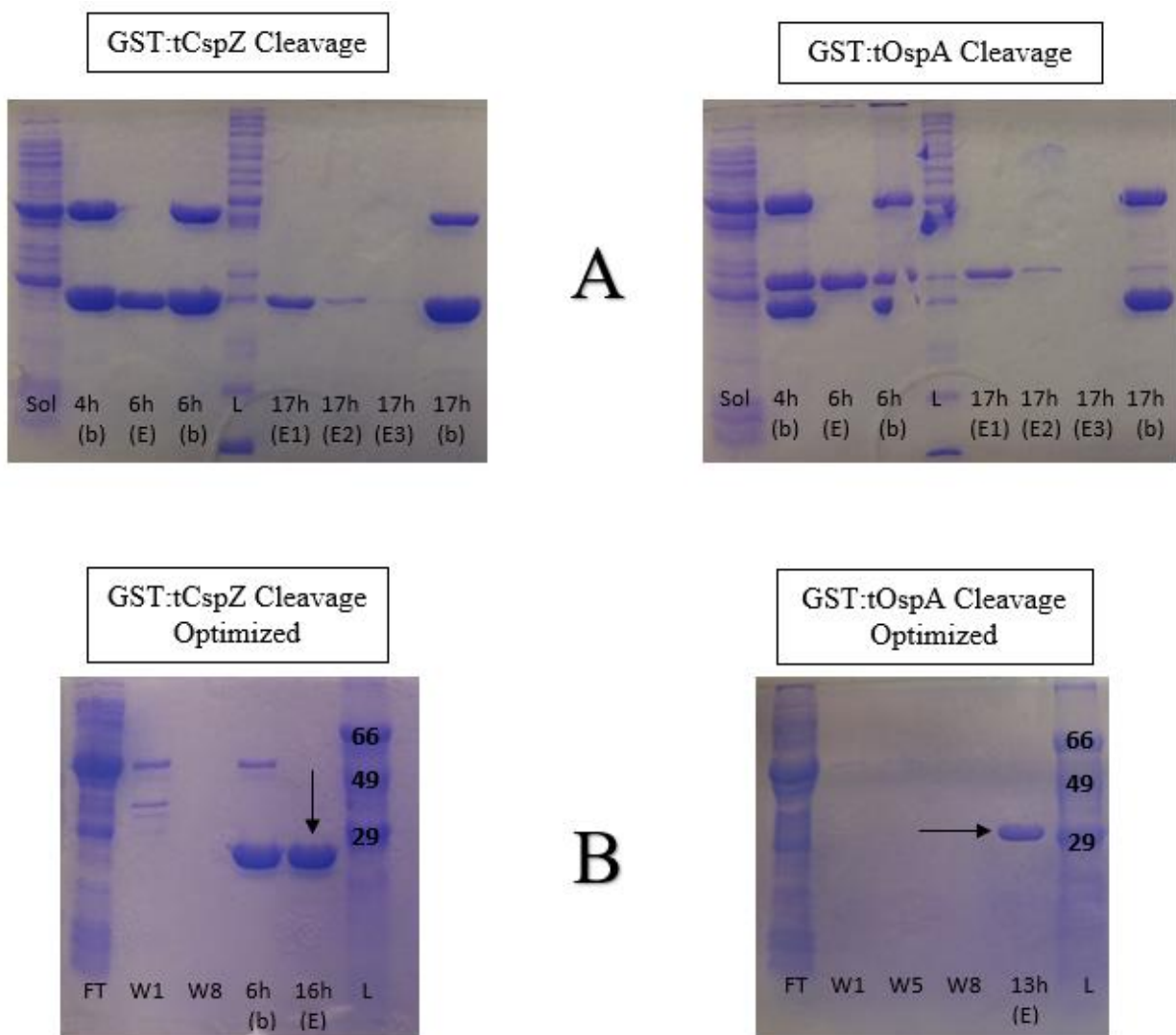


FIG 24. Thrombin cleavage of GST:tCspZ and GST:tOspA. The goal of thrombin cleavage was to free tCspZ and tOspA of the GST moiety. Optimal cleavage conditions were determined through trial. For each protein, the optimal cleavage incubation time was determined by analyzing the contents of the reaction beads (b) and eluates (E) off the beads at different time points (labeled on appropriate lanes) in the reaction shown in panel (A). Once optimized, larger scale reactions were done to produce as much cleaved protein as possible as shown in panel B. Arrows indicate cleaved and purified proteins. After cleavage, tCspZ was ~27kDa and tOspA was ~ 31 kDa as expected.

Dot blot antibody titration and recognition

Antibodies against tCspZ, tOspA, and GST:tFlaB were raised via immunization with the antigens in Long Evans rats. Polyclonal antibody serum was harvested by separation of the serum components from blood cells. Antibody titration was carried out to determine the optimal concentrations to use for downstream experiments and to examine if antibody generation was successful by recognition of purified recombinant proteins. Figure 14 shows the outline of how the titrations were performed. Briefly as a summary, equal amounts of each recombinant protein were spotted onto PVDF membranes that were gridded and allowed to air dry. The gridded squares containing antibody were then incubated with various primary (polyclonal serum from immunized rats) and secondary antibody concentrations to determine optimal combinations for blotting procedures. Results of titration for each recombinant protein is displayed in figure 25. Of the primary antibody, anti-GST:FlaB (B) resulted in the best signal across a wide range of concentrations followed by anti-OspA (C), while anti-CspZ (A) had the weakest signal. The type of membrane used could also be the cause for this, however, since not all proteins bind PVDF the same. When nitrocellulose was used, anti-CspZ showed better specificity (data not shown). All antibodies recognized the appropriate recombinant protein to some capacity. No reactivity was observed for the gridded square that lacked both primary and secondary antibody (denoted as 1 in the figure). Additionally, controls were placed in both the column and the row of the gridded square labeled one. The row control was incubation with primary antibody but no secondary. The column control was incubation with secondary but no primary. No color development was observed for any of the controls for all three proteins. Optimal antibody concentrations were decided by what produced an adequate signal but also was feasible for the quantity of serum obtained. For GST:tFlaB and tOspA, a 1:1000 dilution of primary antibody

and a 1:2000 of secondary antibody was sufficient enough to produce a good signal but also economical with the amount of serum to be used. For tCspZ, however, the highest tested concentrations of primary and secondary antibody were needed to produce a signal. A 1:500 primary and 1:2000 secondary antibody dilutions will be used for tCspZ in blotting experiments.

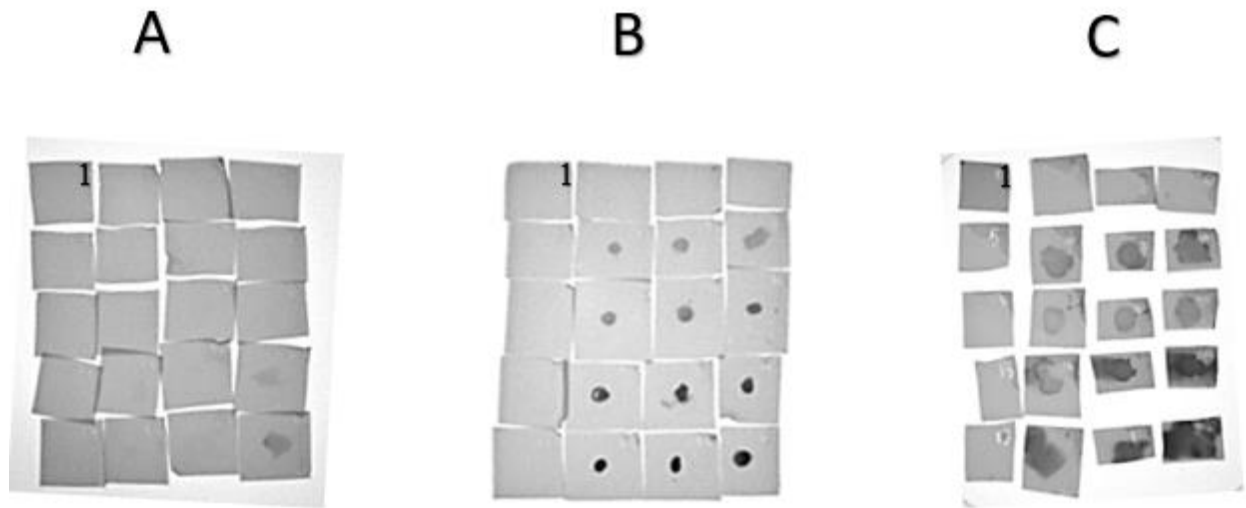


FIG 25. Dot blot antibody titration with recombinant proteins on PVDF membranes. Dot blots follow the pattern depicted in figure 14. The concentration of primary antibody increases from left to right while the secondary antibody concentration increases from top to bottom. Anti-CspZ antibodies (A) only showed recognition to 100ng of recombinant protein at high antibody dilutions (1:500, 1:1000 and 1:500, 1:2000). Anti-FlaB (B) and anti-OspA showed antibody recognition across all antibody concentrations tested.

Immunoblotting for recombinant proteins

Before immunoblotting for determining protein expression profiles from whole cell lysates of *Borrelia*, western blotting was performed on recombinant proteins to determine the best transfer conditions, antibody incubation times, and blocking buffers to use. Antibodies were already determined to recognize the recombinant proteins via the dot blot titration, but specificity is not able to be discerned from dot blots. It was determined that a transfer time of one hour was sufficient to transfer the proteins from the gel to the membrane. This was confirmed by Coomassie staining of the gel after transfer. In addition, blocking and antibody incubation time was sufficient at one hour. Since BSA was available, it was used as the blocking agent in the blocking buffer. The optimal BSA concentration was determined to be 1-2%. Higher percentages did not improve blotting and even resulted in higher background. When 500ng of recombinant proteins were separated via SDS-PAGE and transferred onto a PVDF membrane, some non-specific binding to impurities was revealed by anti-rOspA and anti-rGST:tFlaB primary antibodies likely due to the presence of *E. coli* proteins carried over from the purification process. Fortunately, the non-specific bands are less prominent than the bands for the actual recombinant proteins. Anti-rCspZ antibodies showed the highest specificity producing a single band. Bands with the most prominent signals were of the correct size for the recombinant proteins. It is worth noting that the substrate used for these preliminary blots, 4-chloro-naphthol, is the least sensitive colorimetric HRP substrate and can only detect 1ng or greater amounts of protein. Therefore, other bands could be present that are not in high enough concentration to be detected with this particular substrate. Figure 26 shows a blot of recombinant proteins after probing with the appropriate antibodies.

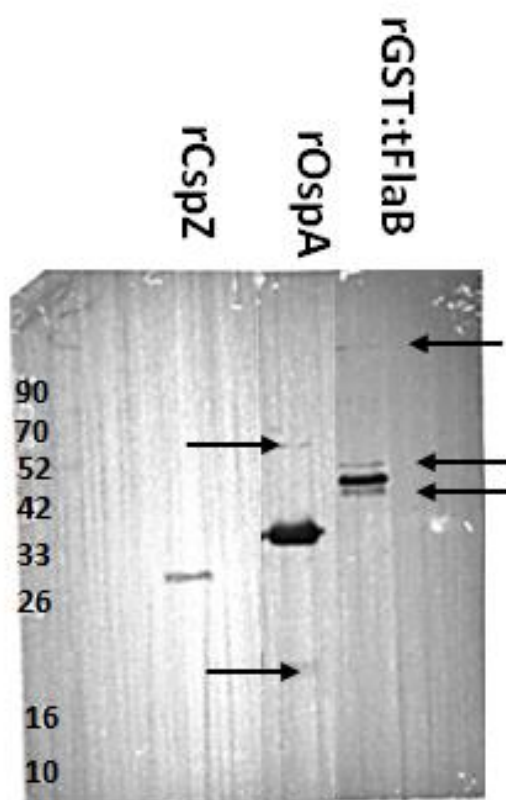


FIG 26. Immunoblots of 500ng of recombinant protein probed with the proper antibodies. Anti-rCspZ had the highest specificity with only one band recognized. Blotting revealed impurities (arrows) with host *E. coli* proteins in the recombinant protein solutions of rOspA and rGST:tFlaB. The non-specific bands produced by the impurities did not produce more intense signals than the bands correlating to the recombinant proteins. As expected, rCspZ was ~27kDa, rOspA was ~31kDa, and rGST:tFlaB was ~ 45kDa. Protein standards (kDa) are indicated to the left of the image.

***Borrelia burgdorferi* expression of CspZ in different host environments**

For protein expression analysis of CspZ in *B. burgdorferi*, spirochetes were grown at 23°C (tick environment), temperature-shifted from 23°C to 34°C (transmission from tick to mammalian host), or host adapted (HA, mammalian environment) in dog serum to mimic the enzootic life cycle of *B. burgdorferi*. Two strains of *B. burgdorferi* were used: B31MI which is infectious and contains the entire genome with all plasmids and B31cF which is clone lacking several plasmids including lp28-3 which harbors CspZ. B31cF should be positive for FlaB and OspA but negative for CspZ. Whole cell lysates were prepared from the cultures grown at the various conditions above to examine if CspZ is upregulated in mammalian environments by *B. burgdorferi*. B31cF was not host adapted in dog serum as it does not survive. *Borrelial* whole cell lysates were then separated via SDS-PAGE and transferred to nitrocellulose membranes for detection with enhanced chemiluminescence (ECL). FlaB, a constitutively expressed protein, was used as a loading control to ensure equal loading of whole cell lysates to each lane. OspA was used to ensure proper conditions were achieved during *in vitro* cultivation as the protein's response to these conditions is well documented (108, 109). Recombinant proteins were also loaded to ensure antibodies used were working properly.

Results of ECL immunoblotting to determine protein expression profiles of the proteins is shown in figure 27. Whole cell lysates were visually determined to be loaded equally as FlaB bands were of similar intensity across all lysates. OspA was able to be detected in all lysates, but no discernable difference was observed in the expression of OspA across the different conditions except in host-adapted lysate. CspZ was unable to be detected in any of the whole cell lysate preparations. The ECL kit used can detect proteins to the low picogram and high femtogram, yet

a band of 27kDa was never detected in any lysate when probed with anti-rCspZ. Recombinant CspZ was detected by the antibodies on the blot.

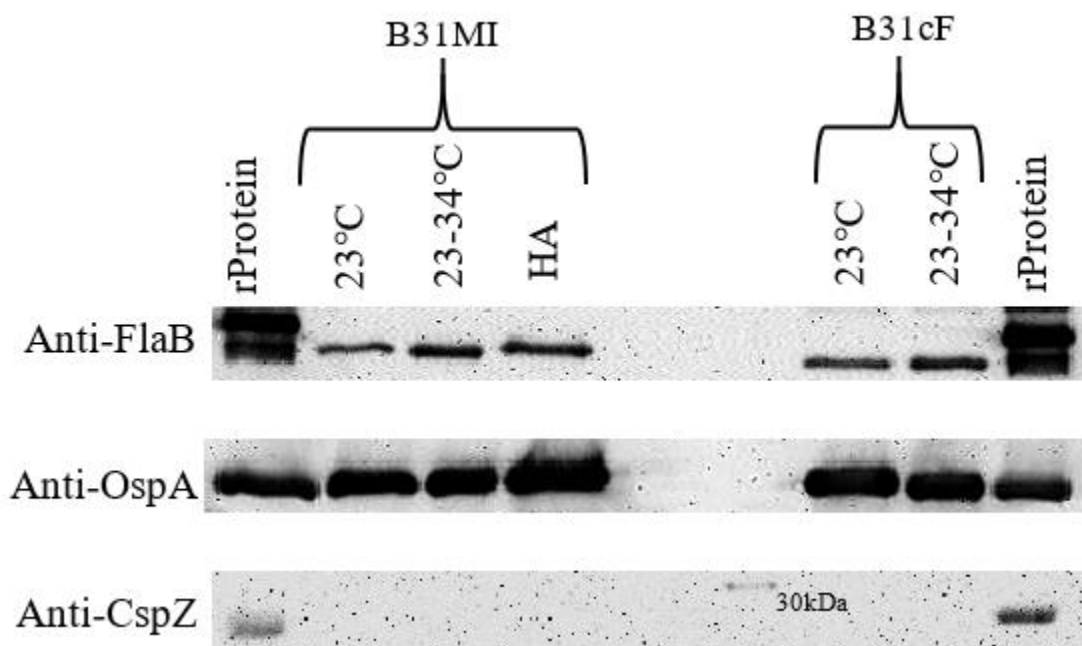


FIG 27. ECL immunoblotting of *Borrelia* whole cell lysates. FlaB was expressed across all lysates and demonstrates visually the lysates were loaded equally across the lanes and different blots. OspA showed similar expression levels in both B31MI and B31cF regardless of environmental conditions except for the host-adapted lysate (HA). OspA appears to be expressed slightly higher in B31MI when cultivated in 20% dog serum. CspZ was not able to be detected in any whole cell lysate preparation regardless of strain. Prestained protein markers are not visible under chemiluminescence except for the 80kDa and 30kDa bands. The 30kDa band is visible and labeled above.

Recognition of native CspZ protein by anti-CspZ

CspZ was undetectable in whole cell lysates when the lysates were prepared for SDS-PAGE resulting in denaturation and then used for immunoblotting. To see if this was due to a lack of detectable CspZ in lysates or if the antibodies raised in rats can only recognize native (non-reduced and non-denatured) CspZ protein, a dot-blot was performed on temperature shifted B31MI whole cell lysates that were not treated with sampling buffer containing β -mercaptoethanol (β ME, reducing agent) and SDS (denaturing agent) but rather resuspended in 1X PBS only. Anti-CspZ was indeed able to detect native protein located in the whole cell lysates which is shown in figure 28 below. It is visually evident that CspZ is not expressed as much as FlaB and OspA when the dot-blot is compared. Given that all the controls resulted in minimal or no background signal, the majority of the signal visualized is due to an antibody-antigen interaction.

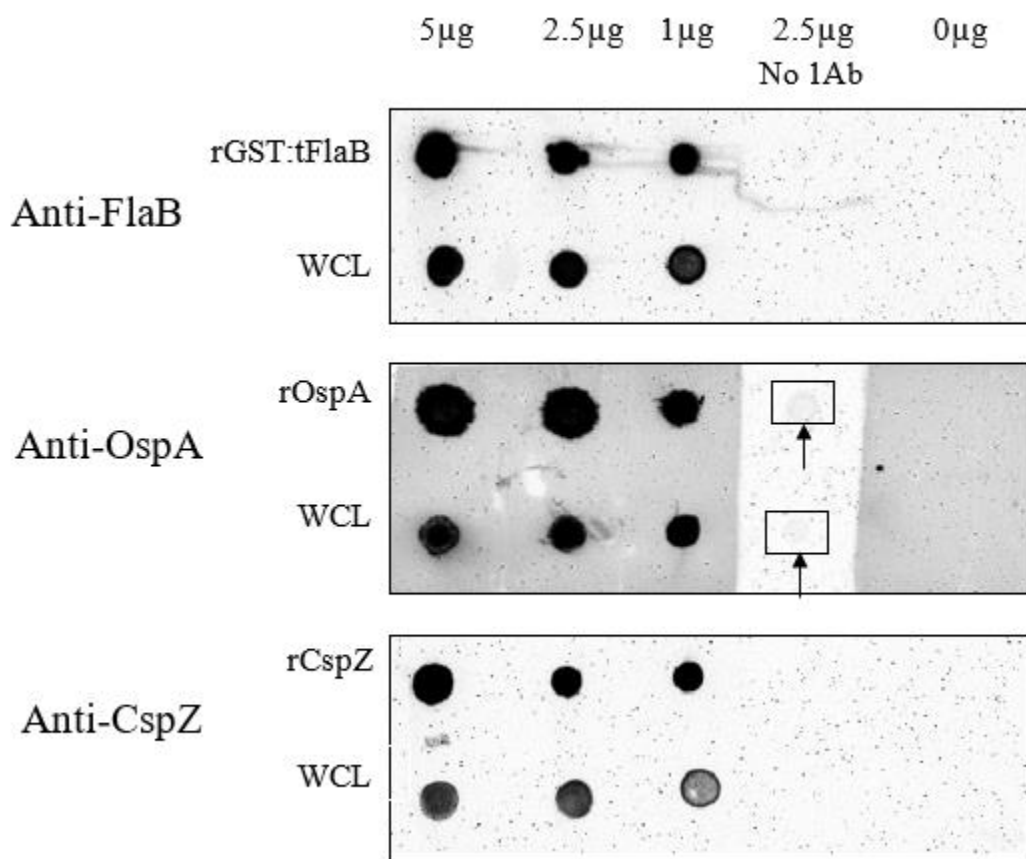


FIG 28. Native dot-blot of recombinant proteins and *Borrelia* whole cell lysates. Different amounts of recombinant protein (rProtein) or whole cell lysate (WCL) indicated above were spotted onto gridded squares of a nitrocellulose membrane strip and incubated with appropriate antibody indicated to the left. No signal was detected for the 0µg of protein controls. rFlaB and rCspZ had no background signal produced in the no primary antibody control (No 1Ab). rOspA had a slight signal produced (arrow and box) with just secondary antibody, but it was hardly visible. WCL incubated with no primary antibody also produced a small signal (arrow and box) shown in the anti-OspA strip. The signal intensities for the three proteins is much higher than the background indicating the background is not the predominant signal observed. All three antibodies recognize native protein located in the WCL. Images displayed are after 5 min exposure.

Cell surface localization of CspZ via indirect immunofluorescence

In order to be a good vaccine target, the target antigen must be accessible to the immune system of the host. Since CspZ is known to be insensitive to protease treatment such as with proteinase K, an indirect immunofluorescence assay (IFA) was used to determine the cell surface localization of CspZ (89, 95). FlaB is located in the periplasmic space and therefore not cell surface localized. It was used as a negative cell surface control. OspA on the other hand is a known outer surface protein of *B. burgdorferi* and was used as a positive outer surface control. B31MI spirochetes were incubated with the appropriate primary antibodies either after acetone permeabilization (fixed control) or prior to acetone fixation (unfixed). Slides for both the fixed and unfixed cells were counterstained with DAPI to locate spirochetes within a given field. The fixed control was performed to ensure antibody recognition of the proteins and serve as a comparison to the unfixed cells. All three proteins, CspZ, FlaB, and OspA were detected with antibodies in the fixed control. The IFA results of the fixed control are below in figure 29.

Results of the cell surface localization IFA are shown in figure 30. Both the FlaB and OspA controls worked as expected indicating the assay was performed correctly. No green fluorescence by the Alex Fluor 488 conjugated secondary antibody was detected in the unfixed FlaB slide. DAPI counterstaining indicated that there were spirochetes in the observed field of view. This indicates that the spirochete membranes were intact, and any cell-surface localization detected in the other samples was not due to membrane damage from miss-handling of the cells. Anti-OspA antibodies produced a continuous green signal spanning the entirety of a cell, and every cell identified in the given field of view by DAPI was fluorescing. IFA of unfixed cells treated with anti-CspZ yielded mixed results. The majority of spirochetes identified by DAPI in a given field of view did not produce a green fluorescence, however, every few fields a spirochete

or two were visible and green. A spirochete that was detected by both DAPI and Alexa Fluor 488 is circled in figure 30.

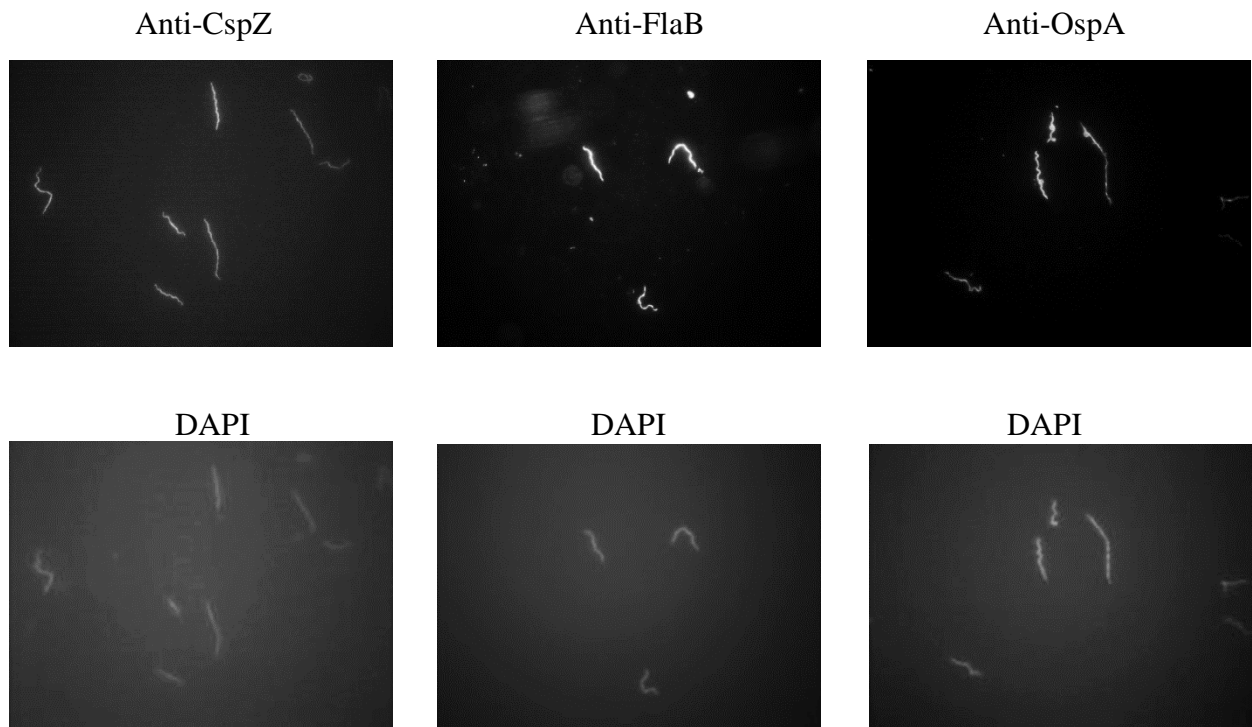


FIG 29. A control of fixed spirochetes via indirect immunofluorescence. Permeabilization of cells followed by primary antibody incubation produced fluorescence in all spirochetes within a given field of view for all three protein targets. All images are at 1000x magnification.

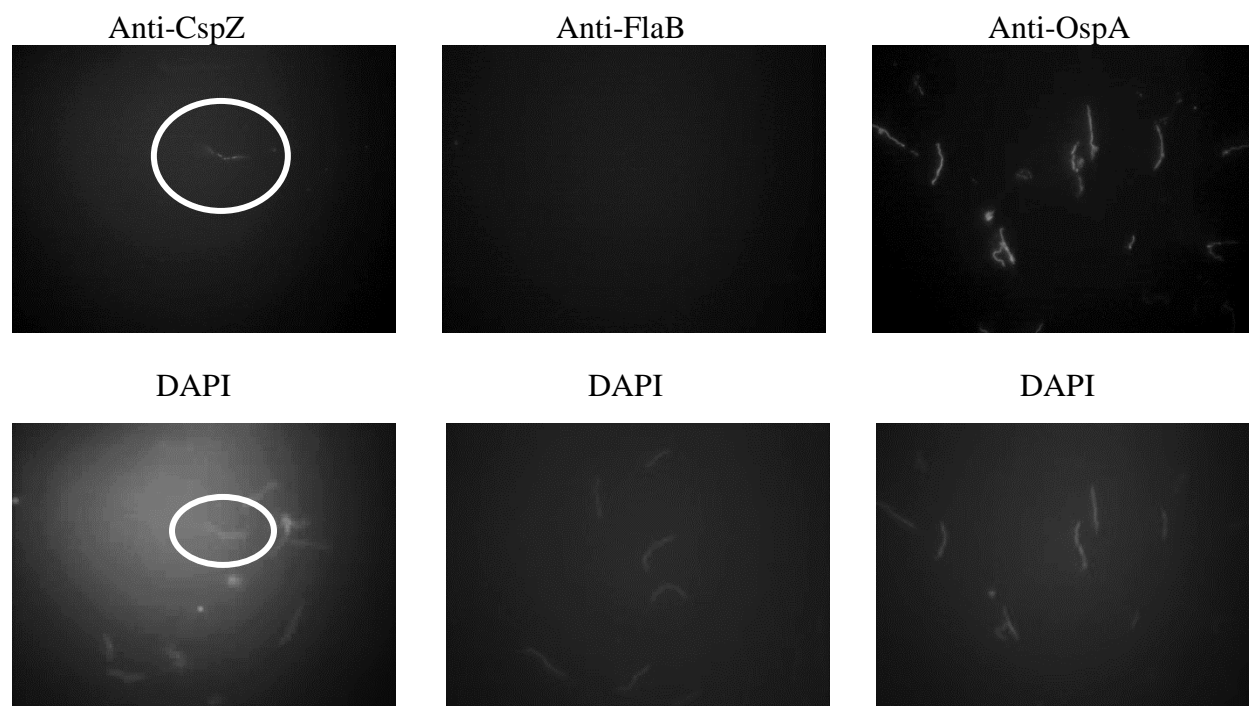


FIG 30. Cell-surface (unfixed cells) localization via indirect immunofluorescence. FlaB was not detected by anti-FlaB antibodies resulting in no fluorescence. The spirochete membrane was therefore intact. OspA was identified on the surface of spirochetes indicating the procedure was performed correctly. CspZ was not detected on the surface of every spirochete visualized by DAPI counterstaining per field of view. A few spirochetes, however, were detected and potentially have CspZ surface exposed such as the one circled above. The same spirochete is circled in the DAPI image to show it is not an artifact. All images are at 1000x magnification.

CspZ deficient B31cF dies in the presence of dog serum

The serum sensitivity of two *B. burgdorferi* strains B31MI and B31cF was tested. The results of the assay are displayed below in figure 31. Both B31MI and B31cF survived in heat inactivated serum. B31MI was resistant to 20% normal dog serum showing no statistical significance in spirochete concentration when compared to the heat inactivated control over the course of 16 hours. B31cF, however, was serum sensitive with total death occurring at 16h. A significant difference ($p < 0.05$) was found between B31cF exposed to normal dog serum when compared to the heat inactivated control.

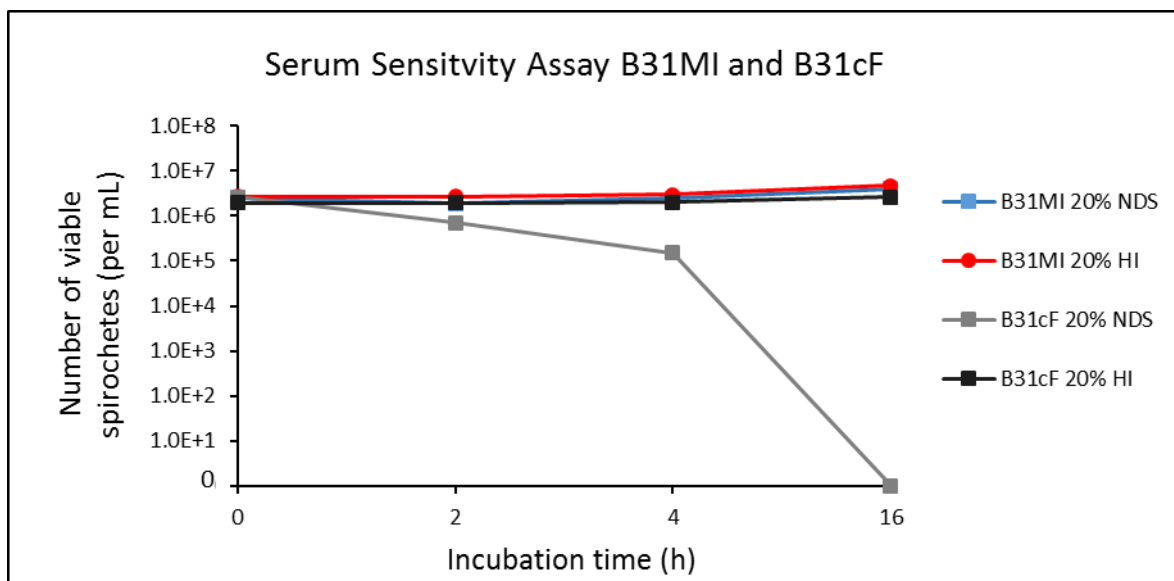


FIG 31. Serum sensitivity assay results. *B. burgdorferi* strains B31MI and B31cF were both challenged to 20% dog serum. The concentration of surviving spirochetes was measured over time. Both were compared to their respective heat inactivated controls. B31MI survives in the presence of 20% dog serum. There was no significant difference detected between B31MI exposed to normal dog serum versus the heat inactivated control. B31cF does not survive in the presence of normal dog serum. A significant difference was detected between B31cF exposed to normal dog serum versus the heat inactivated control ($p < 0.05$).

CHAPTER IV

Discussion

Generation of the plasmid constructs pGEX:tcspZ, pGEX:tospA, and pGEX:tflaB

To be able to generate recombinant proteins, plasmid constructs must be designed to ensure proper transcription and translation of the gene and protein in the chosen host. For protein expression to be successful, it is crucial that the gene of interests be inserted in frame with the GST fusion protein. The first step of creating the plasmid constructs for each gene of interest *cspZ*, *ospA*, and *flaB* was designing primers to include restriction sites for BamHI and XhoI located within the multiple cloning site of pGEX 4T-3. The sequences of the genes and vector were analyzed to ensure primers resulted in in-frame cloning and proper orientation of the insert within the expression vector using the ExPASy Translate Tool (Swiss Institute of Bioinformatics, Lausanne, Switzerland), NCBI nucleotide database, and BLAST (Basic Local Alignment Search Tool) (National Center for Biotechnology Information, Bethesda, MD). In addition, hydrophobicity plots were created and examined to determine the signal peptide sequence of the proteins. The genes of interest were then truncated by designing primers that exclude the signal peptide sequence to result in the mature version of the proteins.

Correct cloning of the plasmid constructs was confirmed by colony PCR and restriction enzyme analysis. All amplicons resulted in the appropriate sizes of the genes. Restriction enzyme analyses showed that the linearized constructs are larger than parental pGEX 4T-3 indicating the presence of an insert. Double digestion with BamHI and XhoI of the recombinant plasmids produced two bands corresponding to the size of linearized pGEX 4T-3 and the genes of interest. Orientation specific primers used for colony PCR on selected transformants resulted in

amplicons which can only result if the genes are inserted properly. Sequencing of pGEX:*tcspZ* revealed a single point mutation, but it did not result in a different amino acid being translated. This indicates a 100% sequence homology to native *cspZ* in the BLAST database and that the proper and functional protein will be generated during expression. Taken collectively the data shows that the genes of interest were properly inserted into the expression vector pGEX 4T-3 to result in three constructs: pGEX:*tcspZ*, pGEX:*tospA*, and pGEX:*tflaB*. Each construct did result in protein expression of their respective proteins.

Protein expression and purification

Protein expression and purification was achieved for each truncated protein of interest. Optimization of protein induction and expression included altering IPTG concentration, length of incubation, incubation temperature and utilization of an *E. coli* host strain BL21 DE3 which is optimized for protein expression. For GST:tCspZ and GST:tOspA, using 0.5mM IPTG and incubation for four hours at 34-37°C resulted in optimal protein overexpression. Initially, purification of the full length flagellar protein FlaB was attempted. If the fusion proteins are soluble, insoluble fractions should not show protein bands at the approximate kDa, while soluble fractions do. Although plenty of GST:FlaB was overexpressed, all of the fusion protein remained in the insoluble fraction likely in inclusion bodies. Attempts were made to shift the expression into the soluble fraction by changing the induction parameters listed previously, but it was not successful. Extraction from inclusion bodies is possible through methods such as urea denaturation and then refolding, however, the construct was instead re-cloned to produce a truncated version of FlaB (110, 111). This truncated version of FlaB is the immunodominant region of the protein that is roughly 13kDa (105). For GST:tFlaB, induction had to be performed at room temperature overnight with 0.5mM or 1mM IPTG to result in soluble protein expression.

Successful protein expression can be visualized after SDS-PAGE via Coomassie blue staining by comparing whole cell lysates of induced cultures versus un-induced (no IPTG) cultures. New protein bands appeared in the whole cell lysates of *E. coli* containing the recombinant expression vectors at a size corresponding to GST plus the size of the protein of interest. The parental pGEX 4T-3 vector had a protein band corresponding to the size of the fusion partner GST only. At the anticipated fusion protein sizes, a protein band appeared

indicating overexpression of the fusion proteins. All plasmid constructs resulted in successful protein expression as protein bands were seen in each whole cell lysate preparation.

Protein studies and immunization, however, need to be done on purified proteins. The proteins of interest were separated from host *E. coli* proteins through ligand affinity chromatography. Sepharose beads covalently bound to glutathione capture glutathione S-transferase (GST) tagged proteins while the *E. coli* host proteins are washed away (111). In addition, if the proteins need to be freed of GST moiety, a thrombin cleavage site is built into the expression vector. Due to the small size of tFlaB, it was left fused to GST to ensure it was large enough for antibodies to be produced. GST:tFlaB was able to be purified away from the majority of host proteins resulting in about 80-85% purity assessed visually by Coomassie staining after SDS-PAGE. It should be noted that Coomassie staining has a sensitivity of approximately 100ng of protein so impurities below that limit would not be detected. The bands that carried over from the purification process were likely caused by over-sonication of the lysates and are likely *E. coli* chaperones aiding the folding of the proteins which are commonly the cause of erroneous bands present after purification (111).

The GST moiety was cleaved by thrombin from tCspZ and tOspA. The cleavage incubation time that resulted in the lowest amount of fusion protein (examined band visually) left in the beads and most cleaved protein in the eluate was chosen as optimal. After cleavage, proteins were separated by SDS-PAGE and stained to estimate purity. Upon cleavage of proteins, most proteins are approximately 90% pure (111). The gels of cleaved tCspZ and tOspA did not reveal any impurities and were likely ~90% pure, and the proteins were of the anticipated sizes at ~27kDa and ~31kDa respectively. For the purposes of this study, no further purification was required. A total of 300 μ g of each recombinant protein was required for the immunization of

two rats for each protein. Quantitation of the proteins was carried out through a Bradford Coomassie assay and through generation of the standard curve using BSA. Although the Bradford assay has a lot of variation depending on the standard used and amino acid content of the proteins of interest, it was reliable enough that immunizations with 50 μ g of protein calculated by the assay resulted in successful antibody generation.

Immunoblotting of recombinant proteins

Before any experimental procedures were performed that required the generated antibodies, they were titrated to determine the optimal concentration of primary and secondary antibody to use with dot blotting. While dot-blotting provides quick information on the quantities of proteins and optimal antibody concentrations, they are limited in that there is no information provided about antibody specificity. In addition, dot-blotting does not require the transferring of proteins from a gel to a membrane which requires optimization to ensure proteins are transferred properly and able to be detected. Before western blotting was performed on precious experimental lysates, blotting was performed on purified recombinant proteins to ensure that there was recognition of denatured proteins and to optimize transfer conditions. Antibodies against rCspZ, rOspA, and rFlaB resulted in predominant bands at the appropriate sizes for each protein. The impurities carried over from protein purification of rOspA and rFlaB were visible on the immunoblot that were not on the Coomassie stained gels, however, the signal produced by the bands corresponding to the actual proteins was much higher than the erroneous bands. If some cross-reactivity of the antibodies occurs due to these *E. coli* proteins to *Borrelia* proteins, the erroneous bands are not the same size of the target proteins and should be discernable. Overall, the proteins purified were pure enough to create specific antibodies against the target proteins.

Determining CspZ expression in Borrelia burgdorferi grown in vitro

The results of the immunoblot revealed that FlaB was expressed consistently across all conditions and that equal amounts of lysate were loaded in each lane for each experimental condition. This means that changes observed for the other proteins were not due to over or underloading of the gel in certain lanes but to the actual conditions exposed on the spirochetes. OspA showed no substantial changes in protein expression across the temperature conditions consistent with other work done on this protein (86, 109, 112). There was also no discernable difference in OspA expression between the two strains either. For the host adapted condition, however, OspA produced a band with greater intensity. OspA is largely involved in allowing spirochete survival in the midguts of ticks, not in mammalian infection (113). Unfortunately, CspZ was undetectable in all whole cell lysate preparations including host adaptation in normal dog serum. Even when the amount of whole cell lysate added to each well was quadrupled (data not shown), no CspZ was detected.

In vitro culture conditions have been shown to alter protein expression of many proteins of *Borrelia* in comparison to natural infections (114). Other aspects of laboratory cultivation that affect expression of proteins in *Borrelia* include pH and cell density (88, 115). Since the host adapted condition used was temperature shifting spirochetes into media containing 20% dog serum, acidification of the media could have occurred much faster as some spirochetes initially might not have survived the exposure. Bykowski et al. postulated that media acidification could send mixed environmental cues as the tick midgut is acidic. This could explain the observed increase in OspA expression as well as decreased CspZ expression as it is a protein expressed during established mammalian infection and not tick midguts. In general, CspZ is poorly expressed *in vitro*. In the Bykowski et al. study, the highest level of *cspZ* expression achieved in

culture was at 23°C at a pH of 8.0 resulting in 0.025ng of *cspZ* mRNA expressed for every 1ng of *flaB* expressed. *In vivo* *cspZ* is expressed far more. Infected mouse tissues yielded 0.44ng of *cspZ* mRNA for every 1ng of *flaB* (88). This makes it difficult to study CspZ, and its overall suitability as a vaccine candidate since most *B. burgdorferi* research is done *in vitro*. More methods like host adaptation will likely have to be employed to illicit better expression of this gene. One such example is using dialysis membrane chambers inoculated with spirochetes which are then implanted into the peritoneal cavities of small mammals such as rodents to mimic the host stage of Lyme disease infection. This method has shown to improve the expression of proteins that express poorly via conventional temperature shift experiments. This method also more accurately depicts the mammalian environment as proteins thought to be downregulated in mammals were indeed downregulated whereas during temperature shift experiments in culture they are still expressed (108).

Another possibility as to why CspZ was not detected in whole cell lysates could be the antibodies generated against rCspZ in the rats can only recognize full length CspZ in its native three-dimensional form. Native dot-blotting did result in the detection of proteins by anti-CspZ in whole cell lysates. Indirect immunofluorescence discussed below also resulted in detection of protein within spirochetes by anti-CspZ. Dot-blotting and immunofluorescence do not guarantee that CspZ was the main or single protein detected by the antibody, however, given the specificity of anti-CspZ for rCspZ, the fact that the *cspZ* gene is unlike any other gene in *B. burgdorferi*, and that the CspZ protein is highly divergent from the other CRASPs, native CspZ likely was the main protein detected in the lysates (89, 97, 98). Removal of the signal peptide, which corresponds to amino acids 1-19, should not have interrupted any ligand binding sites that might alter the immune response to CspZ. N-terminal truncations after the signal peptide do result in

ligand binding site interruption, but no such truncation was done in this study (89, 116, 117). While denaturing proteins for immunoblotting linearizes them and exposes all epitopes, the antibodies were raised against the protein in its three-dimensional shape. The epitopes the antibodies recognize could be grouped together and then become too spaced apart when denatured for the antibodies to bind. Adopting more native blotting conditions such as removal of reducing and denaturing agents might result in detection of CspZ by the anti-CspZ in lysate. In addition, rats might only raise sera against CspZ that are directed at native structural determinants. A different species of animal, such as a mouse, might raise antibodies that can detect the denatured protein as mouse anti-CspZ antibodies used in other studies have been able to detect this protein in a denatured state when immunoblotting (89, 88, 95, 98). Alternatively, a switch from antigen antibody blotting (CspZ→anti-CspZ) to ligand affinity blotting (CspZ→Factor H or FH-1 protein→anti-Factor H or FH-1) might be the better alternative as this technique has extensively been used in the study of CRASPs (83, 89, 87, 98, 100, 117, 118, 94).

Cell surface localization of CspZ

For the fixed cell control, anti-CspZ antibodies were able to detect the presence of CspZ proteins within fixed cells. FlaB and OspA were also detected indicating successful permeabilization of the cells. This ensured that when the cell-surface localization IFA was performed, a negative result was not due to the antibodies not binding antigen or recognizing CspZ. FlaB was not detected in the cell surface localization IFA. This means that the spirochete membranes remained intact and that only proteins on the surface were available for antibody binding. The OspA cell surface IFA was positive indicating the procedure worked. While CspZ was detected within cells of the fixed control, an inconclusive result was obtained for cell surface localization. For OspA, every spirochete within a field of view displayed green fluorescence strongly supporting prior data indicating OspA is cell surface localized.

Staining for CspZ, however, resulted in only one to two spirochetes per field displaying green fluorescence. DAPI counterstaining showed more than just the one or two spirochetes were present in the fields observed. Since the FlaB control showed the membrane was intact, the fluorescence observed had to come from an outer surface protein. The cell surface localization IFA was performed a total of three times. Each time the same result was achieved for CspZ. Hartmann et al. and Bykowski et al. performed cell surface localization of CspZ using IFA. CspZ was shown to be sparsely expressed on the surface of spirochetes indicated by a beaded pattern in both studies (89, 88). The Alexa Fluor 488 conjugate produced more nonspecific fluorescence when anti-CspZ was the primary antibody as compared to anti-OspA for the unfixed slides. Clarification of the image was made difficult because of this. Perhaps the use of a higher resolution microscope, such as a confocal, would reveal if the few spirochetes observed positive for CspZ did indeed display a beaded pattern of expression on the surface of the cell.

Serum sensitivity of B31MI and B31cF

If CspZ is required for *B. burgdorferi* to survive dog complement and establish infection, then B31cF, which lacks the plasmid carrying the *cspZ* gene, should die in the presence of normal dog serum. The serum sensitivity assay performed revealed B31MI to be dog serum resistant, while B31cF was serum sensitive. This corroborates with previous work done by Kay and Lund, however, B31cF took 16h for total killing to occur in this study but as little as 4h in the Lund study (101, 102). This variation may be attributed to the way the serum was handled and stored and how scoring of death was carried out, which is why some studies classify *B. burgdorferi* as intermediate dog serum sensitive while others classify it as fully dog serum resistant (119).

B31cF contains lp54 and therefore has *cspA*, which is thought to be the main CRASP for spirochete survival in other mammalian hosts such as humans. It also harbors a circular plasmid that contains the *erp* genes. These data supports that *B. burgdorferi* activates different complement regulators in a host dependent fashion (120). It also means that CspA and Erp proteins are not capable of imparting canine serum resistance to *B. burgdorferi*. Since rescuing Bb31cF with *cspZ* does provide canine serum resistance (102), a few hypotheses can be made:

1. CspZ alone is the main complement regulator for *B. burgdorferi* in canine hosts.
2. CspZ and CspA both contribute to spirochete complement resistance in canines by working in tandem.
3. CspZ alone does not confer resistance but must work with an Erp protein to result in *B. burgdorferi* canine serum resistance.

CHAPTER V

Conclusion

In conclusion, CspZ is a contributing factor to the survival of *B. burgdorferi* in a canine host. However, the present study could not determine if CspZ is the minimally necessary and sufficient CRASP in canine hosts or if it is a suitable vaccine target. This is due to the antibodies generated against CspZ only detecting native proteins, which hindered the ability to perform crucial experiments regarding protein expression such as western blotting and cellular localization via Triton X-114 phase partitioning that rely on immunoblotting. Using indirect immunofluorescence produced conflicting results with those in literature about the cell surface localization of CspZ and will require optimization of the protocol. In addition, the overall poor expression of CspZ *in vitro* makes it difficult to study in terms of determining how suitable of a vaccine target it is.

When B31cF, a clone lacking CspZ, are exposed to dog serum the culture dies by 16h. Rescuing B31cF with a shuttle vector containing *cspZ* denoted a pBSV2(FlgB:CspZ) results in B31cF regaining dog serum resistance and surviving (102). This does not however answer the question of if CspZ is the necessary and sufficient complement regulator-acquiring surface protein of *Borrelia burgdorferi* in canines, since B31cF still contains other CRASPs including CspA and the various Erp proteins. To determine if CspZ is the predominant CRASP, a knockout mutant deficient of all other CRASPs needs to be created and then subsequently rescued with CspZ. If that results in survival of the knockout strain when exposed to dog serum, then CspZ likely is the major CRASP involved in the survival of *B. burgdorferi* in canine hosts. If confirmed to be cell surface localized and responsible for dog serum resistance, CspZ would be an ideal vaccine target against canine Lyme disease, since it is a well conserved protein within *B.*

burgdorferi species, is involved in persistent mammalian infection, and produces a good immune response within hosts of the same species (88, 97–99)

REFERENCES

1. Mather TN, Fish D, Coughlin RT. 1994. Competence of dogs as reservoirs for Lyme disease spirochetes (*Borrelia burgdorferi*). *J. Am. Vet. Med. Assoc.* 205:186–188.
2. Stevenson B, El-hage N, Hines MA, Miller C, Miller JC, Babb K. 2002. Differential binding of host complement inhibitor factor H by *Borrelia burgdorferi* Erp surface proteins: a possible mechanism underlying the expansive host range of Lyme disease spirochetes. *Infect. Immun.* 70:491–497.
3. Burgdorfer W, Barbour AG, Hayes SF, Benach JL, Davis JP. 1982. Lyme disease a tick-borne spirochetosis? *Science* 216:1317–1319.
4. Steere AC, Grodzicki RL, Kornblatt AN, Craft JE, Barbour AG, Burgdorfer W, Schmid GP, Johnson E, Malawista SE. 1983. The spirochetal etiology of Lyme disease. *N. Engl. J. Med.* 308:733–740.
5. Johnson RC, Schmid GP, Hyde FW, Steigerwalt AG, Brenner DJ. 1984. *Borrelia burgdorferi* sp. nov.: etiologic agent of Lyme disease. *Int. J. Syst. Bacteriol.* 34:496–497.
6. Holt SC. 1978. Anatomy and chemistry of spirochetes. *Microbiol. Rev.* 42:114–60.
7. Barbour AG, Hayes SF. 1986. Biology of *Borrelia* species. *Microbiol. Rev.* 50:381–400.
8. Fraser CM, Casjens S, Huang WM, Sutton GG, Clayton R, Lathigra R, White O, Ketchum KA, Dodson R, Hickey EK, Gwinn M, Dougherty B, Tomb JF, Fleischmann RD, Richardson D, Peterson J, Kerlavage AR, Quackenbush J, Salzberg S, Hanson M, van Vugt R, Palmer N, Adams MD, Gocayne J, Weidman J, Utterback T, Wathley L, McDonald L, Artiach P, Bowman C, Garland S, Fuji C, Cotton MD, Horst K, Roberts K, Hatch B, Smith HO, Venter JC. 1997. Genomic sequence of a Lyme disease spirochaete, *Borrelia burgdorferi*. *Nature* 390:580–586.

9. Li C, Motaleb A, Sal M, Goldstein SF, Charon NW. 2000. Spirochete periplasmic flagella and motility. *J. Mol. Microbiol. Biotechnol.* 2:345–354.
10. Singh SK, Girschick HJ. 2004. Molecular survival strategies of the Lyme disease spirochete *Borrelia burgdorferi*. *Lancet Infect. Dis.* 4:575–583.
11. Srivastava SY, de Silva AM. 2009. Characterization of *Borrelia burgdorferi* aggregates. *Vector Borne Zoonotic Dis.* 9:323–9.
12. Sapi E, Bastian SL, Mpoy CM, Scott S, Rattelle A, Pabbati N, Poruri A, Burugu D, Theophilus PAS, Pham T V., Datar A, Dhaliwal NK, MacDonald A, Rossi MJ, Sinha SK, Luecke DF. 2012. Characterization of biofilm formation by *Borrelia burgdorferi* *in vitro*. *PLoS One* 7:1–11.
13. Margos G, Vollmer SA, Ogden NH, Fish D. 2011. Population genetics, taxonomy, phylogeny and evolution of *Borrelia burgdorferi* sensu lato. *Infect. Genet. Evol.* 11:1545–1563.
14. Baranton GUY, Postic D, Girons S, Boerlin P, Piffaretti J, Assous M, Grimont PAD. 1992. Delineation of *Borrelia burgdorferi* sensu stricto, *Borrelia garinii* sp. nov., and Group VS461 associated with Lyme borreliosis. *Int. J. Syst. Bacteriol.* 42:378–383.
15. Canica MM, Nato F, du Merle L, Mazie JC, Baranton G, Postic D. 1993. Monoclonal antibodies for identification of *Borrelia afzelii* sp. nov. associated with late cutaneous manifestations of Lyme borreliosis. *Scand. J. Infect. Dis.* 25:441–448.
16. Van Dam AP, Kuiper H, Vos K, Widjojokusumo A, de Jongh BM, Spanjaard L, Ramselaar ACP, Kramer MD, Dankert J. 1993. Different genospecies of *Borrelia burgdorferi* are associated with distinct clinical manifestations of Lyme borreliosis. *Clin. Infect. Dis.* 17:708–717.

17. Casjens S, Palmer N, Van Vugt R, Huang WM, Stevenson B, Rosa P, Lathigra R, Sutton G, Peterson J, Dodson RJ, Haft D, Hickey E, Gwinn M, White O, Fraser CM. 2000. A bacterial genome in flux: The twelve linear and nine circular extrachromosomal DNAs in an infectious isolate of the Lyme disease spirochete *Borrelia burgdorferi*. *Mol. Microbiol.* 35:490–516.
18. Barbour AG. 1984. Isolation and cultivation of Lyme disease spirochetes. *Yale J. Biol. Med.* 57:521–525.
19. Stevenson B, Schwan TG, Rosa PA. 1995. Temperature-related differential expression of antigens in the Lyme disease spirochete, *Borrelia burgdorferi*. *Infect. Immun.* 63:4535–4539.
20. Zückert WR. 2007. Laboratory maintenance of *Borrelia burgdorferi*. *Curr. Protoc. Microbiol.* 12C.1: doi: 10.1002/9780471729259.mc12c01s4.
21. Hyde, J.A., Weening, E.H. Skare JT. 2011. Genetic manipulation of *Borrelia Burgdorferi*. *Curr. Protoc. Microbiol.* 12C.4: doi: 10.1002/9780471729259.mc12c04s20.
22. Yang X, Popova TG, Goldberg MS, Norgard M V. 2001. Influence of cultivation media on genetic regulatory patterns in *Borrelia burgdorferi*. *Infect. Immun.* 69:4159–4163.
23. Wang G, Iyer R, Bittker S, Cooper D, Wormser GP, Schwartz I. 2004. Variations in Barbour-Stoenner-Kelly culture medium modulate infectivity and pathogenicity of *Borrelia burgdorferi* clinical isolates. *Infect. Immun.* 72:6702–6706.
24. Babb K, El-Hage N, Miller JC, Carroll JA, Stevenson B. 2001. Distinct regulatory pathways control expression of *Borrelia burgdorferi* infection-associated Ospc and Erp surface proteins. *Infect. Immun.* 69:4146–4153.

25. Barbour AG. 1988. Plasmid analysis of *Borrelia burgdorferi*, the Lyme disease agent. J. Clin. Microbiol. 26:475–478.
26. Schwan TG, Burgdorfer W, Garon CF. 1988. Changes in infectivity and plasmid profile of the Lyme disease spirochete, *Borrelia burgdorferi*, as a result of *in vitro* cultivation. Infect. Immun. 56:1831–1836.
27. Biškup UG, Strle F, Ružić-Sabljić E. 2011. Loss of plasmids of *Borrelia burgdorferi* sensu lato during prolonged *in vitro* cultivation. Plasmid 66:1–6.
28. Afzelius A. 1910. Report to Verhandlungen der dermatologischen Gesellschaft zu Stockholm on December 16, 1909. Arch. Dermatol. Syph. 101:405–406.
29. Steere AC, Malawista SE, Snyderman DR, Shope RE, Andiman WA, Ross MR, Steele FM. 1977. Lyme arthritis an epidemic of oligoarticular arthritis in children and adults in three Connecticut communities. Arthritis Rheum. 20:7–17.
30. Steere A. 2001. Lyme disease. N. Engl. J. Med. 345:115–125.
31. Bauman, RW, Primm, TP, Machunis-Masuoka E. 2017. Rickettsias, Chlamydias, Spirochetes, and Vibrios, p. 611–637. *In* Microbiology With Disease By Taxonomy. Fifth. Pearson Education , Inc.
32. Steere AC, Malawista SE, Bartenhagen NH, Spieler PN, Newman JH, Rahn DW, Hutchinson GJ, Green J, Snyderman DR, Taylor E. 1984. The clinical spectrum and treatment of Lyme disease. Yale J. Biol. Med. 57:453–461.
33. Center for Disease Control, CDC. 2017. Signs and Symptoms | Lyme Disease | CDC. http://www.cdc.gov/lyme/signs_symptoms/index.html

34. Steere AC, Batsford WP, Weinberg M, Alexander J, Berger HJ, Wolfson S, Malawista SE. 1980. Lyme carditis: cardiac abnormalities of Lyme disease. *Ann. Intern. Med.* 93:8–16.
35. Schwartz, AM, Hinckley, AK, Mead PS, Hook SA, Kugeler KJ. 2017. Surveillance for Lyme disease - United States, 2008-2015. *MMWR* 66:1–12.
36. Sigal LH. 1997. Lyme disease: a review of aspects of its immunology and immunopathogenesis. *Annu. Rev. Immunol.* 15:63–92.
37. Littman MP, Goldstein RE, Labato MA, Lappin MR, Moore GE. 2006. ACVIM small animal consensus statement on Lyme disease in dogs: diagnosis, treatment, and prevention. *J. Vet. Intern. Med.* 20:422–434.
38. Little SE, Heise SR, Blagburn BL, Callister SM, Mead PS. 2010. Lyme borreliosis in dogs and humans in the USA. *Trends Parasitol.* 26:213–8.
39. Center for Disease Control, CDC. 2017. Treatment | Lyme Disease | CDC. <https://www.cdc.gov/lyme/treatment/index.html>
40. Steere AC, Angelis SM. 2006. Therapy for Lyme arthritis strategies for the treatment of antibiotic-refractory arthritis. *Arthritis Rheum.* 54:3079–3086.
41. Piesman J, Eisen L. 2008. Prevention of tick-borne diseases*. *Annu. Rev. Entomol.* 53:323–343.
42. Garnett JM, Connally NP, Stafford KC, Cartter ML. 2011. Evaluation of deer-targeted interventions on Lyme disease incidence in Connecticut. *Public Health Rep.* 126:446–54.
43. Piesman J, Mather TN, Sinsky RJ, Spielman A. 1987. Duration of tick attachment and *Borrelia burgdorferi* transmission. *J. Clin. Microbiol.* 25:557–558.

44. Steere AC, Sikand VK, Meurice F, Parenti DL, Fikrig E, Schoen RT, Nowakowski J, Schmid CH, Laukamp S, Buscarino C, Krause DS. 1998. Vaccination against Lyme disease with recombinant *Borrelia burgdorferi* outer-surface lipoprotein A with adjuvant. *N. Engl. J. Med.* 339:209–215.
45. Poland GA. 2011. Vaccines against lyme disease: What happened and what lessons can we learn? *Clin. Infect. Dis.* 52:253–258.
46. Fikrig E, Barthold SW, Kantor FS, Flavell RA. 1990. Protection of mice against the Lyme disease. *Science* 250:553–556.
47. de Silva AM, Telford SR, Brunet LR, Barthold SW, Fikrig E. 1996. *Borrelia burgdorferi* OspA is an arthropod-specific transmission-blocking Lyme disease vaccine. *J. Exp. Med.* 183:271–5.
48. Dennis DT, Hayes EB, Orloski KA, Meltzer MI. 1999. Recommendations for the use of Lyme disease vaccine recommendations of the advisory committee on immunization practices (ACIP). *MMWR* 48:1–17.
49. Steere AC, Drouin EE, Glickstein LJ. 2011. Relationship between immunity to *Borrelia burgdorferi* Outer-surface Protein A (OspA) and lyme arthritis. *Clin. Infect. Dis.* 52:259–265.
50. Bacon RM, Kugeler KJ, Mead PS. 2008. Surveillance for Lyme disease--United States, 1992-2006. *MMWR Surveill. Summ.* 57:1–9.
51. Eisen RJ, Eisen L, Beard C. 2016. County-scale distribution of *Ixodes scapularis* and *Ixodes pacificus* (Acari: Ixodidae) in the continental United States. *J. Med. Entomol.* 53:349–386.

52. Töpfer KH, Straubinger RK. 2007. Characterization of the humoral immune response in dogs after vaccination against the Lyme borreliosis agent. A study with five commercial vaccines using two different vaccination schedules. *Vaccine* 25:314–326.
53. Center for Disease Control, CDC. 2017. Data and Statistics | Lyme Disease | CDC. <http://www.cdc.gov/lyme/stats/index.html>
54. Center for Disease Control, CDC. 2017. How many people get Lyme disease? | Lyme Disease | CDC. <http://www.cdc.gov/lyme/stats/humancases.html>
55. Lane RS, Piesman J, Burgdorfer W. 1991. Lyme borreliosis : relation of its causative agent to its vectors and hosts in North America and Europe. *Annu. Rev. Entomol.* 36:587–509.
56. Barbour A, Fish D. 1993. The biological and social phenomenon of Lyme disease. *Science* 260:1610–1616.
57. Steere AC, Malawista SE. 1977. Cases of Lyme disease in the United States: localities correlated with distribution of *Ixodes dammini*. *Ann. Intern. Med.* 91:730–733.
58. Jones CG, Ostfeld RS, Richard MP, Schaubert EM, Wolff JO. 1998. Chain reactions linking acorns to gypsy moth outbreaks and Lyme disease risk. *Science* 279:1023–1026.
59. Lastavica CC, Wilson ML, Berardi VP, Spielman A, Deblinger RD. 1989. Rapid emergence of a focal epidemic of Lyme disease in coastal Massachusetts. *N. Engl. J. Med.* 320:133–137.
60. Dennis DT, Nekomoto TS, Victor JC, Paul WS, Piesman J. 1998. Reported distribution of *Ixodes scapularis* and *Ixodes pacificus* (Acari: Ixodidae) in the United States. *J. Med. Entomol.* 35:629–638.

61. Steere AC, Coburn J, Glickstein L. 2004. The emergence of Lyme disease. *J. Clin. Invest.* 113:1093–1101.
62. Radolf JD, Caimano MJ, Stevenson B, Hu LT. 2012. Of ticks, mice and men: understanding the dual-host lifestyle of Lyme disease spirochaetes. *Nat. Rev. Microbiol.* 10:87–99.
63. Hovius JWR, van Dam AP, Fikrig E. 2007. Tick–host–pathogen interactions in Lyme borreliosis. *Trends Parasitol.* 23:434–438.
64. Center for Disease Control, CDC. 2017. Lyme disease transmission| Lyme Disease | CDC. <http://www.cdc.gov/lyme/transmission/index.html>
65. Schwan TG, Piesman J, Golde WT, Dolan MC, Rosa PA. 1995. Induction of an outer surface protein on *Borrelia burgdorferi* during tick feeding. *Proc. Natl. Acad. Sci. USA* 92:2909–2913.
66. Suk K, Das S, Sun W, Jwang B, Barthold SW, Flavell RA, Fikrig E. 1995. *Borrelia burgdorferi* genes selectively expressed in the infected host. *Proc. Natl. Acad. Sci. USA* 92:4269–4273.
67. Schwan TG, Piesman J. 2000. Temporal changes in outer surface proteins A and C of the Lyme disease- associated spirochete, *Borrelia burgdorferi*, during the chain of infection in ticks and mice. *J. Clin. Microbiol.* 38:382–388.
68. Hefty PS, Jolliff SE, Caimano MJ, Wikel SK, Akins DR. 2002. Changes in temporal and spatial patterns of outer surface lipoprotein expression generate population heterogeneity and antigenic diversity in the Lyme disease spirochete, *Borrelia burgdorferi*. *Infect. Immun.* 70:3468–3478.

69. Brooks CS, Hefty PS, Jolliff SE, Akins DR. 2003. Global analysis of *Borrelia burgdorferi* genes regulated by mammalian host-specific signals. *Infect. Immun.* 71:3371–3383.
70. Pal U, Yang X, Chen M, Bockenstedt LK, Anderson JF, Flavell RA, Norgard MV, Fikrig E. 2004. OspC facilitates *Borrelia burgdorferi* invasion of *Ixodes scapularis* salivary glands. *J. Clin. Invest.* 113:220–30.
71. Grimm D, Tilly K, Byram R, Stewart PE, Krum JG, Bueschel DM, Schwan TG, Policastro PF, Elias AF, Rosa PA. 2004. Outer-surface protein C of the Lyme disease spirochete: a protein induced in ticks for infection of mammals. *Proc. Natl. Acad. Sci. USA* 101:3142–7.
72. Yang XF, Pal U, Alani SM, Fikrig E, Norgard MV. 2004. Essential role for OspA/B in the life cycle of the Lyme disease spirochete. *J. Exp. Med.* 199:641–8.
73. Zhang JR, Hardham JM, Barbour AG, Norris SJ. 1997. Antigenic variation in Lyme disease *Borreliae* by promiscuous recombination of VMP-like sequence cassettes. *Cell* 89:275–285.
74. Zhang JR, Norris SJ. 1998. Genetic variation of the *Borrelia burgdorferi* gene vlsE involves cassette-specific, segmental gene conversion. *Infect. Immun.* 66:3698–3704.
75. Eicken C, Sharma V, Klabunde T, Lawrenz MB, Hardham JM, Norris SJ, Sacchettini JC. 2002. Crystal structure of Lyme disease variable surface antigen vlsE of *Borrelia burgdorferi*. *J. Biol. Chem.* 277:21691–21696.
76. McDowell JV., Sung SY, Hu LT, Marconi RT. 2002. Evidence that the variable regions of the central domain of VlsE are antigenic during infection with Lyme disease spirochetes. *Infect. Immun.* 70:4196–4203.

77. Posey JE. 2000. Lack of a role for iron in the Lyme disease pathogen. *Science* 288:1651–1653.
78. Stevenson B, Tilly K, Rosa PA. 1996. A family of genes located on four separate 32-kilobase circular plasmids in *Borrelia burgdorferi* B31. *J. Bacteriol.* 178:3508–3516.
79. Casjens S, Van Vugt R, Tilly K, Rosa PA, Stevenson B. 1997. Homology throughout the multiple 32-kilobase circular plasmids present in lyme disease spirochetes. *J. Bacteriol.* 179:217–227.
80. Stevenson B, Casjens S, Rosa P. 1998. Evidence of past recombination events among the genes encoding the Erp antigens of *Borrelia burgdorferi*. *Microbiology* 144:1869–1879.
81. Stewart PE, Byram R, Grimm D, Tilly K, Rosa PA. 2005. The plasmids of *Borrelia burgdorferi*: essential genetic elements of a pathogen. *Plasmid* 53:1–13.
82. Purser JE, Norris SJ. 2000. Correlation between plasmid content and infectivity in *Borrelia burgdorferi*. *Proc. Natl. Acad. Sci. USA* 97:13865–13870.
83. Zipfel PF, Skerka C, Hellwage J, Jokiranta ST, Meri S, Brade V, Kraiczy P, Noris M, Remuzzi G. 2002. Factor H family proteins: on complement, microbes and human diseases. *Biochem. Soc. Trans.* 30:971–978.
84. de Taeye SW, Kreuk L, van Dam AP, Hovius JW, Schuijt TJ. 2013. Complement evasion by *Borrelia burgdorferi*: It takes three to tango. *Trends Parasitol.* 29:119–128.
85. Kraiczy P, Skerka C. 2001. Immune evasion of *Borrelia burgdorferi* by acquisition of human complement regulators FHL-1/reconnectin and Factor H. *Eur. J. Immunol.* 31:1674–1684.
86. Brooks CS, Vuppala SR, Jett AM, Akins DR. 2006. Identification of *Borrelia burgdorferi* outer surface proteins. *Infect. Immun.* 74:296–304.

87. Kraiczy P, Skerka C, Brade V, Peter F. 2001. Further characterization of complement regulator-acquiring surface proteins of *Borrelia burgdorferi*. *Infect. Immun.* 69:7800–7809.
88. Bykowski T, Woodman ME, Cooley AE, Brissette CA, Brade V, Wallich R, Kraiczy P, Stevenson B. 2007. Coordinated expression of *Borrelia burgdorferi* complement regulator-acquiring surface proteins during the Lyme disease spirochete's mammal-tick infection cycle. *Infect. Immun.* 75:4227–36.
89. Hartmann K, Corvey C, Skerka C, Kirschfink M, Karas M, Brade V, Miller JC, Stevenson B, Wallich R, Zipfel PF, Kraiczy P. 2006. Functional characterization of BbCRASP-2, a distinct outer membrane protein of *Borrelia burgdorferi* that binds host complement regulators factor H and FHL-1. *Mol. Microbiol.* 61:1220–1236.
90. Kraiczy P, Hellwage J, Skerka C, Becker H, Kirschfink M, Simon MM, Brade V, Zipfel PF, Wallich R. 2004. Complement resistance of *Borrelia burgdorferi* correlates with the expression of BbCRASP-1, a novel linear plasmid-encoded surface protein that interacts with human factor H and FHL-1 and is unrelated to Erp proteins. *J. Biol. Chem.* 279:2421–9.
91. Kraiczy P, Hellwage J, Skerka C, Kirschfink M, Brade V, Zipfel PF, Wallich R. 2003. Immune evasion of *Borrelia burgdorferi*: mapping of a complement inhibitor factor H-binding site of BbCRASP-3, a novel member of the Erp protein family. *Eur. J. Immunol.* 33:697–707.
92. Haupt K, Kraiczy P, Wallich R, Brade V, Skerka C, Zipfel PF. 2007. Binding of human factor H-related protein 1 to serum-resistant *Borrelia burgdorferi* is mediated by *Borrelial* complement regulator-acquiring surface proteins. *J. Infect. Dis.* 196:124–133.

93. Siegel C, Hallström T, Skerka C, Eberhardt H, Uzonyi B, Beckhaus T, Karas M, Wallich R, Stevenson B, Zipfel PF, Kraiczy P. 2010. Complement factor H-related proteins CFHR2 and CFHR5 represent novel ligands for the infection-associated CRASP proteins of *Borrelia burgdorferi*. PLoS One 5:e13519. doi:10.1371/journal.pone.0013519
94. Hammerschmidt C, Hallström T, Skerka C, Wallich R, Stevenson B, Zipfel PF, Kraiczy P. 2012. Contribution of the infection-associated complement regulator-acquiring surface protein 4 (ErpC) to complement resistance of *Borrelia burgdorferi*. Clin. Dev. Immunol. 2012: doi:10.1155/2012/349657.
95. Coleman AS, Yang X, Kumar M, Zhang X, Promnares K, Shroder D, Kenedy MR, Anderson JF, Akins DR, Pal U. 2008. *Borrelia burgdorferi* complement regulator-acquiring surface protein 2 does not contribute to complement resistance or host infectivity. PLoS One 3:3010e. doi:10.1371/journal.pone.0003010
96. Kraiczy P, Stevenson B. 2013. Complement regulator-acquiring surface proteins of *Borrelia burgdorferi*: structure, function and regulation of gene expression. Ticks Tick Borne Dis. 4:26–34.
97. Kraiczy P, Seling A, Brissette CA, Rossmann E, Hunfeld KP, Bykowski T, Burns LH, Troese MJ, Cooley AE, Miller JC, Brade V, Wallich R, Casjens S, Stevenson B. 2008. *Borrelia burgdorferi* complement regulator-acquiring surface protein 2 (CspZ) as a serological marker of human Lyme disease. Clin. Vaccine Immunol. 15:484–491.
98. Rogers EA, Marconi RT. 2007. Delineation of species-specific binding properties of the CspZ protein (BBH06) of Lyme disease spirochetes: Evidence for new contributions to the pathogenesis of *Borrelia* spp. Infect. Immun. 75:5272–5281.

99. Baum E, Grosenbaugh DA, Barbour AG. 2014. Diversity of antibody responses to *Borrelia burgdorferi* in experimentally infected beagle dogs. *Clin. Vaccine Immunol.* 21:838–46.
100. Brooks CS, Vuppala SR, Jett AM, Meri S, Akins DR, Alitalo A. 2005. Complement regulator-acquiring surface protein 1 imparts resistance to human serum in *Borrelia burgdorferi*. *J. Immunol.* 175:3299–308.
101. Kay J. 2009. Correlating *Borrelia burgdorferi* plasmids with survival in different animal sera. Master's Thesis, Austin Peay State University, Clarksville, TN.
102. Lund Takalo E. 2011. CspZ, the immunological determinant for plasmid maintenance in Lyme disease. Master's Thesis, Austin Peay State University, Clarksville, TN.
103. Tokarz R, Anderton JM, Katona LI, Benach L, Benach JL. 2004. Combined effects of blood and temperature shift on *Borrelia burgdorferi* gene expression as determined by whole genome DNA array. *Infect. Immun.* 72:5419–5432.
104. Kyte J, Doolittle RF. 1982. A simple method for displaying the hydropathic character of a protein. *J. Mol. Biol.* 157:105–132.
105. Berland R, Fikrig E, Rahn D, Hardin J, Flavell RA. 1991. Molecular characterization of the humoral response to the 41-kilodalton flagellar antigen of *Borrelia burgdorferi*, the Lyme disease agent. *Infect. Immun.* 59:3531–3535.
106. Alitalo A, Meri T, Rämö L, Jokiranta TS, Heikkilä T, Seppälä IJT, Oksi J, Viljanen M, Meri S. 2001. Complement evasion by *Borrelia burgdorferi*: serum-resistant strains promote C3b inactivation. *Infect. Immun.* 69:3685–3691.
107. Kenedy MR, Lenhart TR, Akins DR. 2012. The role of *Borrelia burgdorferi* outer surface proteins. *FEMS Immunol. Med. Microbiol.* 66:1–19.

108. Akins DR, Bourell KW, Caimano MJ, Norgard MV., Radolf JD. 1998. A new animal model for studying Lyme disease spirochetes in a mammalian host-adapted state. *J. Clin. Invest.* 101:2240–2250.
109. Hefty PS, Jolliff SE, Caimano MJ, Wikel SK, Radolf JD, Akins DR. 2001. Regulation of OspE-related, OspF-related, and Elp lipoproteins of *Borrelia burgdorferi* strain 297 by mammalian host-specific signals. *Infect. Immun.* 69:3618–3627.
110. Rebay I, Fehon RG. 2009. Preparation of insoluble GST fusion proteins. *Cold Spring Harb. Protoc.* 4: doi: 10.1101/pdb.prot4997.
111. Harper S, Speicher DW. 2011. Purification of proteins fused to glutathione S-transferase. *Methods Mol. Biol.* 681:259–280.
112. Radolf JD, Bourell KW, Akins DR, Brusca JS, Norgard MV. 1994. Analysis of *Borrelia burgdorferi* membrane architecture by freeze-fracture electron microscopy. *J. Bacteriol.* 176:21–31.
113. Pal U, De Silva AM, Montgomery RR, Fish D, Anguita J, Anderson JF, Lobet Y, Fikrig E. 2000. Attachment of *Borrelia burgdorferi* within *Ixodes scapularis* mediated by outer surface protein A. *J. Clin. Invest.* 106:561–569.
114. Ramamoorthy R, Philipp MT. 1998. Differential expression of *Borrelia burgdorferi* proteins during growth *in vitro*. *Infect. Immun.* 66:5119–5124.
115. Arnold WK, Savage CR, Brissette CA, Seshu J, Livny J, Stevenson B. 2016. RNA-Seq of *Borrelia burgdorferi* in multiple phases of growth reveals insights into the dynamics of gene expression, transcriptome architecture, and noncoding RNAs. *PLoS One* 11:e0164165. doi:10.1371/journal.pone.0164165.

116. Brangulis K, Petrovskis I, Kazaks A, Bogans J, Otikovs M, Jaudzems K, Ranka R, Tars K. 2014. Structural characterization of CspZ, a complement regulator factor H and FHL-1 binding protein from *Borrelia burgdorferi*. FEBS J. 281:2613–2622.
117. Siegel C, Schreiber J, Haupt K, Skerka C, Brade V, Simon MM, Stevenson B, Wallich R, Zipfel PF, Kraiczy P. 2008. Deciphering the ligand-binding sites in the *Borrelia burgdorferi* complement regulator-acquiring surface protein 2 required for interactions with the human immune regulators factor H and factor H-like protein 1. J. Biol. Chem. 283:34855–34863.
118. Rogers EA, Abdunnur SV, McDowell JV, Marconi RT. 2009. Comparative analysis of the properties and ligand binding characteristics of CspZ, a factor H binding protein, derived from *Borrelia burgdorferi* isolates of human origin. Infect. Immun. 77:4396–4405.
119. Kraiczy P. 2016. Travelling between two worlds: complement as a gatekeeper for an expanded host range of Lyme disease spirochetes. Vet. Sci. 3: 12. doi:10.3390/vetsci3020012.
120. Kišová-Vargová L, Mucha R, Čerňanská D, Bhide M. 2011. Host-dependent differential expression of factor H binding proteins, their affinity to factor H and complement evasion by Lyme and relapsing fever *Borreliae*. Vet. Microbiol. 148:341–347.

VITAE

Nerina Jusufovic immigrated to the United States from Bosnia and Herzegovina with her family in 1996. They settled in the town of Smyrna, TN. She attended La Vergne High School where she graduated as salutatorian. After high school, she attended Middle Tennessee State University in Murfreesboro, TN, and she graduated cum laude with a BS in Biology with a concentration in Microbiology in 2013.

After a year off from school, Nerina decided to pursue a master's degree in science at Austin Peay State University. She decided to complete a thesis studying the Lyme disease spirochete *Borrelia burgdorferi* and was awarded a graduate tuition assistantship grant. In addition, she taught both lecture and laboratory courses of microbiology to undergraduate nursing and medical technology students. Nerina won second place in microbiology oral presentations at the Tennessee Academy of Sciences annual meeting in 2017. She intends to apply to PhD programs to study infectious diseases in 2018 to start in the fall 2019 semester. As of Jan. 2018, she will continue to teach at Austin Peay State University as an adjunct professor.